

CP Symmetry and Lepton Mixing from a Scan of Finite Discrete Groups

Chang-Yuan Yao*, Gui-Jun Ding†

*Interdisciplinary Center for Theoretical Study and Department of Modern Physics,
University of Science and Technology of China, Hefei, Anhui 230026, China*

Abstract

Including the generalized CP symmetry, we have performed a comprehensive scan of leptonic mixing patterns which can be obtained from finite discrete groups with order less than 2000. Both the semidirect approach and its variant are considered. The lepton mixing matrices which can admit a good agreement with experimental data can be organized into eight different categories up to possible row and column permutations. These viable mixing patterns can be completely obtained from the discrete flavor groups $\Delta(6n^2)$, $D_{9n,3n}^{(1)}$, A_5 and $\Sigma(168)$ combined with CP symmetry. We perform a detailed analytical and numerical analysis for each possible mixing patterns. The resulting predictions for lepton mixing parameter, neutrinoless double decay and flavored leptogenesis are studied.

arXiv:1606.05610v1 [hep-ph] 17 Jun 2016

*E-mail: phyman@mail.ustc.edu.cn

†E-mail: dinggj@ustc.edu.cn

1 Introduction

The origin of fermion mass and flavor mixing is one of longstanding open questions beyond the Standard Model physics. The discovery of neutrino oscillations and the precise measurements of the three lepton mixing angles θ_{12} , θ_{23} and θ_{13} shed light on the flavor puzzle and help to establish underlying physics principle. One most popular approach is to invoke a discrete flavor symmetry to explain the observed patterns. In this paradigm, a given mixing pattern is related to certain residual symmetry of the leptonic mass matrices, and the residual symmetry may arise from the breaking of the complete flavor symmetry group G_f of some unknown extension of the Standard Model. The residual symmetry groups and their embedding in G_f is sufficient to predict the values of the mixing angles, and the detailed dynamics of symmetry breaking is not necessary. Many different discrete flavor symmetry groups and their application in model building have been studied in the literature, please see Refs. [1–3] for review.

In recent years, the flavor symmetry is extended to include the generalized CP symmetry in order to understand the observed values of the mixing angles and simultaneously predict the unknown CP violating phases [4, 5]. Note that low significance hints for a maximal Dirac CP phase $\delta_{CP} \simeq -\pi/2$ has been reported [6], and the measurement of the Dirac CP phase is an important physical motivation of forthcoming neutrino oscillation experiments. From the bottom-up view, the neutrino and the charged lepton mass matrices admit both residual flavor symmetry and residual CP symmetry, and the residual flavor symmetry can be generated by the residual CP transformations [7, 8]. One generally presumes that these residual symmetries originate from a large symmetry group (a flavor symmetry G_f and the generalized CP) at high energy scale whose breaking leads to the symmetries of the mass matrices. Imposing a flavor symmetry as well as generalized CP symmetry, one can constrain the CP violation phases besides mixing angles. This can lead to very predictive scenarios in which the mixing angles and CP phases are determined in terms of few input parameters [4, 7, 8]. Discrete flavor symmetry combined with CP symmetry turns out to be a rather powerful framework. A variety of flavor symmetry groups and their interplay with the CP symmetry have been studied such as A_4 [9], S_4 [4, 10–14], $\Delta(27)$ [15], $\Delta(48)$ [16], A_5 [17–19], $\Delta(96)$ [20] and $\Sigma(36 \times 3)$ [21]. In particular the lepton mixing patterns arising from flavor symmetry group series $\Delta(3n^2)$ [22, 23], $\Delta(6n^2)$ [22, 24, 25] and $D_{9n, 3n}^{(1)}$ [26] in combination with a CP symmetry have been analyzed for an arbitrary index n . Some models with flavor and CP symmetry have been constructed [9–14, 16, 17], where the required vacuum alignment needed to achieve the remnant symmetries is dynamically realized. Moreover, the phenomenological implications of residual flavor and CP symmetry in neutrinoless double beta ($0\nu\beta\beta$) decay [10, 11, 17, 25, 26, 28] and leptogenesis [27, 28] have been studied. It is remarkable that the residual CP transformation could be systematically classified according to the number of its zero elements [29].

The powerful computer algebra software GAP [30] has been frequently used to investigate the lepton mixing matrices achievable from finite discrete groups [31–40]. In this paper, we shall include the generalized CP symmetry and performed a comprehensive scan of all finite subgroups up to order 2000 with the help of GAP. The CP transformations are assumed to correspond to class-inverting automorphisms of the flavor symmetry group. All the possible residual flavor symmetries would be considered. We shall find out all the admissible lepton lepton mixing patterns which can be compatible with the experimental data for certain values of the free parameter θ . To our surprise, these viable lepton mixing matrices can be categorized into eight cases up to permutations of rows and columns, and they can be completely reproduced from the $\Delta(6n^2)$, $D_{9n, 3n}^{(1)}$, A_5 and $\Sigma(168)$ flavor symmetry groups and CP symmetry. We give the analytic formulas of mixing angles and CP invariants in each of these cases. Moreover, we present the analytic expressions for the effective Majorana neutrino mass $|m_{ee}|$ in neutrinoless double beta decay and the lepton asymmetry parameters ϵ_α ($\alpha = e, \mu, \tau$) relevant to leptogenesis. Furthermore, the allowed values of $|m_{ee}|$ and the baryon asymmetry Y_B are analyzed numerically for the smallest values of the index n that admit a good agreement with the experimental data on the mixing angles.

This paper is structured as follows: we shall elaborate the method to obtain the lepton mixing PMNS matrix from any given residual symmetry in the semidirect approach and the variant of the

semidirect approach in section 2. The mixing matrix can be determined from the representation matrices of the residual symmetry without reconstructing the lepton mass matrices. We outline the procedure of group scanning in section 3. The resulting mixing patterns which can accommodate the experimental data, and the predictions for mixing angles and CP invariants are presented. Moreover the phenomenological predictions for $0\nu\beta\beta$ decay and flavored thermal leptogenesis are studied. Finally we conclude in section 4. In appendix A, we derive the criteria to determine whether two residual symmetries leads to the same mixing pattern, if the redefinition of the free parameter θ is used.

2 Framework

Both family symmetry and CP symmetry acts on the flavor space in a non-trivial way, and the interplay between them should be treated carefully. In order to consistently combine the generalized CP symmetry with a flavor symmetry group G_f , the CP transformation should be related to an automorphism $u : G_f \rightarrow G_f$, and the so called consistency condition has to be fulfilled [4, 5, 41],

$$X_{\mathbf{r}}\rho_{\mathbf{r}}^*(g)X_{\mathbf{r}}^\dagger = \rho_{\mathbf{r}}(u(g)), \quad \forall g \in G_f, \quad (2.1)$$

where the subscript “ \mathbf{r} ” refers to the representation space acted on, $\rho_{\mathbf{r}}(g)$ is the representation matrix of the element g , and $X_{\mathbf{r}}$ is the generalized CP transformation. For a given CP transformation $X_{\mathbf{r}}$, $\rho_{\mathbf{r}}(h)X_{\mathbf{r}}$ with $h \in G_f$ also satisfies the consistency equation of Eq. (2.1), and consequently it is an admissible CP transformation as well. Obviously $\rho_{\mathbf{r}}(h)X_{\mathbf{r}}$ corresponds to performing a flavor symmetry transformation $\rho_{\mathbf{r}}(h)$ followed by a CP transformation $X_{\mathbf{r}}$. It is easy to check that the generalized CP transformation $\rho_{\mathbf{r}}(h)X_{\mathbf{r}}$ maps the group element g into $hu(g)h^{-1}$. Hence the automorphism related to $\rho_{\mathbf{r}}(h)X_{\mathbf{r}}$ is an composition of u and an inner automorphism $\mu_h : g \rightarrow hgh^{-1}$ with $h, g \in G_f$. This implies that the effect of the inner automorphism μ_h amounts to a flavor symmetry transformation $\rho_{\mathbf{r}}(h)$. As a result, one could focus on the outer automorphism of G_f when searching for the most general CP transformations compatible with G_f . Furthermore, it has been shown that that the physically well-defined CP transformations should be given by class-inverting automorphism of G_f [42]. In other words, the automorphism u should map each class of G_f into its inverse class. In the present work, we shall be concerned with the CP transformations corresponding to the class-inverting automorphisms.

Let us now consider a theory with both flavor symmetry G_f and CP symmetry H_{CP} which denotes the CP transformations consistent with G_f . Thus the original symmetry at high energy scale is generically $G_f \times H_{CP}$. Notice that the mathematical structure of the group comprising G_f and H_{CP} is a semi-direct product [4], because the flavor symmetry and CP transformations are not commutable in general. The experimental data clearly shows that all lepton masses are unequal and there is flavor mixing among the three mass eigenstates. Therefore the parent symmetry $G_f \times H_{CP}$ should be broken down to different residual subgroups $G_l \times H_{CP}^l$ and $G_\nu \times H_{CP}^\nu$ in the charged lepton and neutrino sectors, respectively. It is remarkable that the lepton flavor mixing is fully fixed by the group structure of $G_f \times H_{CP}$ and the residual symmetries [7, 8]. The details of the breaking mechanisms realizing the assumed residual symmetries are irrelevant. Assuming that neutrinos are Majorana particles, the mass terms of leptons obtained through flavor and CP symmetry breaking take the following form:

$$\mathcal{L}_m = -\bar{l}_R m_l l_L - \frac{1}{2} \nu_L^T C m_\nu \nu_L + h.c., \quad (2.2)$$

where C is the charge conjugation matrix, $l_L \equiv (e_L, \mu_L, \tau_L)^T$ and $l_R \equiv (e_R, \mu_R, \tau_R)^T$ denote the three left-handed (LH) and right-handed (RH) charged lepton fields, respectively, and $\nu_L \equiv (\nu_{eL}, \nu_{\mu L}, \nu_{\tau L})^T$ contains the three LH neutrino fields. Both the charged lepton and neutrino mass matrices m_l and m_ν are subject to the constraints of the remnant symmetries, such that the lepton mixing matrix can be fixed. Bottom-up analysis shows that the residual flavor symmetry G_l can be any Abelian subgroup of G_f while G_ν is either a $K_4 \cong Z_2 \times Z_2$ Klein subgroup or a Z_2 subgroup for Majorana neutrinos [7, 8]. If the remnant flavor symmetry G_ν is restricted to be a Klein subgroup of

G_f and the left-handed leptons l_L transform as three unequivalent one dimensional representations under G_l , both the lepton mixing angles and Dirac CP violating phase would be fully determined by residual symmetries. This scenario has been studied comprehensively in the literature [32, 38, 43]. The Majorana CP phase α_{31} would be predicted to be trivial and another Majorana phase α_{21} can only be a rational multiple of π after the CP symmetry is taken into account [8].

In this work, we shall discuss two different types of remnant symmetries dubbed as “semidirect” and “variant of semidirect” approaches. In the semidirect approach, the residual symmetry in the neutrino sector is $Z_2 \times H_{CP}^\nu$ while G_l is able to distinguish among the three generations of charged lepton fields. As a result, one column of the PMNS matrix is completely fixed by the residual symmetries in this case. In the variant of semidirect approach, the remnant symmetries in the charged lepton and neutrino sectors are assumed to be $Z_2 \times H_{CP}^l$ and $K_4 \times H_{CP}^\nu$ respectively, and one row of the PMNS matrix can be fixed. It turns out that the lepton mixing matrix depends on a single real parameter θ in both approaches. Consequently the mixing angles and CP violating phases are strongly correlated with each other. In the following, the master formula of the prediction for lepton flavor mixing would be derived. As usual the three generations of left-handed leptons are assigned to a faithful irreducible three-dimensional representation of G_f which is denoted as $\mathbf{3}$ henceforth.

2.1 Semidirect approach

We first analyze the residual symmetry constraints in the charged lepton sector. The requirement that $G_l \times H_{CP}^l$ is a symmetry of the charged lepton mass matrix m_l entails that the hermitian combination $m_l^\dagger m_l$ should be invariant under the action of $G_l \times H_{CP}^l$, i.e.,

$$\rho_{\mathbf{3}}^\dagger(g_l) m_l^\dagger m_l \rho_{\mathbf{3}}(g_l) = m_l^\dagger m_l, \quad g_l \in G_l, \quad (2.3)$$

$$X_{l\mathbf{3}}^\dagger m_l^\dagger m_l X_{l\mathbf{3}} = (m_l^\dagger m_l)^*, \quad X_{l\mathbf{3}} \in H_{CP}^l. \quad (2.4)$$

The residual flavor symmetry G_l and the residual CP symmetry H_{CP}^l has to be compatible with each other such that the following restricted consistency equation must be satisfied [7, 8, 11],

$$X_{l\mathbf{r}} \rho_{\mathbf{r}}^*(g_l) X_{l\mathbf{r}}^{-1} = \rho_{\mathbf{r}}(g_l^{-1}), \quad g_l \in G_l, \quad X_{l\mathbf{r}} \in H_{CP}^l. \quad (2.5)$$

The hermitian matrix $m_l^\dagger m_l$ is diagonalized by the unitary transformation U_l with $U_l^\dagger m_l^\dagger m_l U_l = \text{diag}(m_e^2, m_\mu^2, m_\tau^2)$. The explicit form of $m_l^\dagger m_l$ could be constructed from Eqs. (2.3, 2.4), and thus U_l can be determined. In fact, one can directly extract the constraints on U_l from Eqs. (2.3, 2.4) without resorting to mass matrix $m_l^\dagger m_l$ as follows

$$U_l^\dagger \rho_{\mathbf{3}}(g_l) U_l = \rho_{\mathbf{3}}^{diag}(g_l), \quad (2.6)$$

$$U_l^\dagger X_{l\mathbf{3}} U_l^* = X_{l\mathbf{3}}^{diag}, \quad (2.7)$$

where $\rho_{\mathbf{3}}^{diag}(g_l)$ and $X_{l\mathbf{3}}^{diag}$ are diagonal phase matrices. We see that the residual CP transformation $X_{l\mathbf{3}}$ should be a symmetric unitary matrix, and $\rho_{\mathbf{3}}(g_l)$ and $m_l^\dagger m_l$ can be diagonalized by the same unitary matrix U_l . Given a specific residual symmetry group G_l and the three-dimensional representation of G_f , the three normalized and mutually orthogonal eigenvectors of $\rho_{\mathbf{3}}(g_l)$ can be easily found and they constitute a unitary matrix Σ_l fulfilling $\Sigma_l^\dagger \rho_{\mathbf{3}}(g_l) \Sigma_l = \rho_{\mathbf{3}}^{diag}(g_l)$. Since we consider a scenario in which the three generations of left-handed leptons can be distinguished by G_l , and no further assumption or prediction is made about the charged lepton masses. Therefore U_l is uniquely fixed up to permutations and phases of its column vectors, i.e.

$$U_l = \Sigma_l P_l Q_l, \quad (2.8)$$

where Q_l is an arbitrary diagonal phase matrix, and P_l is a permutation matrix. Moreover, it is straightforward to check that the constraint of Eq. (2.7) arising from remnant CP is automatically

fulfilled for the admissible CP transformation $X_{l\mathbf{r}}$ satisfying the restricted consistency condition in Eq. (2.5). That is to say, the mixing matrix U_l of charged leptons is fully determined by the residual flavor symmetry G_l , and the residual CP symmetry H_{CP}^l doesn't lead to additional new constraint in the semidirect approach.

Then we proceed to the neutrino sector. The invariance of the neutrino mass matrix m_ν under the action of the residual symmetry $Z_2 \times H_{CP}^\nu$ gives rise to

$$\rho_{\mathbf{3}}^T(g_\nu)m_\nu\rho_{\mathbf{3}}(g_\nu) = m_\nu, \quad g_\nu \in G_\nu, \quad (2.9)$$

$$X_{\nu\mathbf{3}}^T m_\nu X_{\nu\mathbf{3}} = m_\nu^*, \quad X_{\nu\mathbf{3}} \in H_{CP}^\nu, \quad (2.10)$$

where g_ν is the generator of the residual flavor symmetry $G_\nu = Z_2$ such that the equality $g_\nu^2 = 1$ is satisfied. The restricted consistency condition reads as

$$X_{\nu\mathbf{r}}\rho_{\mathbf{r}}^*(g_\nu)X_{\nu\mathbf{r}}^{-1} = \rho_{\mathbf{r}}(g_\nu), \quad g_\nu \in G_\nu, \quad X_{\nu\mathbf{r}} \in H_{CP}^\nu. \quad (2.11)$$

We denote the diagonalization matrix of m_ν as U_ν which fulfills $U_\nu^T m_\nu U_\nu = \text{diag}(m_1, m_2, m_3)$. Neutrino oscillation experiments reveal that three light neutrino masses $m_{1,2,3}$ are not degenerate. Inserting $U_\nu^T m_\nu U_\nu = \text{diag}(m_1, m_2, m_3)$ into Eqs. (2.9, 2.10), we can derive the following constraints on the unitary transformation U_ν ,

$$U_\nu^\dagger \rho_{\mathbf{3}}(g_\nu) U_\nu = \text{diag}(\pm 1, \pm 1, \pm 1), \quad (2.12)$$

$$U_\nu^\dagger X_{\nu\mathbf{3}} U_\nu^* = \text{diag}(\pm 1, \pm 1, \pm 1) \equiv Q_\nu^2, \quad (2.13)$$

where the “ \pm ” signs can be chosen independently. The unitary matrix $Q_\nu = \text{diag}(\sqrt{\pm 1}, \sqrt{\pm 1}, \sqrt{\pm 1})$ is diagonal, and its non-vanishing entries are ± 1 or $\pm i$. Obviously the residual CP transformation $X_{\nu\mathbf{3}}$ is a unitary symmetric matrix as well. Since g_ν is an element of order two and its representation matrix $\rho_{\mathbf{3}}(g_\nu)$ satisfies $\rho_{\mathbf{3}}^2(g_\nu) = 1$, the eigenvalues of $\rho_{\mathbf{3}}(g_\nu)$ can only be $+1$ or -1 . Without loss of generality, we choose the three eigenvalues of $\rho_{\mathbf{3}}(g_\nu)$ to be $+1, -1$ and -1 respectively. In the following, we shall list the procedures of how to extract the prediction for U_ν .

Firstly $\rho_{\mathbf{3}}(g_\nu)$ can be diagonalized by a unitary matrix $\Sigma_{\nu 1}$ with

$$\Sigma_{\nu 1}^\dagger \rho_{\mathbf{3}}(g_\nu) \Sigma_{\nu 1} = \text{diag}(1, -1, -1). \quad (2.14)$$

Note that $\Sigma_{\nu 1}$ is determined up to a unitary rotation of the second and third column vectors because $\rho_{\mathbf{3}}(g_\nu)$ has two degenerate eigenvalues -1 . Subsequently plugging the expression $\rho_{\mathbf{3}}(g_\nu) = \Sigma_{\nu 1} \text{diag}(1, -1, -1) \Sigma_{\nu 1}^\dagger$ into the the consistency condition of Eq. (2.11), we obtain

$$\Sigma_{\nu 1}^\dagger X_{\nu\mathbf{3}} \Sigma_{\nu 1}^* \text{diag}(1, -1, -1) = \text{diag}(1, -1, -1) \Sigma_{\nu 1}^\dagger X_{\nu\mathbf{3}} \Sigma_{\nu 1}^*, \quad (2.15)$$

which implies that $\Sigma_{\nu 1}^\dagger X_{\nu\mathbf{3}} \Sigma_{\nu 1}^*$ is a block-diagonal matrix, and it is of the form

$$\Sigma_{\nu 1}^\dagger X_{\nu\mathbf{3}} \Sigma_{\nu 1}^* = \begin{pmatrix} e^{i\gamma} & 0 \\ 0 & u_{2 \times 2} \end{pmatrix}, \quad (2.16)$$

where $u_{2 \times 2}$ is a symmetric unitary matrix, and it can be written as $u_{2 \times 2} = \sigma_{2 \times 2} \sigma_{2 \times 2}^T$ by performing the Takagi factorization. As a consequence, the residual CP transformation $X_{\nu\mathbf{3}}$ can be factorized as

$$X_{\nu\mathbf{3}} = \Sigma_\nu \Sigma_\nu^T, \quad (2.17)$$

where $\Sigma_\nu = \Sigma_{\nu 1} \Sigma_{\nu 2}$ with

$$\Sigma_{\nu 2} = \begin{pmatrix} e^{i\gamma/2} & 0 \\ 0 & \sigma_{2 \times 2} \end{pmatrix}. \quad (2.18)$$

It is easy to check that the residual flavor symmetry transformation $\rho_{\mathbf{3}}(g_\nu)$ can be diagonalized by Σ_ν as well,

$$\Sigma_\nu^\dagger \rho_{\mathbf{3}}(g_\nu) \Sigma_\nu = \text{diag}(1, -1, -1). \quad (2.19)$$

Then we discuss the constraint on U_ν from the remnant CP. Substituting the relation $X_{\nu\mathbf{3}} = \Sigma_\nu \Sigma_\nu^T$ of Eq. (2.17) into Eq. (2.13), we have

$$\left(Q_\nu^\dagger U_\nu^\dagger \Sigma_\nu\right) \left(Q_\nu^\dagger U_\nu^\dagger \Sigma_\nu\right)^T = \mathbb{1}. \quad (2.20)$$

This implies that the combination $Q_\nu^\dagger U_\nu^\dagger \Sigma_\nu$ is a orthogonal matrix, and it is also a unitary matrix. Therefore $Q_\nu^\dagger U_\nu^\dagger \Sigma_\nu$ is a real orthogonal matrix denoted by $O_{3\times 3}$. Then the unitary transformation U_ν takes the following form

$$U_\nu = \Sigma_\nu O_{3\times 3}^T Q_\nu^\dagger. \quad (2.21)$$

This indicated that U_ν is fixed up to a real orthogonal matrix $O_{3\times 3}$ by the remnant CP transformation $X_{\nu\mathbf{3}}$ [7]. Furthermore, U_ν is subject to the constraint of residual Z_2 flavor symmetry shown in Eq. (2.12), i.e.

$$U_\nu^\dagger \rho_{\mathbf{3}}(g_\nu) U_\nu = P_\nu^T \text{diag}(1, -1, -1) P_\nu, \quad (2.22)$$

where P_ν is a permutation matrix, because the neutrino masses can not be pinned down in this approach and the neutrino mass spectrum can be either normal ordering (NO) or inverted ordering (IO). One finds from Eq. (2.22) that

$$P_\nu Q_\nu O_{3\times 3} \text{diag}(1, -1, -1) = \text{diag}(1, -1, -1) P_\nu Q_\nu O_{3\times 3}, \quad (2.23)$$

which leads to

$$O_{3\times 3} = P_\nu^T S_{23}^T(\theta), \quad (2.24)$$

where $S_{23}(\theta)$ is a rotation matrix, it is given by

$$S_{23}(\theta) = \begin{pmatrix} 1 & 0 & 0 \\ 0 & \cos \theta & -\sin \theta \\ 0 & \sin \theta & \cos \theta \end{pmatrix}. \quad (2.25)$$

As a result, the residual symmetry $Z_2 \times CP$ of the neutrino mass matrix enforces the unitary diagonalization matrix U_ν of the following form

$$U_\nu = \Sigma_\nu S_{23}(\theta) P_\nu Q_\nu^\dagger. \quad (2.26)$$

Thus we summarize the lepton mixing matrix is determined to be

$$U = U_l^\dagger U_\nu = Q_l^\dagger P_l^T \Sigma_l^\dagger \Sigma_\nu S_{23}(\theta) P_\nu Q_\nu^\dagger. \quad (2.27)$$

Note that PMNS matrix only depend on one free parameter θ , the phase matrix Q_l can be absorbed into the charged lepton fields, and the same result has been obtained by using various methods [4, 7]. This is our master formula to extract the mixing matrix from the postulated residual symmetry in semidirect approach. It would be frequently exploited when we scan the finite groups in section 3.

2.2 Variant of semidirect approach

In this scenario, the original symmetry $G_f \times H_{CP}$ is broken down to $Z_2 \times H_{CP}^l$ in the charged lepton sector. The generator of the residual Z_2 flavor symmetry group is called g_l with $g_l^2 = 1$. For the symmetry $Z_2 \times H_{CP}^l$ to hold, the charged lepton mass matrix has to fulfill

$$\rho_{\mathbf{3}}^\dagger(g_l) m_l^\dagger m_l \rho_{\mathbf{3}}(g_l) = m_l^\dagger m_l, \quad (2.28)$$

$$X_{l\mathbf{3}}^\dagger m_l^\dagger m_l X_{l\mathbf{3}} = (m_l^\dagger m_l)^*, \quad X_{l\mathbf{3}} \in H_{CP}^l, \quad (2.29)$$

The remnant symmetry $Z_2 \times H_{CP}^l$ is well defined only if the restricted consistency condition is satisfied,

$$X_{l\mathbf{r}} \rho_{\mathbf{r}}^*(g_l) X_{l\mathbf{r}}^{-1} = \rho_{\mathbf{r}}(g_l), \quad X_{l\mathbf{r}} \in H_{CP}^l. \quad (2.30)$$

From Eqs. (2.28, 2.29), we find that the residual symmetry $Z_2 \times H_{CP}^l$ leads to the following constraints on the unitary transformation U_l ,

$$U_l^\dagger \rho_{\mathbf{3}}(g_l) U_l = \text{diag}(\pm 1, \pm 1, \pm 1), \quad (2.31)$$

$$U_l^\dagger X_{l\mathbf{3}} U_l^* = \text{diag}(e^{i\alpha_e}, e^{i\alpha_\mu}, e^{i\alpha_\tau}) \equiv Q_l^2, \quad (2.32)$$

where $Q_l = \text{diag}(e^{i\alpha_e/2}, e^{i\alpha_\mu/2}, e^{i\alpha_\tau/2})$ and $\alpha_{e,\mu,\tau}$ are real parameters. Note that $X_{l\mathbf{3}}$ should be symmetric, and the entries of the diagonal matrix is ± 1 in Eq. (2.31) because g_l is of order two here. We assume that the eigenvalues of $\rho_{\mathbf{3}}(g_l)$ are $+1$, -1 and -1 without loss of generality. In the same fashion as we analyze the neutrino sector in the semidirect approach, a proper Takagi factorization of $X_{l\mathbf{3}}$ can be found to satisfy

$$X_{l\mathbf{3}} = \Sigma_l \Sigma_l^T, \quad \Sigma_l^\dagger \rho_{\mathbf{3}}(g_l) \Sigma_l = \text{diag}(1, -1, -1), \quad (2.33)$$

where Σ_l is a unitary matrix. Substituting $X_{l\mathbf{3}}$ from this equation in Eq. (2.32) we obtain

$$(Q_l^\dagger U_l^\dagger \Sigma_l)(Q_l^\dagger U_l^\dagger \Sigma_l)^T = \mathbb{1}. \quad (2.34)$$

Hence $Q_l^\dagger U_l^\dagger \Sigma_l$ is a real orthogonal matrix denoted as $O_{3 \times 3}$, and thus U_l can be expressed as

$$U_l = \Sigma_l O_{3 \times 3}^T Q_l^\dagger. \quad (2.35)$$

Furthermore, we take into account the constraint of the residual Z_2 flavor symmetry,

$$U_l^\dagger \rho_{\mathbf{3}}(g_l) U_l = P_l^T \text{diag}(1, -1, -1) P_l, \quad (2.36)$$

where P_l is a permutation matrix since no prediction can be made for the charged lepton masses. Inserting Eq. (2.35) into Eq. (2.36), we obtain

$$(P_l Q_l O_{3 \times 3}) \text{diag}(1, -1, -1) = \text{diag}(1, -1, -1) (P_l Q_l O_{3 \times 3}). \quad (2.37)$$

As a consequence, $O_{3 \times 3}$ can only be a block diagonal rotation matrix

$$O_{3 \times 3} = P_l^T S_{23}^T(\theta). \quad (2.38)$$

Hence the charged lepton mass matrix $m_l^\dagger m_l$ can be diagonalized by

$$U_l = \Sigma_l S_{23}(\theta) P_l Q_l^\dagger. \quad (2.39)$$

In the neutrino sector, the residual flavor symmetry G_ν is identified with a Klein group,

$$G_\nu = \{1, g_{\nu 1}, g_{\nu 2}, g_{\nu 3}\} \quad (2.40)$$

with the properties

$$g_{\nu i}^2 = 1, \quad g_{\nu i} g_{\nu j} = g_{\nu j} g_{\nu i} = g_{\nu k}, \quad \text{for } i \neq j \neq k. \quad (2.41)$$

The residual CP symmetry H_{CP}^ν arises from the breaking of H_{CP} , and it has to be compatible with residual flavor symmetry G_ν ,

$$X_{\nu \mathbf{r}} \rho_{\mathbf{r}}^*(g_{\nu i}) X_{\nu \mathbf{r}}^{-1} = \rho_{\mathbf{r}}(g_{\nu i}), \quad X_{\nu \mathbf{r}} \in H_{CP}^\nu, \quad i = 1, 2, 3. \quad (2.42)$$

The $G_\nu \times H_{CP}^\nu$ transformation on ν_L leaves the Majorana neutrino mass term in Eq. (2.2) invariant. This implies that

$$\rho_{\mathbf{3}}^T(g_{\nu i}) m_\nu \rho_{\mathbf{3}}(g_{\nu i}) = m_\nu, \quad i = 1, 2, 3, \quad (2.43)$$

$$X_{\nu \mathbf{3}}^T m_\nu X_{\nu \mathbf{3}} = m_\nu^*, \quad X_{\nu \mathbf{3}} \in H_{CP}^\nu, \quad (2.44)$$

Equivalently the neutrino diagonalization matrix U_ν should satisfy

$$U_\nu^\dagger \rho_{\mathbf{3}}(g_{\nu i}) U_\nu = \text{diag}(\pm 1, \pm 1, \pm 1), \quad (2.45)$$

$$U_\nu^\dagger X_{\nu \mathbf{3}} U_\nu^* = \text{diag}(\pm 1, \pm 1, \pm 1) \equiv Q_\nu^2, \quad (2.46)$$

where $Q_\nu = \text{diag}(\sqrt{\pm 1}, \sqrt{\pm 1}, \sqrt{\pm 1})$. As $g_{\nu i}$ is of order two, we have $\det(\rho_{\mathbf{3}}(g_{\nu i})) = \pm 1$. Thus each residual flavor symmetry transformation $\rho_{\mathbf{3}}(g_{\nu i})$ has a unique normalized eigenvector v_i with eigenvalue equal to $\det(\rho_{\mathbf{3}}(g_{\nu i}))$. These three unique eigenvectors v_i ($i = 1, 2, 3$, one for each non-trivial Klein group element) constitute a unitary matrix $\Sigma'_\nu \equiv (v_1, v_2, v_3)$. It is easy to see that Σ'_ν simultaneously diagonalizes all the three representation matrices $\rho_{\mathbf{3}}(g_{\nu i})$. Therefore U_ν coincides with Σ'_ν up to an arbitrary diagonal phase matrix Q'_ν and permutation matrix P_ν multiplied from the right-handed side,

$$U_\nu = \Sigma'_\nu P_\nu Q'_\nu. \quad (2.47)$$

From the consistency condition of Eq. (2.42), we can straightforwardly derive that the remnant CP transformation $X_{\nu \mathbf{3}}$ would be diagonalized by Σ'_ν as follow:

$$\Sigma_\nu'^\dagger X_{\nu \mathbf{3}} \Sigma_\nu'^* = \text{diag}(e^{i\beta_e}, e^{i\beta_\mu}, e^{i\beta_\tau}) \equiv D_\nu^2, \quad (2.48)$$

where $D_\nu = \text{diag}(e^{i\beta_e/2}, e^{i\beta_\mu/2}, e^{i\beta_\tau/2})$, and $\beta_{e,\mu,\tau}$ are real. The diagonal matrix Q'_ν would contribute to the Majorana CP phases. Considering the constraint of the remnant CP transformation in Eq. (2.46) and using the relation of Eq. (2.48), we find

$$Q'_\nu = P_\nu^T D_\nu P_\nu Q_\nu^\dagger. \quad (2.49)$$

Therefore the unitary matrix U_ν is uniquely determined (up to permutations and phases of the column vectors)

$$U_\nu = \Sigma'_\nu D_\nu P_\nu Q_\nu^\dagger \equiv \Sigma_\nu P_\nu Q_\nu^\dagger, \quad (2.50)$$

where we have denoted $\Sigma_\nu = \Sigma'_\nu D_\nu$. Hence in this approach, the master formula for constructing the PMNS matrix is given by

$$U = U_l^\dagger U_\nu = Q_l P_l^T S_{23}^T(\theta) \Sigma_l^\dagger \Sigma_\nu P_\nu Q_\nu^\dagger, \quad (2.51)$$

where Q_l is unphysical as it can be absorbed by redefinition of the charged lepton fields. In contrast with the semidirect approach, one row instead of one column is fixed by the remnant symmetries while the PMNS matrix depends on a single free parameter θ in both cases.

Notice that if another pair of remnant subgroups $\{G'_l \times H'_{CP}, G'_\nu \times H'_{CP}\}$ are conjugate to $\{G_l \times H_{CP}, G_\nu \times H_{CP}\}$ under a group element of G_f , i.e.,

$$G'_l = h G_l h^{-1}, \quad G'_\nu = h G_\nu h^{-1}, \quad h \in G_f, \quad (2.52)$$

$$H'_{CP} = \rho_{\mathbf{r}}(h) H_{CP} \rho_{\mathbf{r}}^T(h), \quad H'_{CP} = \rho_{\mathbf{r}}(h) H_{CP} \rho_{\mathbf{r}}^T(h), \quad (2.53)$$

The unitary diagonalization matrices of the charged lepton and neutrino would be related by $U'_l = \rho_{\mathbf{3}}(h) U_l$ and $U'_\nu = \rho_{\mathbf{3}}(h) U_\nu$. As a consequence, the same result for the PMNS matrix would be obtained. In Appendix A, we present the most general criteria to determine whether the predicted PMNS for different residual symmetries are equivalent.

3 Lepton mixing from scan of finite groups and phenomenology

In this section, we shall perform an exhaustive scan over the discrete groups of order less than 2000 with the help of the computer algebra program GAP [30], and all the possible lepton mixing patterns achievable from the semidirect approach and the variant of the semidirect approach would be studied. In order to avoid duplicating subgroups which have been scanned, we shall only consider the groups with faithful three-dimensional irreducible representations. In our previous work, the possible lepton flavor mixing from flavor symmetry breaking (without generalized CP) have been

systematically analyzed [38], and all discrete groups of size smaller than 2000 are considered by using `GAP`. The CP symmetry would be taken into account further in the present work.

As a proper generalized CP symmetry corresponds to a class-inverting automorphism of the flavor symmetry group [42], we should firstly determine whether a finite group have a class-inverting automorphism. The `GAP` command `AutomorphismGroup(.)` can be exploited to obtain all the automorphisms of a given group G_f , then we can search for the existence of class-inverting automorphisms which map the classes of G_f into their inverse. However, this might be a tough job for groups of large order, since there are generically large amount of automorphisms. We notice that all the automorphisms of G_f constitute a group called automorphism group $\text{Aut}(G_f)$. The inner automorphism group $\text{Inn}(G_f)$ is generated by the group conjugation $\mu_h : g \rightarrow hgh^{-1}$ with $h, g \in G_f$. $\text{Inn}(G_f)$ is a normal subgroup of $\text{Aut}(G_f)$, and it can be easily obtained by using the command `InnerAutomorphismsAutomorphismGroup(.)`. Obviously the inner automorphism maps each conjugacy class into itself. As a result, if \mathbf{u} is a class-inverting automorphism, so will be the composition $\mu_h \circ \mathbf{u}$. The search for class-inverting automorphism can be greatly simplified by considering the quotient group $\text{Out}(G_f) \equiv \text{Aut}(G_f)/\text{Inn}(G_f)$ which is called outer automorphism group. $\text{Out}(G_f)$ can be obtained by the `GAP` command `NaturalHomomorphismByNormalSubgroup(.)`. If there exists a class-inverting outer automorphism, a generalized CP transformation consistent with G_f can be imposed for a generic field content. For a class-inverting outer automorphism \mathbf{u} , the corresponding CP transformation $X_{0\mathbf{r}}$ can be fixed by solving the consistency equation

$$X_{0\mathbf{r}}\rho_{\mathbf{r}}^*(g)X_{0\mathbf{r}}^{-1} = \rho_{\mathbf{r}}(\mathbf{u}(g)), \quad g \in G_f. \quad (3.1)$$

Note that it is sufficient to impose this consistency equation on the generators of G_f . Including the contribution of the inner automorphism, the most general CP transformation compatible with the flavor symmetry G_f takes the form

$$X_{\mathbf{r}} = \rho_{\mathbf{r}}(h)X_{0\mathbf{r}}, \quad h \in G_f. \quad (3.2)$$

On the other hand, if G_f doesn't possess a class-inverting automorphism, CP symmetry can only be introduced in the case that a special subset of irreducible representations is present in a model. We shall not consider such flavor symmetry since the generalized CP symmetry and the resulting predictions for lepton mixing are model dependent.

The residual flavor symmetries G_l and G_ν are Abelian subgroups of the flavor symmetry G_f [7, 8, 38]. Hence we find all the Abelian subgroups of G_f with `GAP`, and the corresponding group structures and generators are extracted. For a generic residual flavor symmetry group G_R which can be either G_l or G_ν , the residual CP transformation $X_{R\mathbf{r}} = \rho_{\mathbf{r}}(f_R)X_{0\mathbf{r}}$ with $f_R \in G_f$ should be a symmetric unitary matrix and it satisfies the consistency condition

$$X_{R\mathbf{r}}\rho_{\mathbf{r}}^*(h_R)X_{R\mathbf{r}}^{-1} = \rho_{\mathbf{r}}(h_R^{-1}), \quad h_R \in G_R, \quad (3.3)$$

which gives rise to

$$f_R^{-1}h_R^{-1}f_R = \mathbf{u}(h_R). \quad (3.4)$$

The permissible solutions to f_R can be straightforwardly found by `GAP`. Notice that G_R is an Abelian group, therefore all the elements in the right coset $G_R f_R$ also satisfy Eq. (3.4) for a given solution f_R . In other words, $\rho_{\mathbf{r}}(h_R)X_{R\mathbf{r}}$ with $h_R \in G_R$ is also an admissible residual CP transformation, and it imposes the same constraints on the lepton mass matrices as $X_{R\mathbf{r}}$ because of the remnant flavor symmetry invariance. In this manner, we can find out all the possible remnant CP symmetries H_{CP}^l and H_{CP}^ν which are compatible with the postulated remnant flavor symmetry groups G_l and G_ν respectively.

Our comprehensive scan over the discrete finite group up to order 2000 reveals that there are 574 groups which possess both faithful three-dimensional irreducible representation and class-inverting automorphism. For each of the 574 groups, the class-inverting automorphism and the corresponding CP transformation $X_{0\mathbf{r}}$ in the triplet representation, its Abelian subgroups as well as the residual CP transformations are calculated. Furthermore, we investigate the possible lepton mixing patterns

achievable from the semidirect approach and the variant of the semidirect approach by considering all the admitted residual symmetries. The predictions for the PMNS matrix are obtained by using the master formulas in Eqs. (2.27, 2.51). In order to measure quantitatively how well the obtained mixing patterns can explain the current experimental data, we perform a conventional χ^2 analysis. The χ^2 function is defined in the usual way

$$\chi^2 = \sum_{ij=12,13,23} \frac{\left(\sin^2 \theta_{ij} - (\sin^2 \theta_{ij})^{\text{bf}}\right)^2}{\sigma_{ij}^2}, \quad (3.5)$$

where $\sin^2 \theta_{ij}$ are the mixing angles predicted for different remnant symmetries, and they depend on the free parameter θ . $(\sin^2 \theta_{ij})^{\text{bf}}$ denote the best fit values of the lepton mixing angles and σ_{ij} their corresponding 1σ errors. We use the current global fit of neutrino oscillation data in Ref. [44]. The results of our analysis are available at the website [45]. It is remarkable that we find many interesting mixing patterns which can accommodate the experimental data on lepton mixing for certain values of θ . Moreover, these phenomenologically viable mixing patterns can be categorized into several cases, as will be shown below.

3.1 Mixing patterns derived from semidirect approach

In this section we shall report the lepton mixing patterns which can be obtained in the semidirect approach. The contributions of the permutations of the rows and columns would be considered. We shall give the analytical expressions for mixing angles and CP invariants J_{CP} , I_1 and I_2 . Moreover, the resulting phenomenological implications in neutrinoless double decay and leptogenesis will be discussed. In the following, three rotation matrices $S_{12}(\theta)$, $S_{13}(\theta)$ and $S_{23}(\theta)$ would be used with the convention

$$\begin{aligned} S_{12}(\theta) &= \begin{pmatrix} \cos \theta & -\sin \theta & 0 \\ \sin \theta & \cos \theta & 0 \\ 0 & 0 & 1 \end{pmatrix}, \\ S_{13}(\theta) &= \begin{pmatrix} \cos \theta & 0 & \sin \theta \\ 0 & 1 & 0 \\ -\sin \theta & 0 & \cos \theta \end{pmatrix}, \\ S_{23}(\theta) &= \begin{pmatrix} 1 & 0 & 0 \\ 0 & \cos \theta & -\sin \theta \\ 0 & \sin \theta & \cos \theta \end{pmatrix}. \end{aligned} \quad (3.6)$$

The permutation matrices P_l and P_ν in Eq. (2.27) can take the following six forms:

$$\begin{aligned} P_{123} &= \begin{pmatrix} 1 & 0 & 0 \\ 0 & 1 & 0 \\ 0 & 0 & 1 \end{pmatrix}, & P_{231} &= \begin{pmatrix} 0 & 1 & 0 \\ 0 & 0 & 1 \\ 1 & 0 & 0 \end{pmatrix}, & P_{312} &= \begin{pmatrix} 0 & 0 & 1 \\ 1 & 0 & 0 \\ 0 & 1 & 0 \end{pmatrix}, \\ P_{132} &= \begin{pmatrix} 1 & 0 & 0 \\ 0 & 0 & 1 \\ 0 & 1 & 0 \end{pmatrix}, & P_{213} &= \begin{pmatrix} 0 & 1 & 0 \\ 1 & 0 & 0 \\ 0 & 0 & 1 \end{pmatrix}, & P_{321} &= \begin{pmatrix} 0 & 0 & 1 \\ 0 & 1 & 0 \\ 1 & 0 & 0 \end{pmatrix}. \end{aligned} \quad (3.7)$$

It is known that if the second and third rows of the PMNS matrix are exchanged, the atmosphere mixing angle θ_{23} becomes $\pi/2 - \theta_{23}$, the Dirac CP phase δ_{CP} becomes $\pi + \delta_{CP}$, and other mixing parameters are invariant. Therefore generically the two permutations of a certain pattern related through the exchange of the second and third rows of the PMNS matrix can (or can't) accommodate the experimental data on mixing angles simultaneously, as will be shown in the following.

Case I(a)

$$U^{I(a)} = \frac{1}{\sqrt{3}} \begin{pmatrix} \sqrt{2} \sin \varphi_1 & e^{i\varphi_2} & \sqrt{2} \cos \varphi_1 \\ \sqrt{2} \cos(\varphi_1 - \frac{\pi}{6}) & -e^{i\varphi_2} & -\sqrt{2} \sin(\varphi_1 - \frac{\pi}{6}) \\ \sqrt{2} \cos(\varphi_1 + \frac{\pi}{6}) & e^{i\varphi_2} & -\sqrt{2} \sin(\varphi_1 + \frac{\pi}{6}) \end{pmatrix} S_{23}(\theta) Q_\nu^\dagger, \quad (3.8)$$

where φ_1 and φ_2 are rational angles, and they are determined by the residual symmetries. The mixing patterns originating from the permutations of rows are related to this matrix through a redefinition of the parameters φ_1 and θ . The viable values of φ_1 and φ_2 and the corresponding representative flavor symmetry groups are collected in table 1. Note that the mixing patterns with the signs of φ_1 and φ_2 reversed can also be produced, and the same predictions for the mixing angles are obtained except all the CP phases become their opposite. However, these viable values are not shown in table 1 in order not to appear too lengthy. From this table, we can see that most of the groups can predict more than one mixing patterns, and some groups predict the same mixing patterns. We only show one or two representative flavor symmetry groups in table 1, and a full summary of the results is available at our website [45]. The subscripts Δ and Δ' of the group identity denote that the corresponding groups belong to the type D group series $D_{n,n}^{(0)} \cong \Delta(6n^2)$ and $D_{9n',3n'}^{(1)} \cong (Z_{9n'} \times Z_{3n'}) \rtimes S_3$, respectively. It is notable that all these interesting mixing patterns can be obtained from the $\Delta(6n^2)$ or $D_{9n',3n'}^{(1)}$ flavor symmetry groups combined with CP symmetry. In particular, widely studied smaller groups $S_4 \cong [24, 12]$ and $\Delta(96) \cong [96, 64]$ can admit a reasonably good fit to the experimental data. This is compatible with the known results in the literature [4, 10, 11, 14, 20]. From the PMNS matrix $U_{PMNS}^{I(a)}$ in Eq. (3.8), we can read out the lepton mixing angles as follow

$$\begin{aligned}\sin^2 \theta_{13} &= \frac{1}{3} \left(1 + \cos^2 \theta \cos 2\varphi_1 - \sqrt{2} \sin 2\theta \cos \varphi_1 \cos \varphi_2 \right), \\ \sin^2 \theta_{12} &= \frac{1 + \sin^2 \theta \cos 2\varphi_1 + \sqrt{2} \sin 2\theta \cos \varphi_1 \cos \varphi_2}{2 - \cos^2 \theta \cos 2\varphi_1 + \sqrt{2} \sin 2\theta \cos \varphi_1 \cos \varphi_2}, \\ \sin^2 \theta_{23} &= \frac{1 - \cos^2 \theta \sin(\pi/6 + 2\varphi_1) + \sqrt{2} \sin 2\theta \cos \varphi_2 \sin(\pi/6 - \varphi_1)}{2 - \cos^2 \theta \cos 2\varphi_1 + \sqrt{2} \sin 2\theta \cos \varphi_1 \cos \varphi_2}.\end{aligned}\tag{3.9}$$

We see that the solar and reactor mixing angles are correlated as,

$$3 \cos^2 \theta_{12} \cos^2 \theta_{13} = 2 \sin^2 \varphi_1,\tag{3.10}$$

For the experimentally measured values $0.270 \leq \sin^2 \theta_{12} \leq 0.344$ and $0.0188 \leq \sin^2 \theta_{13} \leq 0.0251$ at 3σ level [44], we find the allowed intervals of the parameter φ_1 is

$$\varphi_1 \in [0.435\pi, 0.565\pi] \cup [1.435\pi, 1.565\pi]\tag{3.11}$$

Obviously φ_1 should be around $\pi/2$ or $3\pi/2$. Moreover, the three CP rephasing invariants J_{CP} , I_1 and I_2 are predicted to be

$$\begin{aligned}|J_{CP}| &= \frac{1}{6\sqrt{6}} |\sin 2\theta \sin \varphi_2 \sin 3\varphi_1|, \\ |I_1| &= \frac{4}{9} \left| \cos \theta \sin^2 \varphi_1 \sin \varphi_2 \left(\cos \theta \cos \varphi_2 + \sqrt{2} \sin \theta \cos \varphi_1 \right) \right|, \\ |I_2| &= \frac{4}{9} \left| \sin \theta \sin^2 \varphi_1 \sin \varphi_2 \left(\sin \theta \cos \varphi_2 - \sqrt{2} \cos \theta \cos \varphi_1 \right) \right|.\end{aligned}\tag{3.12}$$

The above three CP invariants are conventionally defined as [46–49]

$$\begin{aligned}J_{CP} &\equiv \Im(U_{11}U_{33}U_{13}^*U_{31}^*) = \frac{1}{8} \sin 2\theta_{12} \sin 2\theta_{13} \sin 2\theta_{23} \cos \theta_{13} \sin \delta_{CP}, \\ I_1 &\equiv \Im(U_{11}^{*2}U_{12}^2) = \frac{1}{4} \sin^2 2\theta_{12} \cos^4 \theta_{13} \sin \alpha_{21}, \\ I_2 &\equiv \Im(U_{11}^{*2}U_{13}^2) = \frac{1}{4} \sin^2 2\theta_{13} \cos^2 \theta_{12} \sin(\alpha_{31} - 2\delta_{CP}),\end{aligned}\tag{3.13}$$

where δ_{CP} is the Dirac CP violation phase, α_{21} and α_{31} are the Majorana CP phases in the standard parameterization of the lepton mixing matrix [50]. In this work, we shall present the absolute values of J_{CP} , I_1 and I_2 because the signs of I_1 and I_2 depend on the CP parity of

the neutrino states which is encoded in the matrix Q_ν and the overall signs of all the three CP invariant would be changed if the left-handed lepton doublets are assigned to conjugate triplet $\bar{\mathbf{3}}$ instead of $\mathbf{3}$.

Furthermore, we can derive the following exact sum rule among the mixing angles and Dirac CP phase,

$$\cos \delta_{CP} = \frac{\cos 2\theta_{23} (3 \cos 2\theta_{12} - 2 \sin^2 \varphi_1) + \sqrt{3} \sin 2\varphi_1}{3 \sin 2\theta_{12} \sin \theta_{13} \sin 2\theta_{23}}. \quad (3.14)$$

This sum rule can also be obtained from $|U_{\mu 1}|^2 = 2 \cos^2(\varphi_1 - \pi/6)/3$ and $|U_{\tau 1}|^2 = 2 \cos^2(\varphi_1 + \pi/6)/3$. Because the parameter φ_1 should be around $\pi/2$ or $3\pi/2$ as shown in Eq. (3.11), the sum rule of Eq. (3.14) is approximately

$$\cos \delta_{CP} \simeq \frac{(3 \cos 2\theta_{12} - 2) \cot 2\theta_{23}}{3 \sin 2\theta_{12} \sin \theta_{13}}. \quad (3.15)$$

This implies that δ_{CP} would be nearly maximal if the atmospheric angle θ_{23} takes the maximal value $\theta_{23} = \pi/4$. We allow the three mixing angles to freely vary in the experimentally preferred 3σ ranges [44], then the sum rule Eq. (3.15) leads to

$$-0.643 \leq \cos \delta_{CP} \leq 0.819. \quad (3.16)$$

Needless to say, the improved measurement of the mixing angles particularly θ_{12} and θ_{23} could help to make more precise prediction for δ_{CP} in our framework.

If the light neutrinos with definite mass ν_i are Majorana fermions, their exchange can trigger the neutrinoless double beta ($0\nu\beta\beta$) decay processes $(A, Z) \rightarrow (A, Z + 2) + e^- + e^-$ in which the total lepton number changes by two units. Most importantly, the experimental detection of this lepton number violating decay will proof the Majorana nature of neutrinos. In addition, the lifetime of the $0\nu\beta\beta$ decay is related to the neutrino masses so that its measurement will also probe the unknown absolute neutrino mass and hierarchy. The $0\nu\beta\beta$ decay amplitude has the form $\mathcal{A}^{0\nu\beta\beta} = G_F^2 m_{ee} \mathcal{M}^{0\nu\beta\beta}$, where where G_F is the Fermi constant, m_{ee} is the $0\nu\beta\beta$ decay effective Majorana mass and $\mathcal{M}^{0\nu\beta\beta}$ is the nuclear matrix element of the process. The effective mass m_{ee} contains all the dependence of $\mathcal{A}^{0\nu\beta\beta}$ on the neutrino mixing parameters with [50]

$$\begin{aligned} |m_{ee}| &= \left| \sum_{i=1}^3 m_i U_{1i}^2 \right| \\ &= \left| m_1 \cos^2 \theta_{12} \cos^2 \theta_{13} + m_2 \sin^2 \theta_{12} \cos^2 \theta_{13} e^{i\alpha_{21}} + m_3 \sin^2 \theta_{13} e^{i(\alpha_{31} - 2\delta_{CP})} \right|, \end{aligned} \quad (3.17)$$

where $m_{1,2,3}$ are the light Majorana neutrino masses. One can see that m_{ee} depends on the values of the Majorana phase α_{21} and the Majorana-Dirac phase difference $\alpha'_{31} \equiv \alpha_{31} - 2\delta_{CP}$. We recall that the two heavier neutrino masses can be expressed in terms of the lightest neutrino mass and the two neutrino mass-squared differences measured in neutrino oscillation experiments. For the NO spectrum, one gets

$$m_1 = m_{\text{lightest}}, \quad m_2 = \sqrt{m_{\text{lightest}}^2 + \Delta m_{21}^2}, \quad m_3 = \sqrt{m_{\text{lightest}}^2 + \Delta m_{31}^2}, \quad (3.18)$$

while for the IO spectrum:

$$m_1 = \sqrt{m_{\text{lightest}}^2 - \Delta m_{32}^2 - \Delta m_{21}^2}, \quad m_2 = \sqrt{m_{\text{lightest}}^2 - \Delta m_{32}^2}, \quad m_3 = m_{\text{lightest}}, \quad (3.19)$$

where $\Delta m_{ij}^2 = m_i^2 - m_j^2$. In our numerical analysis, we shall use the best fit values of Δm_{21}^2 and $\Delta m_{31(32)}^2$ obtained in the global analysis [44],

$$\Delta m_{21}^2 = 7.50 \times 10^{-5} \text{eV}^2, \quad \Delta m_{31}^2 = 2.457 \times 10^{-3} \text{eV}^2, \quad \Delta m_{32}^2 = -2.449 \times 10^{-3} \text{eV}^2, \quad (3.20)$$

where the quoted values of Δm_{31}^2 and Δm_{32}^2 correspond to the NO and IO spectrums, respectively. The numerical results would only change a little bit if the experimental uncertainties of the neutrino mass squared splittings are considered. For the mixing pattern $U^{I(a)}$, the effective Majorana mass $|m_{ee}|$ is given by

$$|m_{ee}| = \frac{1}{3} \left| 2m_1 \sin^2 \varphi_1 + q_1 m_2 \left(e^{i\varphi_2} \cos \theta + \sqrt{2} \cos \varphi_1 \sin \theta \right)^2 + q_2 m_3 \left(\sqrt{2} \cos \theta \cos \varphi_1 - e^{i\varphi_2} \sin \theta \right)^2 \right|, \quad (3.21)$$

where $q_1, q_2 = \pm 1$ originates from the ambiguity of the CP parity matrix Q_ν . We show $|m_{ee}|$ versus the lightest neutrino mass m_{lightest} in Fig. 1, where the three mixing angles are required to lie in the 3σ regions. We display the allowed ranges of the effective mass $|m_{ee}|$ under the assumption of φ_1 and φ_2 as free continuous parameters and for the specific value of $(\varphi_1, \varphi_2) = (\pi/2, \pi/2)$. The case of $(\varphi_1, \varphi_2) = (\pi/2, \pi/2)$ can be naturally reproduced from the S_4 flavor symmetry combined with CP symmetry. Accordingly $|m_{ee}|$ is predicted to close to 0.017eV or around the upper bound 0.048eV for IO neutrino mass spectrum, which are within the future sensitivity of forthcoming $0\nu\beta\beta$ decay experiments. However, for NO spectrum, $|m_{ee}|$ strongly depends on the lightest neutrino mass m_{lightest} , and it can even be approximately vanishing for particular value of m_{lightest} . Although exploring the NO region experimentally is beyond the reach of any planned experiment, if $0\nu\beta\beta$ decays are not observed and neutrino oscillation experiments establish that the neutrino masses are NO, it would be important to test $|m_{ee}|$ values in the NO region by combining the information on the absolute mass scale from cosmology.

It is recently found that lepton flavor mixing as well as leptogenesis is strongly constrained by the residual discrete flavor and CP symmetries of the neutrino and charged lepton sectors [27]. For the widely studied scenario of leptogenesis in type-I seesaw model with a hierarchical heavy neutrinos mass spectrum $M_{2,3} \gg M_1$, the CP asymmetry generated by the N_1 decay process $N_1 \rightarrow l_\alpha + H$, $\alpha = e, \mu, \tau$ process is approximately given by [51–55]

$$\begin{aligned} \epsilon_\alpha &\equiv \frac{\Gamma(N_1 \rightarrow Hl_\alpha) - \Gamma(N_1 \rightarrow \overline{H}l_\alpha)}{\sum_\alpha [\Gamma(N_1 \rightarrow Hl_\alpha) + \Gamma(N_1 \rightarrow \overline{H}l_\alpha)]} \\ &= -\frac{3M_1}{16\pi v^2} \frac{\Im \left(\sum_{ij} \sqrt{m_i m_j} m_j R_{1i} R_{1j} U_{\alpha i}^* U_{\alpha j} \right)}{\sum_j m_j |R_{1j}|^2}, \end{aligned} \quad (3.22)$$

where v is the Higgs vacuum expectation value given by $v = 174$ GeV, U is the PMNS matrix, and R is the Casas-Ibarra parametrization of the neutrino Yukawa matrix λ [56]:

$$R = v M^{-\frac{1}{2}} \lambda U m^{-\frac{1}{2}}, \quad (3.23)$$

where $M \equiv \text{diag}(M_1, M_2, M_3)$ and $m \equiv \text{diag}(m_1, m_2, m_3)$. One sees that R is a generic complex orthogonal matrix fulfilling $RR^T = R^T R = 1$. Besides the CP asymmetry parameter ϵ_α , the final baryon asymmetry depends on washout mass parameter \tilde{m}_α for each flavor α with

$$\tilde{m}_\alpha = \left| \sum_j m_j^{1/2} R_{1j} U_{\alpha j}^* \right|^2. \quad (3.24)$$

In the present work we will be concerned with temperature window $10^9 \text{ GeV} \leq T \sim M_1 \leq 10^{12} \text{ GeV}$. In this range only the interactions mediated by the τ Yukawa coupling are in equilibrium, and the final baryon asymmetry is well approximated by

$$Y_B \simeq -\frac{12}{37 g^*} \left[\epsilon_2 \eta \left(\frac{417}{589} \tilde{m}_2 \right) + \epsilon_\tau \eta \left(\frac{390}{589} \tilde{m}_\tau \right) \right], \quad (3.25)$$

where g_* is the effective number of spin-degrees of freedom in thermal equilibrium with $g_* = 106.75$ in the standard model, $\epsilon_2 = \epsilon_e + \epsilon_\mu$, $\tilde{m}_2 = \tilde{m}_e + \tilde{m}_\mu$ and

$$\eta(\tilde{m}_\alpha) \simeq \left[\left(\frac{\tilde{m}_\alpha}{8.25 \times 10^{-3} \text{ eV}} \right)^{-1} + \left(\frac{0.2 \times 10^{-3} \text{ eV}}{\tilde{m}_\alpha} \right)^{-1.16} \right]^{-1}. \quad (3.26)$$

Then we recapitulate the main results for leptogenesis predicted by residual flavor and CP symmetries in Ref. [27]. If both the neutrino Yukawa coupling and the RH neutrino mass matrix (after the electroweak and flavor symmetries breaking) are invariant under two set of residual CP transformation $X_{\nu 1}$, $X_{\nu 2}$ of the LH neutrino fields ν_L and X_{N1} , X_{N2} of the RH neutrino fields, or equivalently a Z_2 flavor symmetry and a CP symmetry are preserved in the neutrino sector, the R -matrix would be constrained to be block diagonal [27],

$$P_N R P_\nu^T = \begin{pmatrix} \times & 0 & 0 \\ 0 & \times & \times \\ 0 & \times & \times \end{pmatrix}, \quad (3.27)$$

where the notation “ \times ” denotes a nonzero matrix element, P_N and P_ν are the permutation matrices. In order to generate a nonvanishing lepton asymmetry, there cannot be two zero elements in the first row of the R -matrix. As a consequence, depending on the values of P_ν , we have three possible cases named C_{12} , C_{13} and C_{23} [27],

$$C_{12} : R = \begin{pmatrix} \times & \times & 0 \\ \dots & & \end{pmatrix}, \quad C_{13} : R = \begin{pmatrix} \times & 0 & \times \\ \dots & & \end{pmatrix}, \quad C_{23} : R = \begin{pmatrix} 0 & \times & \times \\ \dots & & \end{pmatrix}. \quad (3.28)$$

Furthermore, each element of R -matrix is either real or purely imaginary because of the residual CP invariance. To facilitate the discussion, we introduce the notations

$$U' = U Q_{\nu 1}, \quad R' = Q_{N1} R Q_{\nu 1}, \quad (3.29)$$

where Q_{N1} and $Q_{\nu 1}$ are the CP parity matrices of the RH and LH neutrino fields respectively, they are diagonal matrices with entries ± 1 and $\pm i$, and their values are not constrained by residual symmetries. Thus R' would be a block diagonal real matrix, and it satisfies

$$\sum_{i=1}^3 R'_{1i}{}^2 K_i = 1, \quad (3.30)$$

where K_i is equal to $+1$ or -1 with

$$K_i = (Q_{N1}^2)_{11} (Q_{\nu 1}^2)_{ii}. \quad (3.31)$$

Moreover, for each case C_{ab} with $ab = 12, 13$ and 23 listed in Eq. (3.28), the lepton asymmetry ϵ_α and washout mass \tilde{m}_α can be written into a quite simple form

$$\epsilon_\alpha = -\frac{3M_1}{16\pi v^2} W_{ab} I_{ab}^\alpha, \quad (3.32)$$

$$\tilde{m}_\alpha = \left| m_a^{1/2} R'_{1a} U'_{\alpha a} + m_b^{1/2} R'_{1b} U'_{\alpha b} \right|^2, \quad (3.33)$$

where

$$W_{ab} = \frac{\sqrt{m_a m_b} R'_{1a} R'_{1b} (m_a K_a - m_b K_b)}{m_a (R'_{1a})^2 + m_b (R'_{1b})^2}, \quad I_{ab}^\alpha = \text{Im}(U'_{\alpha a} U'_{\alpha b}^*). \quad (3.34)$$

We would like to remind the readers that the repeated indices are not summed over in Eqs. (3.32, 3.33, 3.34). We notice that the lepton asymmetry ϵ_α are closely related to the lower energy CP phases in this framework. The observation of CP violation in future neutrino oscillation and neutrinoless double decay experiments would imply the existence of a baryon asymmetry. We

give the most general parametrization of the first column of R' and corresponding expressions of W_{12} , W_{13} and W_{23} in table 2. For the predicted mixing pattern $U^{I(a)}$ in Eq. (3.8), the rephasing invariants I_{23}^α are of the form

$$\begin{aligned} I_{23}^e &= \frac{\sqrt{2}}{3} \cos \varphi_1 \sin \varphi_2, \\ I_{23}^\mu &= -\frac{\sqrt{2}}{3} \sin\left(\frac{\pi}{6} - \varphi_1\right) \sin \varphi_2, \\ I_{23}^\tau &= -\frac{\sqrt{2}}{3} \sin\left(\frac{\pi}{6} + \varphi_1\right) \sin \varphi_2. \end{aligned} \quad (3.35)$$

As shown in table 1, the parameter values $(\varphi_1, \varphi_2) = (\pi/2, \pi/2)$ can be obtained when the flavor symmetry group G_f is S_4 . Accordingly both atmospheric mixing angle and Dirac CP phase are predicted to be maximal. We find that the best fit value of the parameter θ is $\theta_{\text{bf}} = \pm 0.082\pi (\pm 0.083\pi)$, and the global minimum of the χ^2 function is $\chi_{\text{min}}^2 = 2.089(5.783)$ for NO (IO) spectrum. The predictions for Y_B as a function of the parameter η are plotted in figure 2. We see that the realistic value of Y_B can be reproduced for appropriate values of η except in the case of NO with $(K_1, K_2, K_3) = (\pm, -, +)$, while for IO spectrum the correct value of Y_B can be achieved when $(K_1, K_2, K_3) = (\pm, +, -)$ for $\theta_{\text{bf}} = 0.083\pi$ or $(K_1, K_2, K_3) = (\pm, +, -), (\pm, -, +)$ for $\theta_{\text{bf}} = -0.083\pi$.

Case I(b)

$$U^{I(b)} = \frac{1}{\sqrt{3}} \begin{pmatrix} \sqrt{2} \cos \varphi_1 & e^{i\varphi_2} & \sqrt{2} \sin \varphi_1 \\ -\sqrt{2} \sin\left(\varphi_1 - \frac{\pi}{6}\right) & -e^{i\varphi_2} & \sqrt{2} \cos\left(\varphi_1 - \frac{\pi}{6}\right) \\ -\sqrt{2} \sin\left(\varphi_1 + \frac{\pi}{6}\right) & e^{i\varphi_2} & \sqrt{2} \cos\left(\varphi_1 + \frac{\pi}{6}\right) \end{pmatrix} S_{12}(\theta) Q_\nu^\dagger, \quad (3.36)$$

where the admissible values of φ_1 and φ_2 and the corresponding representative flavor symmetry groups are listed in table 4. One can refer to the full results at the website [45]. It is remarkable that all these phenomenological viable mixing patterns can be achieved from the type D group series $\Delta(6n^2)$ or $D_{9n,3n}^{(1)}$ combined with CP symmetry. The smallest group which can admit a good fit to the experimental data is $[649, 259] \cong D_{9 \times 2, 3 \times 2}^{(1)}$ in this case. The PMNS matrix $U^{I(b)}$ is related to $U^{I(a)}$ by column permutations, and the constant column vector $(\sqrt{2} \sin \varphi_1, \sqrt{2} \cos(\varphi_1 - \frac{\pi}{6}), \sqrt{2} \cos(\varphi_1 + \frac{\pi}{6}))^T$ enforced by residual symmetries is arranged at the third column in this case. The patterns originating from the six possible row permutations of $U^{I(b)}$ can be obtained through redefinitions of φ_1 and θ . We can extract the mixing angles from Eq. (3.36) in the usual way and find

$$\begin{aligned} \sin^2 \theta_{13} &= \frac{2}{3} \sin^2 \varphi_1, & \sin^2 \theta_{23} &= \frac{1 + \sin(\pi/6 + 2\varphi_1)}{2 + \cos 2\varphi_1}, \\ \sin^2 \theta_{12} &= \frac{1 + \sin^2 \theta \cos 2\varphi_1 - \sqrt{2} \sin 2\theta \cos \varphi_2 \cos \varphi_1}{2 + \cos 2\varphi_1}. \end{aligned} \quad (3.37)$$

Notice that both the reactor angle θ_{13} and the atmospheric mixing angle θ_{23} only depend on the discrete parameter φ_1 while all the three parameters θ , φ_1 and φ_2 are involved in the solar mixing angle θ_{12} . Moreover, we easily see that the mixing angles fulfill the following sum rule

$$2 \sin^2 \theta_{23} = 1 \pm \tan \theta_{13} \sqrt{2 - \tan^2 \theta_{13}}. \quad (3.38)$$

Using the best fit value $\sin^2 \theta_{13} = 0.0218$ [44], we obtain

$$\sin^2 \theta_{23} \simeq 0.395, \quad \text{or} \quad \sin^2 \theta_{23} \simeq 0.605. \quad (3.39)$$

Consequently θ_{23} deviates from maximal mixing but it is in the experimentally preferred 3σ

Group Id	(φ_1, φ_2)
$[24, 12]_\Delta, [48, 48]$	$(\frac{\pi}{2}, \frac{\pi}{2})$
$[150, 5]_\Delta, [300, 26]$	$(\frac{7\pi}{15}, -\frac{\pi}{5}), (\frac{7\pi}{15}, 0), (\frac{7\pi}{15}, \frac{2\pi}{5}), (\frac{8\pi}{15}, -\frac{\pi}{5}), (\frac{8\pi}{15}, 0), (\frac{8\pi}{15}, \frac{2\pi}{5})$
$[162, 10], [162, 12]$	$(\frac{5\pi}{9}, 0), (\frac{5\pi}{9}, \frac{\pi}{3})$
$[294, 7]_\Delta, [588, 39]$	$(\frac{10\pi}{21}, -\frac{3\pi}{7}), (\frac{10\pi}{21}, -\frac{2\pi}{7}), (\frac{10\pi}{21}, -\frac{\pi}{7}), (\frac{10\pi}{21}, 0), (\frac{11\pi}{21}, -\frac{3\pi}{7}), (\frac{11\pi}{21}, -\frac{2\pi}{7}),$ $(\frac{11\pi}{21}, -\frac{\pi}{7}), (\frac{11\pi}{21}, 0)$
$[384, 568]_\Delta,$ $[768, 1085727]$	$(\frac{11\pi}{24}, -\frac{\pi}{4}), (\frac{11\pi}{24}, 0), (\frac{11\pi}{24}, \frac{\pi}{8}), (\frac{11\pi}{24}, \frac{3\pi}{8}), (\frac{11\pi}{24}, \frac{\pi}{2}), (\frac{\pi}{2}, -\frac{3\pi}{8}),$ $(\frac{13\pi}{24}, -\frac{\pi}{4}), (\frac{13\pi}{24}, 0), (\frac{13\pi}{24}, \frac{\pi}{8}), (\frac{13\pi}{24}, \frac{3\pi}{8}), (\frac{13\pi}{24}, \frac{\pi}{2})$
$[600, 179]_\Delta, [1200, 1011]$	$(\frac{7\pi}{15}, \frac{\pi}{10}), (\frac{7\pi}{15}, \frac{3\pi}{10}), (\frac{7\pi}{15}, \frac{\pi}{2}), (\frac{\pi}{2}, -\frac{2\pi}{5}), (\frac{\pi}{2}, -\frac{3\pi}{10}), (\frac{8\pi}{15}, \frac{\pi}{10}), (\frac{8\pi}{15}, \frac{3\pi}{10}),$ $(\frac{8\pi}{15}, \frac{\pi}{2})$
$[648, 259]_{\Delta'}, [648, 260]$	$(\frac{\pi}{2}, \frac{\pi}{3}), (\frac{5\pi}{9}, -\frac{\pi}{6}), (\frac{5\pi}{9}, \frac{\pi}{2})$
$[726, 5]_\Delta, [1452, 23]$	$(\frac{5\pi}{11}, -\frac{2\pi}{11}), (\frac{5\pi}{11}, 0), (\frac{5\pi}{11}, \frac{\pi}{11}), (\frac{5\pi}{11}, \frac{3\pi}{11}), (\frac{5\pi}{11}, \frac{4\pi}{11}), (\frac{5\pi}{11}, \frac{5\pi}{11}), (\frac{16\pi}{33}, -\frac{5\pi}{11}),$ $(\frac{16\pi}{33}, -\frac{3\pi}{11}), (\frac{16\pi}{33}, -\frac{2\pi}{11}), (\frac{16\pi}{33}, -\frac{\pi}{11}), (\frac{16\pi}{33}, 0), (\frac{16\pi}{33}, \frac{4\pi}{11}), (\frac{16\pi}{33}, \frac{5\pi}{11}), (\frac{17\pi}{33}, -\frac{5\pi}{11}),$ $(\frac{17\pi}{33}, -\frac{3\pi}{11}), (\frac{17\pi}{33}, -\frac{2\pi}{11}), (\frac{17\pi}{33}, \frac{4\pi}{11}), (\frac{6\pi}{11}, -\frac{2\pi}{11}), (\frac{6\pi}{11}, 0), (\frac{6\pi}{11}, \frac{\pi}{11}),$ $(\frac{6\pi}{11}, \frac{3\pi}{11}), (\frac{6\pi}{11}, \frac{4\pi}{11}), (\frac{6\pi}{11}, \frac{5\pi}{11})$
$[1014, 7]_\Delta$	$(\frac{6\pi}{13}, -\frac{5\pi}{13}), (\frac{6\pi}{13}, -\frac{3\pi}{13}), (\frac{6\pi}{13}, 0), (\frac{6\pi}{13}, \frac{\pi}{13}), (\frac{6\pi}{13}, \frac{2\pi}{13}), (\frac{6\pi}{13}, \frac{4\pi}{13}), (\frac{6\pi}{13}, \frac{6\pi}{13}),$ $(\frac{19\pi}{39}, -\frac{5\pi}{13}), (\frac{19\pi}{39}, -\frac{3\pi}{13}), (\frac{19\pi}{39}, 0), (\frac{19\pi}{39}, \frac{\pi}{13}), (\frac{19\pi}{39}, \frac{2\pi}{13}), (\frac{19\pi}{39}, \frac{4\pi}{13}),$ $(\frac{19\pi}{39}, \frac{6\pi}{13}), (\frac{20\pi}{39}, -\frac{5\pi}{13}), (\frac{20\pi}{39}, -\frac{3\pi}{13}), (\frac{20\pi}{39}, \frac{4\pi}{13}), (\frac{20\pi}{39}, \frac{6\pi}{13}), (\frac{20\pi}{39}, \frac{8\pi}{13}),$ $(\frac{7\pi}{13}, -\frac{3\pi}{13}), (\frac{7\pi}{13}, 0), (\frac{7\pi}{13}, \frac{\pi}{13}), (\frac{7\pi}{13}, \frac{2\pi}{13}), (\frac{7\pi}{13}, \frac{4\pi}{13}), (\frac{7\pi}{13}, \frac{6\pi}{13})$
$[1176, 243]_\Delta$	$(\frac{19\pi}{42}, -\frac{3\pi}{7}), (\frac{19\pi}{42}, -\frac{2\pi}{7}), (\frac{19\pi}{42}, -\frac{\pi}{7}), (\frac{19\pi}{42}, 0), (\frac{19\pi}{42}, \frac{\pi}{14}), (\frac{19\pi}{42}, \frac{3\pi}{14}),$ $(\frac{19\pi}{42}, \frac{5\pi}{14}), (\frac{19\pi}{42}, \frac{7\pi}{14}), (\frac{19\pi}{42}, \frac{9\pi}{14}), (\frac{19\pi}{42}, \frac{11\pi}{14}), (\frac{19\pi}{42}, \frac{13\pi}{14}), (\frac{19\pi}{42}, \frac{15\pi}{14}),$ $(\frac{\pi}{2}, -\frac{3\pi}{7}), (\frac{\pi}{2}, \frac{2\pi}{7}), (\frac{\pi}{2}, \frac{5\pi}{14}), (\frac{\pi}{2}, \frac{11\pi}{14}), (\frac{11\pi}{21}, \frac{3\pi}{7}), (\frac{11\pi}{21}, \frac{5\pi}{14}), (\frac{11\pi}{21}, \frac{9\pi}{14}),$ $(\frac{11\pi}{21}, \frac{13\pi}{14}), (\frac{23\pi}{42}, -\frac{3\pi}{7}), (\frac{23\pi}{42}, -\frac{2\pi}{7}), (\frac{23\pi}{42}, -\frac{\pi}{7}), (\frac{23\pi}{42}, 0), (\frac{23\pi}{42}, \frac{\pi}{14}), (\frac{23\pi}{42}, \frac{3\pi}{14}),$ $(\frac{23\pi}{42}, \frac{5\pi}{14}), (\frac{23\pi}{42}, \frac{7\pi}{14}), (\frac{23\pi}{42}, \frac{9\pi}{14}), (\frac{23\pi}{42}, \frac{11\pi}{14}), (\frac{23\pi}{42}, \frac{13\pi}{14}), (\frac{23\pi}{42}, \frac{15\pi}{14})$
$[1458, 659]_{\Delta'}, [1458, 663]$	$(\frac{13\pi}{27}, -\frac{2\pi}{9}), (\frac{13\pi}{27}, -\frac{\pi}{9}), (\frac{13\pi}{27}, 0), (\frac{13\pi}{27}, \frac{\pi}{3}), (\frac{13\pi}{27}, \frac{4\pi}{9}), (\frac{14\pi}{27}, -\frac{2\pi}{9}),$ $(\frac{14\pi}{27}, -\frac{\pi}{9}), (\frac{14\pi}{27}, 0), (\frac{14\pi}{27}, \frac{\pi}{3}), (\frac{14\pi}{27}, \frac{4\pi}{9}), (\frac{5\pi}{9}, -\frac{2\pi}{9}), (\frac{5\pi}{9}, \frac{\pi}{9}), (\frac{5\pi}{9}, \frac{4\pi}{9})$
$[1536, 408544632]_\Delta$	$(\frac{11\pi}{24}, -\frac{7\pi}{16}), (\frac{11\pi}{24}, -\frac{5\pi}{16}), (\frac{11\pi}{24}, -\frac{\pi}{16}), (\frac{11\pi}{24}, \frac{3\pi}{16}), (\frac{23\pi}{48}, -\frac{5\pi}{16}),$ $(\frac{23\pi}{48}, -\frac{3\pi}{16}), (\frac{23\pi}{48}, 0), (\frac{23\pi}{48}, \frac{\pi}{16}), (\frac{23\pi}{48}, \frac{3\pi}{16}), (\frac{23\pi}{48}, \frac{5\pi}{16}), (\frac{23\pi}{48}, \frac{7\pi}{16}),$ $(\frac{23\pi}{48}, \frac{9\pi}{16}), (\frac{23\pi}{48}, \frac{11\pi}{16}), (\frac{25\pi}{48}, -\frac{5\pi}{16}), (\frac{25\pi}{48}, -\frac{3\pi}{16}),$ $(\frac{25\pi}{48}, 0), (\frac{25\pi}{48}, \frac{\pi}{16}), (\frac{25\pi}{48}, \frac{3\pi}{16}), (\frac{25\pi}{48}, \frac{5\pi}{16}), (\frac{25\pi}{48}, \frac{7\pi}{16}), (\frac{25\pi}{48}, \frac{9\pi}{16}),$ $(\frac{13\pi}{24}, -\frac{7\pi}{16}), (\frac{13\pi}{24}, -\frac{5\pi}{16}), (\frac{13\pi}{24}, -\frac{\pi}{16}), (\frac{13\pi}{24}, \frac{3\pi}{16}), (\frac{13\pi}{24}, \frac{5\pi}{16}),$ $(\frac{13\pi}{24}, \frac{7\pi}{16}), (\frac{13\pi}{24}, \frac{9\pi}{16}), (\frac{13\pi}{24}, \frac{11\pi}{16}), (\frac{13\pi}{24}, \frac{13\pi}{16}), (\frac{13\pi}{24}, \frac{15\pi}{16})$
$[1734, 5]_\Delta$	$(\frac{23\pi}{51}, -\frac{8\pi}{17}), (\frac{23\pi}{51}, -\frac{6\pi}{17}), (\frac{23\pi}{51}, -\frac{4\pi}{17}), (\frac{23\pi}{51}, -\frac{2\pi}{17}), (\frac{23\pi}{51}, \frac{\pi}{17}),$ $(\frac{23\pi}{51}, \frac{3\pi}{17}), (\frac{23\pi}{51}, \frac{5\pi}{17}), (\frac{23\pi}{51}, \frac{7\pi}{17}), (\frac{8\pi}{17}, -\frac{8\pi}{17}), (\frac{8\pi}{17}, -\frac{7\pi}{17}),$ $(\frac{8\pi}{17}, -\frac{6\pi}{17}), (\frac{8\pi}{17}, -\frac{5\pi}{17}), (\frac{8\pi}{17}, -\frac{4\pi}{17}), (\frac{8\pi}{17}, -\frac{3\pi}{17}), (\frac{8\pi}{17}, -\frac{2\pi}{17}), (\frac{8\pi}{17}, -\frac{\pi}{17}),$ $(\frac{8\pi}{17}, 0), (\frac{25\pi}{51}, -\frac{8\pi}{17}), (\frac{25\pi}{51}, -\frac{6\pi}{17}), (\frac{25\pi}{51}, -\frac{4\pi}{17}), (\frac{25\pi}{51}, -\frac{2\pi}{17}), (\frac{25\pi}{51}, \frac{\pi}{17}),$ $(\frac{25\pi}{51}, \frac{3\pi}{17}), (\frac{26\pi}{51}, -\frac{8\pi}{17}), (\frac{26\pi}{51}, -\frac{6\pi}{17}), (\frac{26\pi}{51}, -\frac{4\pi}{17}), (\frac{26\pi}{51}, -\frac{2\pi}{17}),$ $(\frac{26\pi}{51}, \frac{\pi}{17}), (\frac{26\pi}{51}, \frac{3\pi}{17}), (\frac{9\pi}{17}, -\frac{8\pi}{17}), (\frac{9\pi}{17}, -\frac{7\pi}{17}), (\frac{9\pi}{17}, -\frac{6\pi}{17}), (\frac{9\pi}{17}, -\frac{5\pi}{17}),$ $(\frac{9\pi}{17}, -\frac{4\pi}{17}), (\frac{9\pi}{17}, -\frac{3\pi}{17}), (\frac{9\pi}{17}, -\frac{2\pi}{17}), (\frac{9\pi}{17}, -\frac{\pi}{17}), (\frac{9\pi}{17}, 0), (\frac{28\pi}{51}, -\frac{8\pi}{17}),$ $(\frac{28\pi}{51}, -\frac{6\pi}{17}), (\frac{28\pi}{51}, -\frac{4\pi}{17}), (\frac{28\pi}{51}, -\frac{2\pi}{17}), (\frac{28\pi}{51}, \frac{\pi}{17}), (\frac{28\pi}{51}, \frac{3\pi}{17}),$ $(\frac{28\pi}{51}, \frac{5\pi}{17}), (\frac{28\pi}{51}, \frac{7\pi}{17}), (\frac{28\pi}{51}, \frac{9\pi}{17}), (\frac{28\pi}{51}, \frac{11\pi}{17}), (\frac{28\pi}{51}, \frac{13\pi}{17}), (\frac{28\pi}{51}, \frac{15\pi}{17}),$ $(\frac{28\pi}{51}, \frac{17\pi}{17})$

Table 1: The predictions for PMNS matrix of the form $U^{J(a)}$, where the first column shows the group identification in GAP system, and the second column displays the achievable values of the parameters φ_1 and φ_2 . We have shown at most two representatives flavor symmetry groups in the first column. If there is only one group predicting the corresponding values of φ_1 and φ_2 in the second column, this unique group would be listed. The full results of our analysis are provided at the website [45]. The subscripts Δ and Δ' indicate that the corresponding groups belong to the type D group series $D_{n,n}^{(0)} \cong \Delta(6n^2)$ and $D_{9n',3n'}^{(1)} \cong (Z_{9n'} \times Z_{3n'}) \rtimes S_3$, respectively.

Case C_{ab}	(K_1, K_2, K_3)	$(R'_{11}, R'_{12}, R'_{13})$	W_{ab}
$a = 1, b = 2$	$(+, +, \pm)$	$(\cos \eta, \sin \eta, 0)$	$\frac{\sqrt{m_1 m_2} (m_1 - m_2) \sin \eta \cos \eta}{m_1 \cos^2 \eta + m_2 \sin^2 \eta}$
	$(+, -, \pm)$	$(\cosh \eta, \sinh \eta, 0)$	$\frac{\sqrt{m_1 m_2} (m_1 + m_2) \sinh \eta \cosh \eta}{m_1 \cosh^2 \eta + m_2 \sinh^2 \eta}$
	$(-, +, \pm)$	$(\sinh \eta, \cosh \eta, 0)$	$-\frac{\sqrt{m_1 m_2} (m_1 + m_2) \sinh \eta \cosh \eta}{m_1 \sinh^2 \eta + m_2 \cosh^2 \eta}$
$a = 1, b = 3$	$(+, \pm, +)$	$(\cos \eta, 0, \sin \eta)$	$\frac{\sqrt{m_1 m_3} (m_1 - m_3) \sin \eta \cos \eta}{m_1 \cos^2 \eta + m_3 \sin^2 \eta}$
	$(+, \pm, -)$	$(\cosh \eta, 0, \sinh \eta)$	$\frac{\sqrt{m_1 m_3} (m_1 + m_3) \sinh \eta \cosh \eta}{m_1 \cosh^2 \eta + m_3 \sinh^2 \eta}$
	$(-, \pm, +)$	$(\sinh \eta, 0, \cosh \eta)$	$-\frac{\sqrt{m_1 m_3} (m_1 + m_3) \sinh \eta \cosh \eta}{m_1 \sinh^2 \eta + m_3 \cosh^2 \eta}$
$a = 2, b = 3$	$(\pm, +, +)$	$(0, \cos \eta, \sin \eta)$	$\frac{\sqrt{m_2 m_3} (m_2 - m_3) \sin \eta \cos \eta}{m_2 \cos^2 \eta + m_3 \sin^2 \eta}$
	$(\pm, +, -)$	$(0, \cosh \eta, \sinh \eta)$	$\frac{\sqrt{m_2 m_3} (m_2 + m_3) \sinh \eta \cosh \eta}{m_2 \cosh^2 \eta + m_3 \sinh^2 \eta}$
	$(\pm, -, +)$	$(0, \sinh \eta, \cosh \eta)$	$-\frac{\sqrt{m_2 m_3} (m_2 + m_3) \sinh \eta \cosh \eta}{m_2 \sinh^2 \eta + m_3 \cosh^2 \eta}$

Table 2: The parametrization of the first column of R' -matrix and the corresponding expressions of W_{12} , W_{13} and W_{23} in the three interesting cases C_{12} , C_{13} and C_{23} .

range [44]. As regards the CP invariants, we find

$$\begin{aligned}
|J_{CP}| &= \frac{1}{6\sqrt{6}} |\sin 2\theta \sin 3\varphi_1 \sin \varphi_2|, \\
|I_1| &= \frac{1}{9} \left| \cos \varphi_1 \sin \varphi_2 \left(4 \cos 2\theta \cos \varphi_1 \cos \varphi_2 - \sqrt{2} \sin 2\theta \cos 2\varphi_1 \right) \right|, \\
|I_2| &= \frac{2\sqrt{2}}{9} \left| \sin^2 \varphi_1 \sin \varphi_2 \left(\sqrt{2} \sin^2 \theta \cos \varphi_2 + \sin 2\theta \cos \varphi_1 \right) \right|.
\end{aligned} \tag{3.40}$$

For this mixing pattern $U^{I(b)}$, the effective Majorana mass $|m_{ee}|$ in $0\nu\beta\beta$ is given by

$$\begin{aligned}
|m_{ee}| &= \frac{1}{3} \left| 2m_3 \sin^2 \varphi_1 + q_1 m_2 \left(e^{i\varphi_2} \cos \theta - \sqrt{2} \cos \varphi_1 \sin \theta \right)^2 \right. \\
&\quad \left. + q_2 m_1 \left(\sqrt{2} \cos \theta \cos \varphi_1 + e^{i\varphi_2} \sin \theta \right)^2 \right|,
\end{aligned} \tag{3.41}$$

where $q_1, q_2 = \pm 1$ appears due to the undetermined CP parity of the neutrino states encoded in the matrix Q_ν . In the limit of $|G_f| \rightarrow \infty$, where $|G_f|$ represents the order of G_f , φ_1 and φ_2 tends to be continuous parameters. Then one can almost reproduce the whole regions of $|m_{ee}|$ obtained by varying the oscillation parameters over their current 3σ global ranges, as shown in figure 1. For the smallest group $G_f = [649, 259]$, the admissible values of φ_1 and φ_2 are $(\varphi_1, \varphi_2) = (\frac{\pi}{18}, -\frac{\pi}{6}), (\frac{\pi}{18}, 0), (\frac{\pi}{18}, \frac{\pi}{3}), (\frac{\pi}{18}, \frac{\pi}{2}), (\frac{17\pi}{18}, -\frac{\pi}{6}), (\frac{17\pi}{18}, 0), (\frac{17\pi}{18}, \frac{\pi}{3})$ and $(\frac{17\pi}{18}, \frac{\pi}{2})$. The corresponding predictions for the $0\nu\beta\beta$ decay effective mass $|m_{ee}|$ versus the lightest neutrino mass m_{lightest} are plotted in figure 1. We see that $|m_{ee}|$ is close to 0.029eV or 0.042eV for IO neutrino mass spectrum, which are within the future sensitivity of planned $0\nu\beta\beta$ decay experiments. On the other hand, $|m_{ee}|$ is always bigger than 0.7×10^{-4} eV in the case of NO spectrum.

Now we proceed to discuss the predictions for leptogenesis. The bilinear invariant I_{12}^α can be read

(φ_1, φ_2)	θ_{bf}/π	χ^2_{min}	$\sin^2 \theta_{13}$	$\sin^2 \theta_{12}$	$\sin^2 \theta_{23}$	δ_{CP}/π	α_{21}/π (mod 1)	α'_{31}/π (mod 1)	(K_1, K_2, K_3)
$(\frac{\pi}{18}, -\frac{\pi}{6})$	0.014	11.065 [3.989]	0.0201	0.304	0.601	0.984	0.656	0.010	$(-, +, \pm)$ [[$(-, +, \pm)$]]
	0.367								$(+, -, \pm)$ [[$(+, +, \pm), (+, -, \pm)$]]
$(\frac{\pi}{18}, 0)$	0.012	11.065 [3.989]	0.0201	0.304	0.601	1	0	0	—
	0.384					0	0	0	—
$(\frac{\pi}{18}, \frac{\pi}{3})$	0.026	11.065 [3.989]	0.0201	0.304	0.601	1.049	0.701	0.969	$(+, -, \pm)$ [[$(+, +, \pm), (+, -, \pm), (-, +, \pm)$]]
	0.285					1.629	0.299	0.686	$(+, -, \pm)$ [[$(+, +, \pm), (+, -, \pm), (-, +, \pm)$]]
$(\frac{\pi}{18}, \frac{\pi}{2})$	0	18.807 [11.731]	0.0201	0.340	0.601	1	0	0	$(+, -, \pm), (-, +, \pm)$ [[$(+, +, \pm), (-, +, \pm)$]]
$(\frac{17\pi}{18}, -\frac{\pi}{6})$	0.633	6.432 [26.835]	0.0201	0.304	0.399	1.132	0.344	0.207	$(+, -, \pm), (-, +, \pm)$ [[$(+, +, \pm), (-, +, \pm)$]]
	0.986					1.984	0.656	0.010	$(-, +, \pm)$ [[$(-, +, \pm)$]]
$(\frac{17\pi}{18}, 0)$	0.616	6.432 [26.835]	0.0201	0.304	0.399	1	0	0	—
	0.988					0	0	0	—
$(\frac{17\pi}{18}, \frac{\pi}{3})$	0.715	6.432 [26.835]	0.0201	0.304	0.399	0.629	0.299	0.686	$(+, -, \pm), (-, +, \pm)$ [[$(+, +, \pm), (-, +, \pm)$]]
	0.974					0.049	0.701	0.969	$(+, -, \pm)$ [[$(+, +, \pm), (+, -, \pm), (-, +, \pm)$]]
$(\frac{17\pi}{18}, \frac{\pi}{2})$	0	14.174 [34.576]	0.0201	0.340	0.399	0	0	0	$(+, -, \pm)$ [[$(+, +, \pm), (+, -, \pm), (-, +, \pm)$]]

Table 3: Results of the χ^2 analysis for case I(b) with the flavor symmetry $G_f = [649, 259]$. As shown in table 4, the experimentally measured values of the mixing angles can be accommodated in the case of $(\varphi_1, \varphi_2) = (\frac{\pi}{18}, -\frac{\pi}{6}), (\frac{\pi}{18}, 0), (\frac{\pi}{18}, \frac{\pi}{3}), (\frac{\pi}{18}, \frac{\pi}{2}), (\frac{17\pi}{18}, -\frac{\pi}{6}), (\frac{17\pi}{18}, 0), (\frac{17\pi}{18}, \frac{\pi}{3})$ and $(\frac{17\pi}{18}, \frac{\pi}{2})$. We display the best fit value θ_{bf} for θ , and χ^2_{min} is the smallest value of χ^2 that can be obtained at the best fit value θ_{bf} . The mixing angles and the CP violating phases for $\theta = \theta_{\text{bf}}$ are presented as well. Note that the CP parity matrix Q_ν can shift the Majorana phases α_{21} and α'_{31} by π . In the last column we give the values of $K_{1,2,3}$ for which the observed baryon asymmetry can be generated via leptogenesis. The values in the square brackets are the corresponding results for the case of IO mass spectrum. The net baryon asymmetry can not be generated for $\varphi_2 = 0, \pi$.

out as follow

$$\begin{aligned}
I_{12}^e &= -\frac{\sqrt{2}}{3} \cos \varphi_1 \sin \varphi_2, \\
I_{12}^\mu &= \frac{\sqrt{2}}{3} \sin \left(\frac{\pi}{6} - \varphi_1 \right) \sin \varphi_2, \\
I_{12}^\tau &= \frac{\sqrt{2}}{3} \sin \left(\frac{\pi}{6} + \varphi_1 \right) \sin \varphi_2,
\end{aligned} \tag{3.42}$$

which are generally nonzero except $\varphi_2 = 0, \pi$. The value of baryon asymmetry can be straightforwardly calculated from any given values of φ_1 and φ_2 . We shall study the smallest viable flavor symmetry [649, 259] for illustration. The results of the χ^2 analysis are summarized in table 3. We display the values of the mixing angles and CP phases at θ_{bf} , the best fit points for which the χ^2 function has a global minimum χ^2_{min} . Obviously the mixing angles can be in accordance with the experimental data for particular values of θ . The leptogenesis asymmetries ϵ_α are vanishing for $(\varphi_1, \varphi_2) = (\pi/18, 0), (17\pi/18, 0)$. For the remaining six admissible values of φ_1 and φ_2 , the variations of Y_B as a function of η are plotted in figures (3-8). We see that the correct value of Y_B can be reproduced for certain values of η and $K_{1,2,3}$.

Group Id	(φ_1, φ_2)
$[648, 259]_{\Delta'}, [648, 260]$	$(\frac{\pi}{18}, -\frac{\pi}{6}), (\frac{\pi}{18}, 0), (\frac{\pi}{18}, \frac{\pi}{3}), (\frac{\pi}{18}, \frac{\pi}{2}), (\frac{17\pi}{18}, -\frac{\pi}{6}), (\frac{17\pi}{18}, 0), (\frac{17\pi}{18}, \frac{\pi}{3}), (\frac{17\pi}{18}, \frac{\pi}{2})$
$[726, 5]_{\Delta}, [1452, 23]$	$(\frac{2\pi}{33}, -\frac{2\pi}{11}), (\frac{2\pi}{33}, 0), (\frac{2\pi}{33}, \frac{\pi}{11}), (\frac{2\pi}{33}, \frac{3\pi}{11}), (\frac{2\pi}{33}, \frac{4\pi}{11}), (\frac{2\pi}{33}, \frac{5\pi}{11}), (\frac{31\pi}{33}, -\frac{2\pi}{11}), (\frac{31\pi}{33}, 0), (\frac{31\pi}{33}, \frac{\pi}{11}), (\frac{31\pi}{33}, \frac{3\pi}{11}), (\frac{31\pi}{33}, \frac{4\pi}{11}), (\frac{31\pi}{33}, \frac{5\pi}{11})$
$[1734, 5]_{\Delta}$	$(\frac{\pi}{17}, -\frac{8\pi}{17}), (\frac{\pi}{17}, -\frac{6\pi}{17}), (\frac{\pi}{17}, 0), (\frac{\pi}{17}, \frac{\pi}{17}), (\frac{\pi}{17}, \frac{2\pi}{17}), (\frac{\pi}{17}, \frac{3\pi}{17}), (\frac{\pi}{17}, \frac{4\pi}{17}), (\frac{\pi}{17}, \frac{5\pi}{17}), (\frac{\pi}{17}, \frac{7\pi}{17}), (\frac{16\pi}{17}, -\frac{8\pi}{17}), (\frac{16\pi}{17}, -\frac{6\pi}{17}), (\frac{16\pi}{17}, 0), (\frac{16\pi}{17}, \frac{\pi}{17}), (\frac{16\pi}{17}, \frac{2\pi}{17}), (\frac{16\pi}{17}, \frac{3\pi}{17}), (\frac{16\pi}{17}, \frac{4\pi}{17}), (\frac{16\pi}{17}, \frac{5\pi}{17}), (\frac{16\pi}{17}, \frac{7\pi}{17})$

Table 4: The predictions for PMNS matrix of the form $U^{I(b)}$, where the first column shows the group identification in GAP system, and the second column displays the achievable values of the parameters φ_1 and φ_2 . We have shown at most two representatives flavor symmetry groups in the first column. If there is only one group predicting the corresponding values of φ_1 and φ_2 in the second column, this unique group would be listed. The full results of our analysis are provided at the website [45]. The subscripts Δ and Δ' indicate that the corresponding groups belong to the type D group series $D_{n,n}^{(0)} \cong \Delta(6n^2)$ and $D_{9n',3n'}^{(1)} \cong (Z_{9n'} \times Z_{3n'}) \rtimes S_3$, respectively.

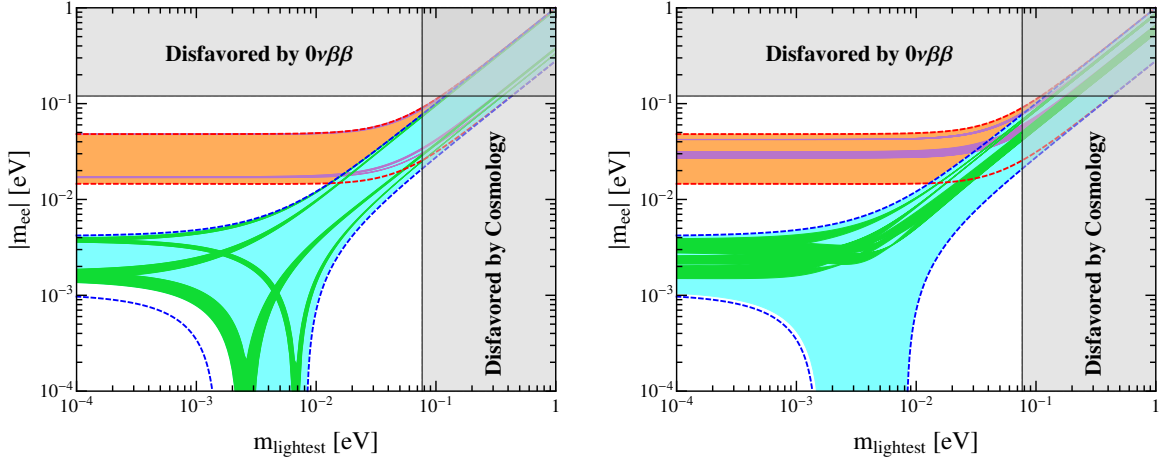


Figure 1: Predictions for the $0\nu\beta\beta$ decay effective mass $|m_{ee}|$ with respect to the lightest neutrino mass m_{lightest} in the case I. The left and right panels are for the mixing patterns $U^{I(a)}$ and $U^{I(b)}$ respectively. The red (blue) dashed lines indicate the most general allowed regions for IO (NO) spectrum obtained by varying the mixing parameters within their 3σ ranges [44]. The orange (cyan) areas denote the achievable values of $|m_{ee}|$ when φ_1 and φ_2 are taken to be free continuous parameters in the case of IO (NO). The purple and green regions are the theoretical predictions of the smallest flavor symmetry group which can generate these two mixing patterns. Note that the purple (green) region overlaps the orange (cyan) one. The present most stringent upper limits $|m_{ee}| < 0.120$ eV from EXO-200 [57,58] and KamLAND-ZEN [59] is shown by horizontal grey band. The vertical grey exclusion band is the current limit on m_{lightest} from the cosmological data of $\sum m_i < 0.230$ eV by the Planck collaboration [60].

Case II

$$U^{II(a)} = \frac{1}{\sqrt{3}} \begin{pmatrix} e^{i\varphi_1} & 1 & e^{i\varphi_2} \\ \omega e^{i\varphi_1} & 1 & \omega^2 e^{i\varphi_2} \\ \omega^2 e^{i\varphi_1} & 1 & \omega e^{i\varphi_2} \end{pmatrix} S_{13}(\theta) Q_\nu^\dagger, \quad (3.43)$$

$$U^{II(b)} = \frac{1}{\sqrt{3}} \begin{pmatrix} e^{i\varphi_1} & 1 & e^{i\varphi_2} \\ \omega^2 e^{i\varphi_1} & 1 & \omega e^{i\varphi_2} \\ \omega e^{i\varphi_1} & 1 & \omega^2 e^{i\varphi_2} \end{pmatrix} S_{13}(\theta) Q_\nu^\dagger, \quad (3.44)$$

where $\omega = e^{i2\pi/3}$. The viable values of φ_1 and φ_2 and corresponding representative flavor symmetry groups are listed in table 5. Please see the website [45] for the full results. The smallest group which can describe the experimentally measured values of the mixing angles for certain values of θ is S_4 . The mixing pattern in Eq. (3.44) results from the permutation of the second and third rows of the PMNS mixing matrix in Eq. (3.43). The second column of $U^{II(a)}$ and $U^{II(b)}$ are

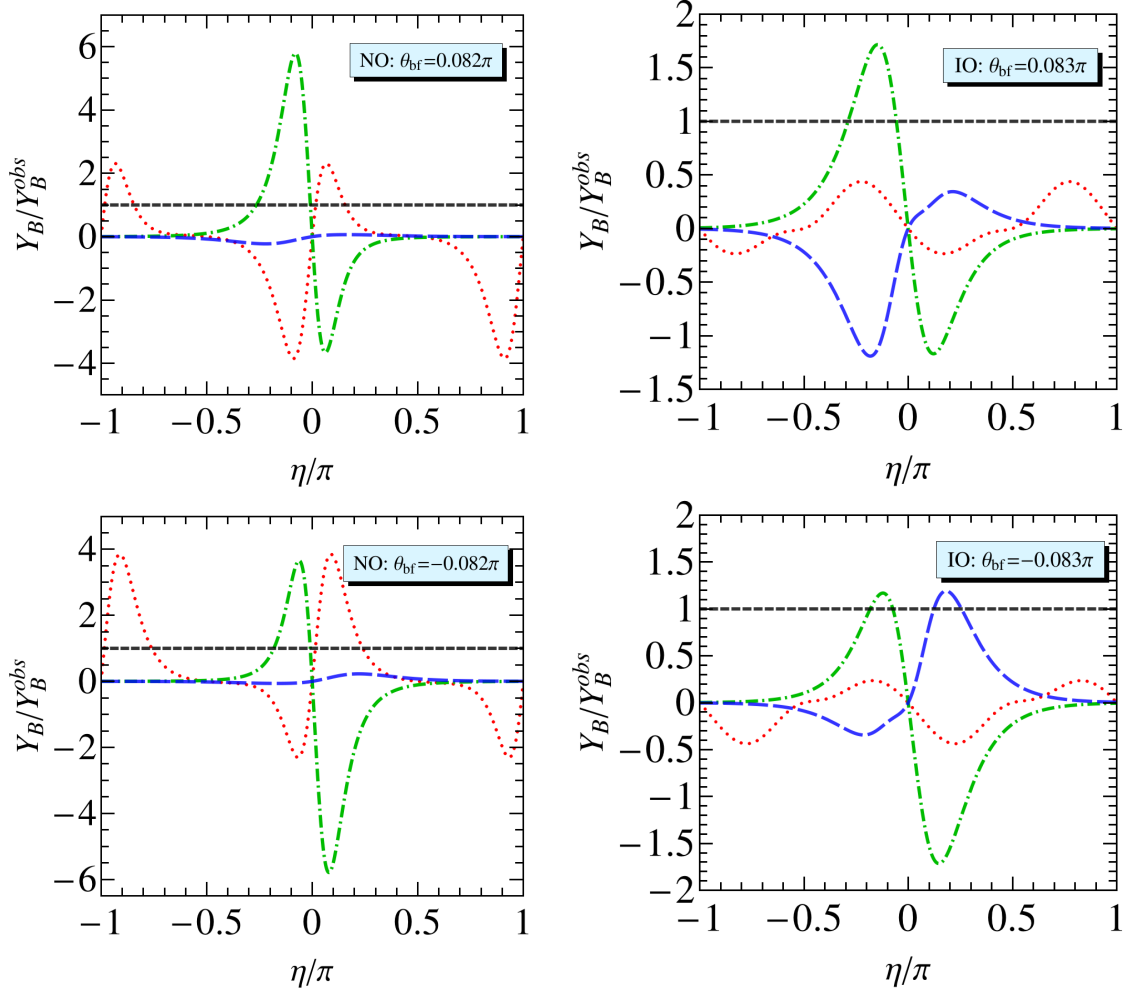


Figure 2: The prediction for Y_B/Y_B^{obs} as a function of η in case I(a) with $(\varphi_1, \varphi_2) = (\frac{\pi}{2}, \frac{\pi}{2})$, where θ_{bf} is the best fit value of θ . Note that minor difference in θ_{bf} is obtained for NO and IO spectrums, because the best fit value as well as 1σ error of $\sin^2 \theta_{13}$ and $\sin^2 \theta_{23}$ slightly depend on the mass ordering [44]. We choose $M_1 = 5 \times 10^{11}$ GeV and the lightest neutrino mass m_1 (or m_3) = 0.01eV. The red dotted, green dot-dashed, blue dashed lines correspond to $(K_1, K_2, K_3) = (\pm, +, +), (\pm, +, -)$ and $(\pm, -, +)$ respectively. The experimentally observed value Y_B^{obs} is represented by the horizontal black dashed line.

$(1, 1, 1)^T/\sqrt{3}$, and consequently they are the trimaximal pattern. We can extract the following results for the lepton mixing angles

$$\begin{aligned}
\sin^2 \theta_{13} &= \frac{1}{3} [1 + \sin 2\theta \cos(\varphi_2 - \varphi_1)], \\
\sin^2 \theta_{12} &= \frac{1}{2 - \sin 2\theta \cos(\varphi_2 - \varphi_1)}, \\
\sin^2 \theta_{23} &= \frac{1 - \sin 2\theta \sin(\varphi_2 - \varphi_1 + \pi/6)}{2 - \sin 2\theta \cos(\varphi_2 - \varphi_1)} \quad \text{for } U^{II(a)}, \\
\sin^2 \theta_{23} &= \frac{1 + \sin 2\theta \sin(\varphi_2 - \varphi_1 - \pi/6)}{2 - \sin 2\theta \cos(\varphi_2 - \varphi_1)} \quad \text{for } U^{II(b)},
\end{aligned} \tag{3.45}$$

Therefore the solar and the reactor mixing angles fulfill the well known sum rule

$$3 \cos^2 \theta_{13} \sin^2 \theta_{12} = 1. \tag{3.46}$$

Hence the solar mixing angle admits a lower bound $\sin^2 \theta_{12} > 1/3$. Using for $\sin^2 \theta_{13}$ its 3σ range $0.0188 \leq \sin^2 \theta_{13} \leq 0.0251$ [44], we find $0.340 \leq \sin^2 \theta_{12} \leq 0.342$. The JUNO experiment will be capable of reducing the error of $\sin^2 \theta_{12}$ to about 0.1° or around 0.3% [61]. Future long

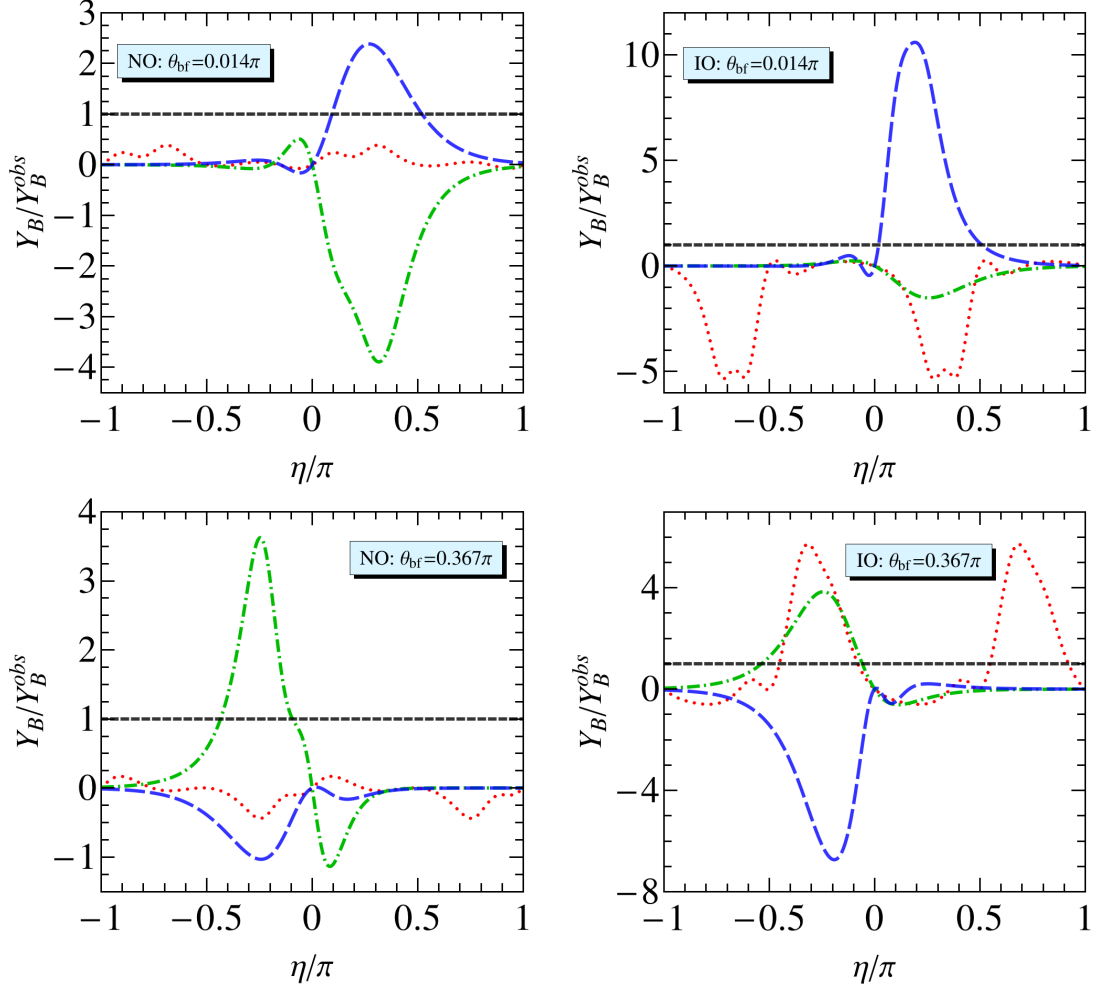


Figure 3: The prediction for Y_B/Y_B^{obs} as a function of η in case I(b) with $(\varphi_1, \varphi_2) = (\frac{\pi}{18}, -\frac{\pi}{6})$, where θ_{bf} is the best fit value of θ . We choose $M_1 = 5 \times 10^{11}$ GeV and the lightest neutrino mass m_1 (or m_3) = 0.01eV. The red dotted, green dot-dashed, blue dashed lines correspond to $(K_1, K_2, K_3) = (+, +, \pm), (+, -, \pm)$ and $(-, +, \pm)$ respectively. The experimentally observed value Y_B^{obs} is represented by the horizontal black dashed line.

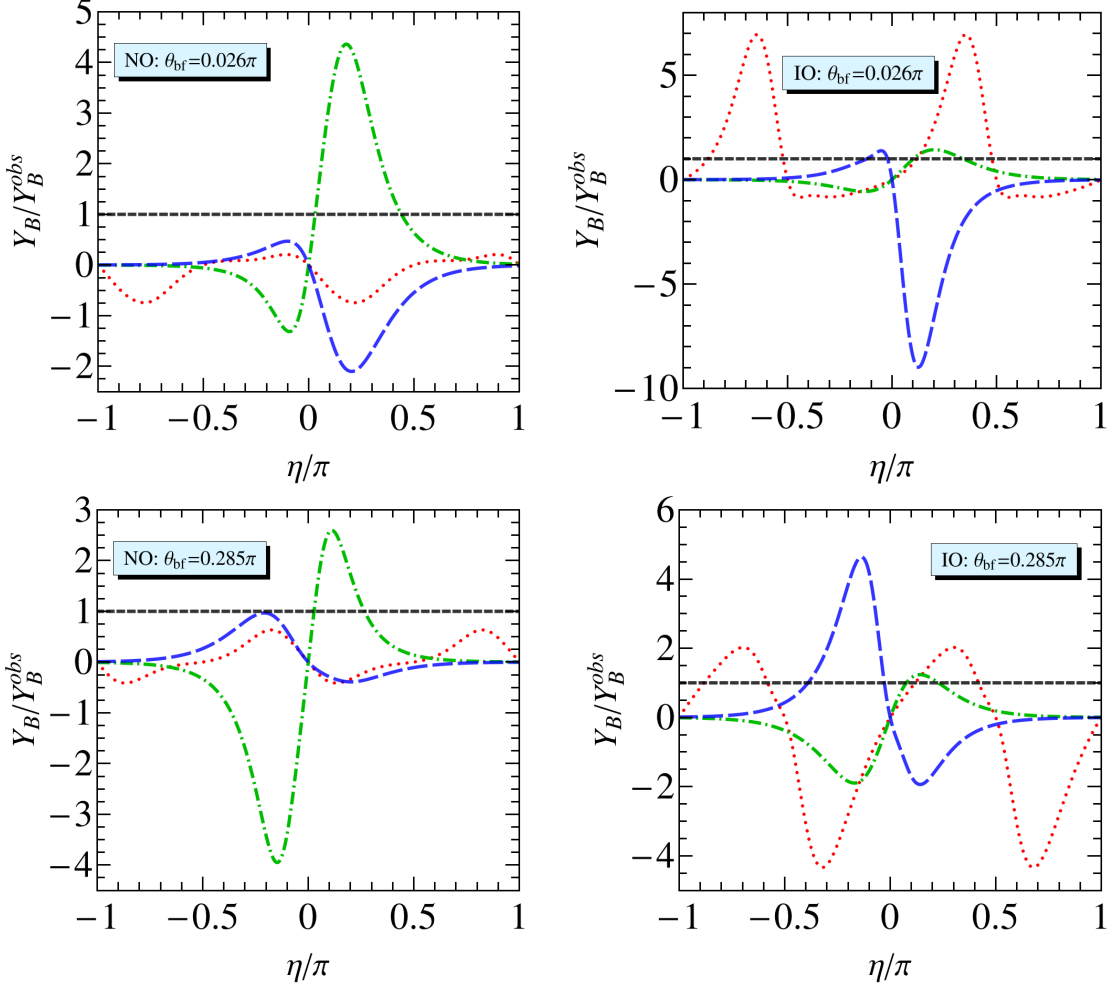


Figure 4: The prediction for Y_B/Y_B^{obs} as a function of η in case I(b) with $(\varphi_1, \varphi_2) = (\frac{\pi}{18}, \frac{\pi}{3})$, where θ_{bf} is the best fit value of θ . We choose $M_1 = 5 \times 10^{11}$ GeV and the lightest neutrino mass m_1 (or m_3) = 0.01eV. The red dotted, green dot-dashed, blue dashed lines correspond to $(K_1, K_2, K_3) = (+, +, \pm), (+, -, \pm)$ and $(-, +, \pm)$ respectively. The experimentally observed value Y_B^{obs} is represented by the horizontal black dashed line.

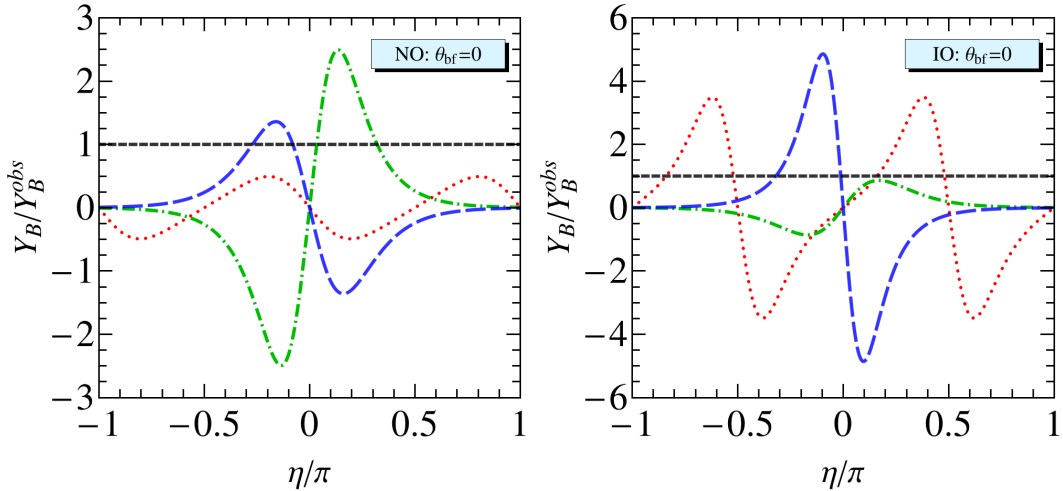


Figure 5: The prediction for Y_B/Y_B^{obs} as a function of η in case I(b) with $(\varphi_1, \varphi_2) = (\frac{\pi}{18}, \frac{\pi}{2})$, where θ_{bf} is the best fit value of θ . We choose $M_1 = 5 \times 10^{11}$ GeV and the lightest neutrino mass m_1 (or m_3) = 0.01eV. The red dotted, green dot-dashed, blue dashed lines correspond to $(K_1, K_2, K_3) = (+, +, \pm), (+, -, \pm)$ and $(-, +, \pm)$ respectively. The experimentally observed value Y_B^{obs} is represented by the horizontal black dashed line.

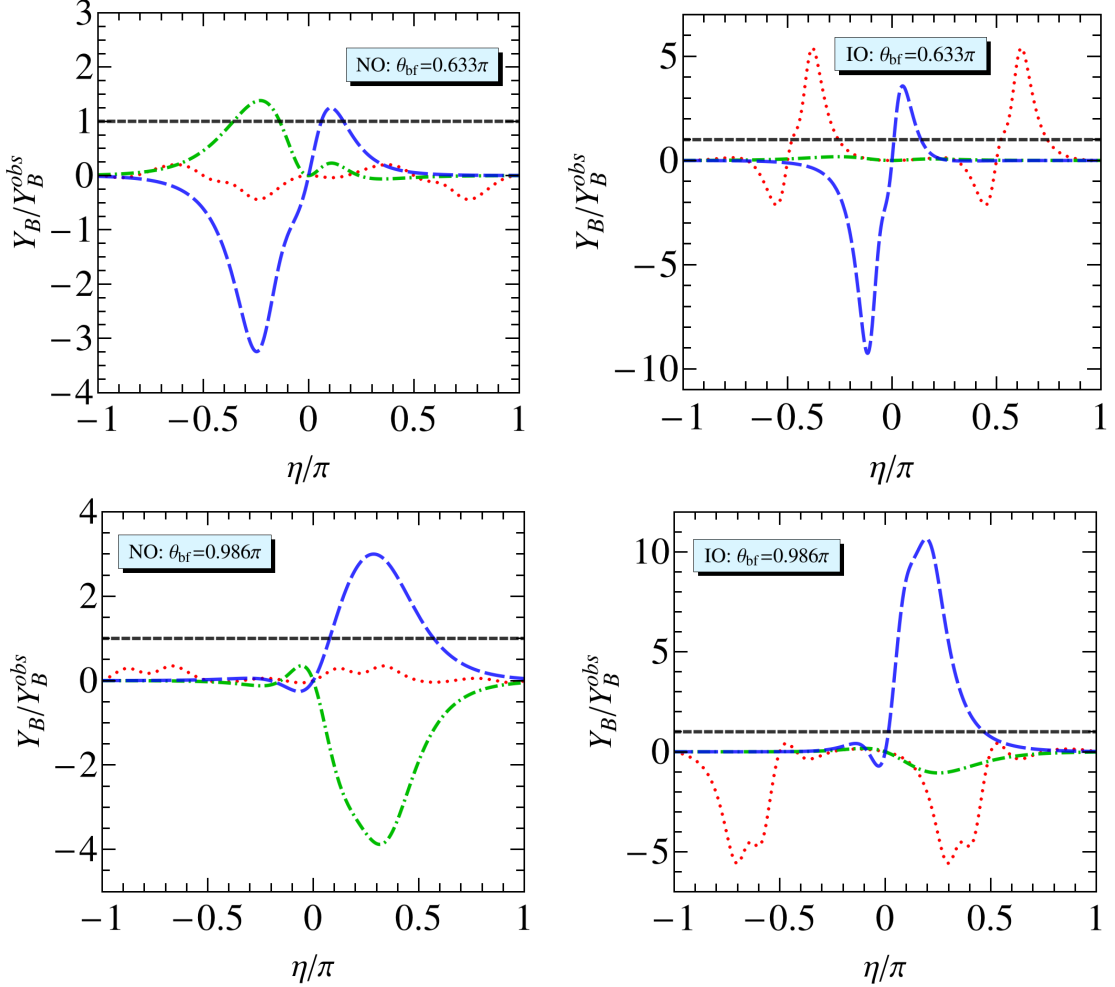


Figure 6: The prediction for Y_B/Y_B^{obs} as a function of η in case I(b) with $(\varphi_1, \varphi_2) = (\frac{17\pi}{18}, -\frac{\pi}{6})$, where θ_{bf} is the best fit value of θ . We choose $M_1 = 5 \times 10^{11}$ GeV and the lightest neutrino mass m_1 (or m_3) = 0.01eV. The red dotted, green dot-dashed, blue dashed lines correspond to $(K_1, K_2, K_3) = (+, +, \pm), (+, -, \pm)$ and $(-, +, \pm)$ respectively. The experimentally observed value Y_B^{obs} is represented by the horizontal black dashed line.

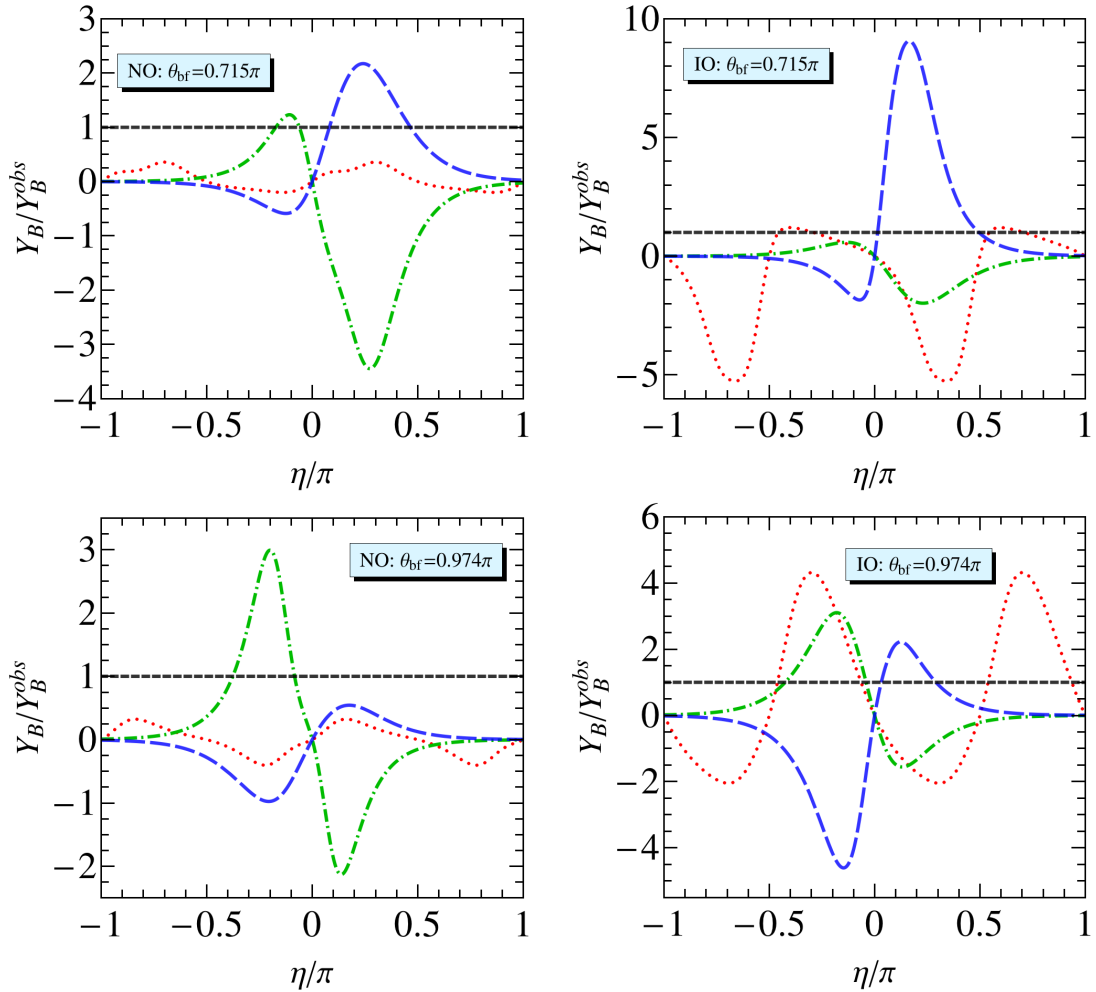


Figure 7: The prediction for Y_B/Y_B^{obs} as a function of η in case I(b) with $(\varphi_1, \varphi_2) = (\frac{17\pi}{18}, \frac{\pi}{3})$, where θ_{bf} is the best fit value of θ . We choose $M_1 = 5 \times 10^{11}$ GeV and the lightest neutrino mass m_1 (or m_3) = 0.01eV. The red dotted, green dot-dashed, blue dashed lines correspond to $(K_1, K_2, K_3) = (+, +, \pm), (+, -, \pm)$ and $(-, +, \pm)$ respectively. The experimentally observed value Y_B^{obs} is represented by the horizontal black dashed line.

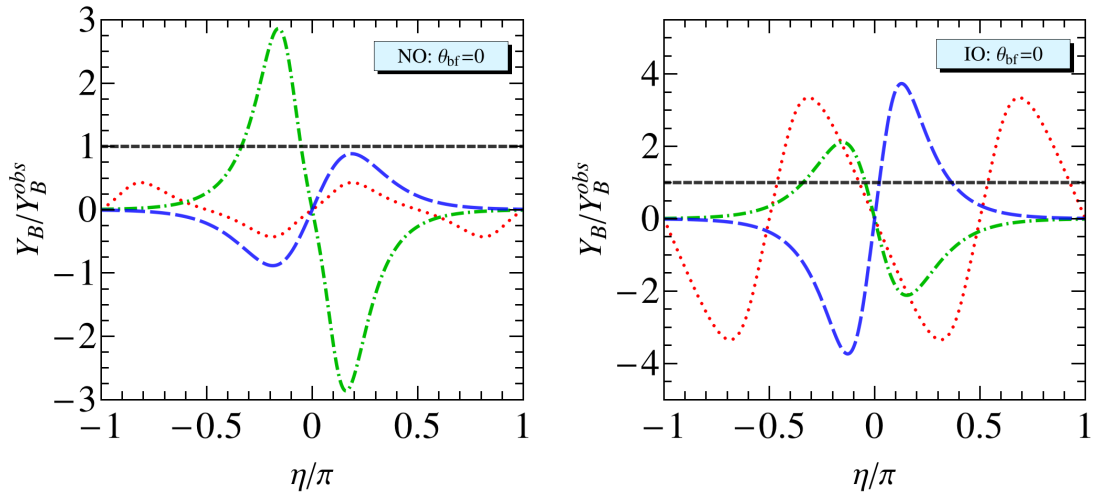


Figure 8: The prediction for Y_B/Y_B^{obs} as a function of η in case I(b) with $(\varphi_1, \varphi_2) = (\frac{17\pi}{18}, \frac{\pi}{2})$, where θ_{bf} is the best fit value of θ . We choose $M_1 = 5 \times 10^{11}$ GeV and the lightest neutrino mass m_1 (or m_3) = 0.01eV. The red dotted, green dot-dashed, blue dashed lines correspond to $(K_1, K_2, K_3) = (+, +, \pm), (+, -, \pm)$ and $(-, +, \pm)$ respectively. The experimentally observed value Y_B^{obs} is represented by the horizontal black dashed line.

baseline experiments such as DUNE [62] and Hyper-Kamiokande [63] can also make very precise measurements of the solar mixing angle. If significant deviations from $1/3$ of $\sin^2 \theta_{12}$ were detected, this mixing pattern would be ruled out. Moreover, the reactor mixing angle and the atmospheric mixing angle are related as follow

$$\begin{aligned} \frac{3 \cos^2 \theta_{13} \sin^2 \theta_{23} - 1}{1 - 3 \sin^2 \theta_{13}} &= \frac{1}{2} + \frac{\sqrt{3}}{2} \tan(\varphi_2 - \varphi_1), \quad \text{for } U^{II(a)}, \\ \frac{3 \cos^2 \theta_{13} \sin^2 \theta_{23} - 1}{1 - 3 \sin^2 \theta_{13}} &= \frac{1}{2} - \frac{\sqrt{3}}{2} \tan(\varphi_2 - \varphi_1), \quad \text{for } U^{II(b)}. \end{aligned} \quad (3.47)$$

For the mixing matrices $U^{II(a)}$ and $U^{II(b)}$, the CP invariants take the form

$$\begin{aligned} |J_{CP}| &= \frac{1}{6\sqrt{3}} |\cos 2\theta|, \\ |I_1| &= \frac{2}{9} |(\cos \theta \cos \varphi_1 - \sin \theta \cos \varphi_2)(\cos \theta \sin \varphi_1 - \sin \theta \sin \varphi_2)|, \\ |I_2| &= \frac{1}{9} |\cos 2\theta \sin(2\varphi_1 - 2\varphi_2)|. \end{aligned} \quad (3.48)$$

We find that the mixing angles and Dirac CP violating phase fulfill the following sum rule

$$\cos \delta_{CP} = \frac{\cos 2\theta_{13} \cot 2\theta_{23}}{\sqrt{3} \cos^2 \theta_{13} - 1 \sin \theta_{13}} \simeq \frac{\sqrt{2}(\pi/4 - \theta_{23})}{\theta_{13}}. \quad (3.49)$$

Therefore the value of δ_{CP} is closely related with the deviation of θ_{23} from maximal mixing. Inputting the 3σ regions $0.0188 \leq \sin^2 \theta_{13} \leq 0.0251$ and $0.385 \leq \sin^2 \theta_{23} \leq 0.644$ from the global fit [44], we see $\cos \delta_{CP}$ can be any value in the interval of $[-1, 1]$. Hence no definite prediction can be made for δ_{CP} at present. However, if the uncertainty of the atmospheric mixing angle θ_{23} is reduced considerably by future neutrino experiments, the above sum rule in Eq. (3.49) could impose a strong constraint on the value of δ_{CP} .

As shown in table 5, the group $G_f = S_4$ can give rise to the mixing patterns $U^{II(a)}$ and $U^{II(b)}$ with $(\varphi_1, \varphi_2) = (\pi, 0)$. Then the atmospheric angle θ_{23} as well as the Dirac CP phase δ_{CP} are predicted to be maximal while both Majorana phases are 0 or π . In fact, $U^{II(a)}$ and $U^{II(b)}$ are essentially the same mixing pattern in this case, since they are related by the redefinition of θ and Q_ν

$$U^{II(b)}(\theta, \varphi_1 = \pi, \varphi_2 = 0) = U^{II(a)}\left(\frac{\pi}{2} - \theta, \varphi_1 = \pi, \varphi_2 = 0\right) \text{diag}(1, 1, -1). \quad (3.50)$$

Furthermore we find there are two best fit solutions $\theta_{\text{bf}} = 0.192\pi, 0.308\pi$ ($0.192\pi, 0.308\pi$) for $U^{II(a)}$ in case of NO (IO) spectrum, and the minimal value of the χ^2 function is $\chi^2_{\text{min}} = 8.843$ (12.565).

Regarding the $0\nu\beta\beta$ decay, the effective mass $|m_{ee}|$ is given by

$$|m_{ee}| = \frac{1}{3} \left| m_1 (e^{i\varphi_1} \cos \theta - e^{i\varphi_2} \sin \theta)^2 + q_1 m_2 + q_2 m_3 (e^{i\varphi_2} \cos \theta + e^{i\varphi_1} \sin \theta)^2 \right|, \quad (3.51)$$

where $q_1, q_2 = \pm 1$. The predicted values of $|m_{ee}|$ are displayed in figure 9, where we require the three lepton mixing angles are within the experimentally preferred 3σ ranges. For the smallest group $G_f = S_4$, one sees that $|m_{ee}|$ is determined to be around 0.015eV or 0.048eV in case of IO spectrum, which are accessible to the future experiments searching for $0\nu\beta\beta$ decay. In the case of NO, $|m_{ee}|$ could be smaller than 10^{-4} eV for certain values of the lightest neutrino mass, because cancellation between different terms in the expression of $|m_{ee}|$ can take place.

The residual symmetry enforces the second column of the PMNS to be trimaximal in this case. Therefore the R -matrix is of the form of C_{13} given in Eq. (3.28). We can read out the CP invariants I_{13}^α relevant to leptogenesis as

$$\begin{aligned} I_{13}^e &= \frac{1}{3} \sin(\varphi_1 - \varphi_2), \\ I_{13}^\mu &= -\frac{1}{3} \cos\left(\frac{\pi}{6} - \varphi_1 + \varphi_2\right), \\ I_{13}^\tau &= \frac{1}{3} \cos\left(\frac{\pi}{6} + \varphi_1 - \varphi_2\right). \end{aligned} \quad (3.52)$$

Group Id	(φ_1, φ_2)
$[24, 12]_\Delta, [48, 30]$	$(\pi, 0)$
$[96, 64]_\Delta, [192, 182]$	$(-\frac{7\pi}{12}, \frac{\pi}{3}), (-\frac{7\pi}{12}, \frac{\pi}{3}), (-\frac{3\pi}{4}, \frac{\pi}{4})$
$[384, 568]_\Delta,$ $[768, 1085335]$	$(\frac{\pi}{24}, -\frac{\pi}{24}), (\frac{\pi}{24}, -\frac{\pi}{24}), (\frac{\pi}{6}, -\frac{19\pi}{24}), (\frac{\pi}{6}, -\frac{19\pi}{24}), (-\frac{7\pi}{24}, -\frac{5\pi}{24}),$ $(-\frac{7\pi}{24}, -\frac{5\pi}{24}), (-\frac{5\pi}{12}, \frac{13\pi}{24}), (-\frac{5\pi}{12}, \frac{13\pi}{24}), (\frac{\pi}{8}, -\frac{7\pi}{8})$
$[600, 179]_\Delta, [1200, 682]$	$(-\frac{\pi}{5}, \frac{7\pi}{10}), (-\frac{\pi}{5}, \frac{7\pi}{10}), (-\frac{\pi}{5}, \frac{4\pi}{5}), (-\frac{\pi}{5}, \frac{9\pi}{10}), (-\frac{\pi}{5}, \frac{9\pi}{10}), (-\frac{7\pi}{15}, \frac{7\pi}{15}),$ $(-\frac{7\pi}{15}, \frac{7\pi}{15}), (-\frac{\pi}{10}, 0), (-\frac{\pi}{10}, 0), (-\frac{23\pi}{30}, \frac{4\pi}{15}), (-\frac{23\pi}{30}, \frac{4\pi}{15}), (-\frac{3\pi}{5}, \frac{2\pi}{5}),$ $(\frac{11\pi}{15}, \frac{2\pi}{3}), (\frac{11\pi}{15}, \frac{2\pi}{3}), (-\frac{2\pi}{3}, -\frac{19\pi}{30}), (-\frac{2\pi}{3}, -\frac{19\pi}{30}), (\frac{2\pi}{15}, \frac{\pi}{15}), (\frac{2\pi}{15}, \frac{\pi}{15}),$ $(-\frac{8\pi}{15}, \frac{13\pi}{30}), (-\frac{8\pi}{15}, \frac{13\pi}{30})$
$[648, 259]_{\Delta'}, [648, 260]$	$(\frac{5\pi}{9}, -\frac{7\pi}{18}), (\frac{5\pi}{9}, -\frac{7\pi}{18}), (\frac{2\pi}{3}, -\frac{\pi}{3}), (-\frac{7\pi}{9}, \frac{5\pi}{18}), (-\frac{7\pi}{9}, \frac{5\pi}{18}), (-\frac{4\pi}{9}, -\frac{5\pi}{9}),$ $(-\frac{4\pi}{9}, -\frac{5\pi}{9}), (-\frac{2\pi}{9}, -\frac{\pi}{9}), (-\frac{2\pi}{9}, -\frac{\pi}{9})$
$[1176, 243]_\Delta$	$(-\frac{2\pi}{7}, \frac{5\pi}{7}), (\frac{20\pi}{21}, \frac{\pi}{21}), (\frac{20\pi}{21}, \frac{\pi}{21}), (\frac{3\pi}{7}, -\frac{4\pi}{7}), (\frac{19\pi}{21}, \frac{17\pi}{21}), (\frac{19\pi}{21}, \frac{17\pi}{21}),$ $(\frac{5\pi}{21}, -\frac{2\pi}{3}), (\frac{5\pi}{21}, -\frac{2\pi}{3}), (\frac{19\pi}{42}, -\frac{2\pi}{3}), (\frac{19\pi}{42}, -\frac{2\pi}{3}), (-\frac{\pi}{6}, \frac{17\pi}{21}), (-\frac{\pi}{6}, \frac{17\pi}{21}),$ $(-\frac{17\pi}{21}, -\frac{29\pi}{42}), (-\frac{17\pi}{21}, -\frac{29\pi}{42}), (-\frac{\pi}{7}, \frac{6\pi}{7}), (\frac{11\pi}{21}, \frac{17\pi}{42}), (\frac{11\pi}{21}, \frac{17\pi}{42}),$ $(-\frac{17\pi}{21}, \frac{5\pi}{42}), (-\frac{17\pi}{21}, \frac{5\pi}{42}), (-\frac{11\pi}{21}, \frac{8\pi}{21}), (-\frac{11\pi}{21}, \frac{8\pi}{21}), (-\frac{11\pi}{21}, \frac{11\pi}{21}), (-\frac{11\pi}{21}, \frac{11\pi}{21}),$ $(-\frac{11\pi}{21}, \frac{11\pi}{21}), (\frac{\pi}{7}, -\frac{11\pi}{14}), (\frac{\pi}{7}, -\frac{11\pi}{14}), (-\frac{11\pi}{21}, -\frac{23\pi}{42}), (-\frac{11\pi}{21}, -\frac{23\pi}{42}),$ $(\frac{2\pi}{21}, -\frac{20\pi}{21}), (\frac{2\pi}{21}, -\frac{20\pi}{21}), (0, -\frac{13\pi}{14}), (0, -\frac{13\pi}{14}), (-\frac{13\pi}{21}, \frac{11\pi}{42}),$ $(-\frac{13\pi}{21}, \frac{11\pi}{42}), (-\frac{11\pi}{14}, -\frac{5\pi}{7}), (-\frac{11\pi}{14}, -\frac{5\pi}{7}), (-\frac{11\pi}{42}, \frac{16\pi}{21}), (-\frac{11\pi}{42}, \frac{16\pi}{21}),$ $(-\frac{8\pi}{21}, \frac{2\pi}{3}), (-\frac{8\pi}{21}, \frac{2\pi}{3}), (-\frac{8\pi}{21}, -\frac{17\pi}{42}), (-\frac{8\pi}{21}, -\frac{17\pi}{42}), (\frac{4\pi}{7}, \frac{9\pi}{14}), (\frac{4\pi}{7}, \frac{9\pi}{14})$
$[1536, 408544632]_\Delta$	$(-\frac{47\pi}{48}, -\frac{23\pi}{24}), (-\frac{47\pi}{48}, -\frac{23\pi}{24}), (\frac{5\pi}{16}, \frac{5\pi}{16}), (-\frac{11\pi}{48}, -\frac{7\pi}{48}), (-\frac{11\pi}{48}, -\frac{7\pi}{48}),$ $(-\frac{7\pi}{16}, \frac{9\pi}{16}), (\frac{23\pi}{48}, -\frac{29\pi}{48}), (\frac{23\pi}{48}, -\frac{29\pi}{48}), (-\frac{23\pi}{48}, -\frac{7\pi}{12}), (-\frac{23\pi}{48}, -\frac{7\pi}{12}),$ $(-\frac{\pi}{8}, -\frac{\pi}{16}), (-\frac{\pi}{8}, -\frac{\pi}{16}), (\frac{9\pi}{16}, -\frac{\pi}{2}), (\frac{9\pi}{16}, -\frac{\pi}{2}), (-\frac{5\pi}{48}, -\frac{\pi}{12}),$ $(-\frac{5\pi}{48}, -\frac{\pi}{12}), (\frac{37\pi}{48}, \frac{35\pi}{48}), (\frac{37\pi}{48}, \frac{35\pi}{48}), (-\frac{29\pi}{48}, \frac{17\pi}{48}), (-\frac{29\pi}{48}, \frac{17\pi}{48}),$ $(\frac{35\pi}{48}, -\frac{\pi}{6}), (\frac{35\pi}{48}, -\frac{\pi}{6}), (\frac{11\pi}{16}, -\frac{\pi}{4}), (\frac{11\pi}{16}, -\frac{\pi}{4}), (-\frac{31\pi}{48}, \frac{11\pi}{24}),$ $(-\frac{31\pi}{48}, \frac{11\pi}{24}), (\frac{\pi}{48}, \frac{47\pi}{48}), (\frac{\pi}{48}, \frac{47\pi}{48}), (\frac{3\pi}{16}, \frac{\pi}{8}), (\frac{3\pi}{16}, \frac{\pi}{8}), (-\frac{5\pi}{24}, -\frac{11\pi}{48}),$ $(-\frac{5\pi}{24}, -\frac{11\pi}{48}), (\frac{\pi}{6}, \frac{7\pi}{48}), (\frac{\pi}{6}, \frac{7\pi}{48}), (\frac{17\pi}{24}, -\frac{19\pi}{48}), (\frac{17\pi}{24}, -\frac{19\pi}{48})$

Table 5: The predictions for PMNS matrix of the form $U^{II(a)}$ and $U^{II(b)}$, where the first column shows the group identification in **GAP** system, and the second column displays the achievable values of the parameters φ_1 and φ_2 . We have shown at most two representatives flavor symmetry groups in the first column. If there is only one group predicting the corresponding values of φ_1 and φ_2 in the second column, this unique group would be listed. The full results of our analysis are provided at the website [45]. The subscripts Δ and Δ' indicate that the corresponding groups belong to the type D group series $D_{n,n}^{(0)} \cong \Delta(6n^2)$ and $D_{9n',3n'}^{(1)} \cong (Z_{9n'} \times Z_{3n'}) \rtimes S_3$, respectively.

The numerical results of the baryon asymmetry for $(\varphi_1, \varphi_2) = (\pi, 0)$ are shown in figure 10. It is easy to see that the observed baryon asymmetry could be generated via leptogenesis except in the case of NO spectrum with $(K_1, K_2, K_3) = (-, \pm, +)$.

Case III

$$U^{III} = \frac{1}{\sqrt{3}} \begin{pmatrix} \sqrt{2}e^{i\varphi_1} \sin \varphi_2 & 1 & \sqrt{2}e^{i\varphi_1} \cos \varphi_2 \\ \sqrt{2}e^{i\varphi_1} \cos(\varphi_2 + \frac{\pi}{6}) & 1 & -\sqrt{2}e^{i\varphi_1} \sin(\varphi_2 + \frac{\pi}{6}) \\ -\sqrt{2}e^{i\varphi_1} \cos(\varphi_2 - \frac{\pi}{6}) & 1 & \sqrt{2}e^{i\varphi_1} \sin(\varphi_2 - \frac{\pi}{6}) \end{pmatrix} S_{13}(\theta) Q_\nu^\dagger, \quad (3.53)$$

where φ_1 and φ_2 are rational angles, and their values are determined by the residual symmetries. The admissible values of φ_1 and φ_2 and the representative flavor symmetry groups found from our group scan up to order 2000 are summarized in table 6. The full results are available at our website [45]. Similar to case II, the second column of the mixing matrix is $(1, 1, 1)^T/\sqrt{3}$ as well. In particular, all the six row permutations lead to the same mixing pattern, if the freedom of redefining the parameters θ , φ_1 and φ_2 is taken into account. For this mixing matrix $U^{(III)}$ in Eq. (3.53), the mixing angles read

$$\sin^2 \theta_{13} = \frac{2}{3} \cos^2(\theta - \varphi_2), \quad \sin^2 \theta_{12} = \frac{1}{3 - 2 \cos^2(\theta - \varphi_2)}, \quad \sin^2 \theta_{23} = \frac{\sin(2\theta - 2\varphi_2 + \frac{\pi}{6}) - 1}{\cos(2\theta - 2\varphi_2) - 2}, \quad (3.54)$$

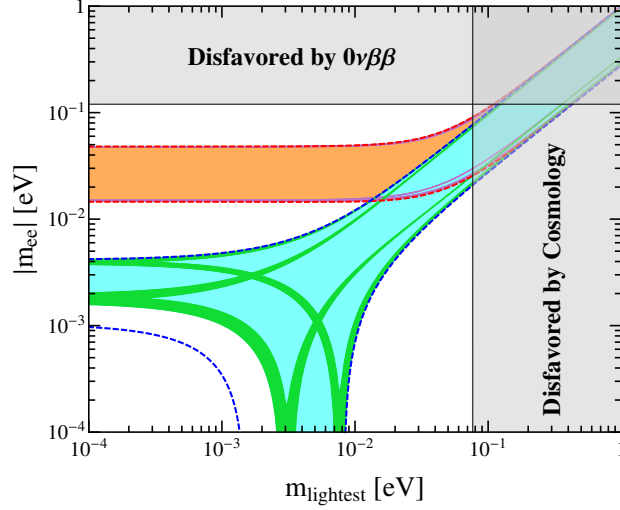


Figure 9: Predictions of the $0\nu\beta\beta$ decay effective mass $|m_{ee}|$ with respect to the lightest neutrino mass m_{lightest} for the mixing patterns $U^{II(a)}$ and $U^{II(b)}$. The red (blue) dashed lines indicate the most general allowed regions for IO (NO) spectrum obtained by varying the mixing parameters within their 3σ ranges [44]. The orange (cyan) areas denote the achievable values of $|m_{ee}|$ when φ_1 and φ_2 are taken to be free continuous parameters in the case of IO (NO). The purple and green regions are the theoretical predictions of the smallest flavor symmetry group which can generate this two mixing pattern. Note that the purple (green) region overlaps the orange (cyan) one. The present most stringent upper limits $|m_{ee}| < 0.120$ eV from EXO-200 [57, 58] and KamLAND-ZEN [59] is shown by horizontal grey band. The vertical grey exclusion band is the current limit on m_{lightest} from the cosmological data of $\sum m_i < 0.230$ eV by the Planck collaboration [60].

which fulfill the following sum rules

$$3 \cos^2 \theta_{13} \sin^2 \theta_{12} = 1, \quad \sin^2 \theta_{23} = \frac{1}{2} \pm \frac{1}{2} \tan \theta_{13} \sqrt{2 - \tan^2 \theta_{13}}. \quad (3.55)$$

Inserting the best fit value $\sin^2 \theta_{13} = 0.0218$ [44], we obtain

$$\sin^2 \theta_{12} \simeq 0.341, \quad \sin^2 \theta_{23} \simeq 0.395 \text{ or } 0.605, \quad (3.56)$$

which are compatible with the present experimental data. By precisely measuring the solar and atmospheric mixing angles, the reactor neutrino experiment JUNO and long baseline neutrino oscillation experiments DUNE and Hyper-Kamiokande are able to exclude this mixing pattern or provide strong evidence for its relevance. Furthermore, the CP invariants are given by

$$J_{CP} = I_2 = 0, \quad |I_1| = \frac{2}{9} |\sin 2\varphi_1| \sin^2(\theta - \varphi_2), \quad (3.57)$$

which leads to

$$\delta_{CP}, \alpha_{31} = 0 \text{ or } \pi, \quad \alpha_{21} \pmod{\pi} = \pm 2\varphi_1. \quad (3.58)$$

This indicates that both Dirac CP phase δ_{CP} and Majorana phase α_{31} are always trivial in this case. Subsequently we find for the effective Majorana mass $|m_{ee}|$ the following expression

$$|m_{ee}| = \frac{1}{3} |2m_1 e^{2i\varphi_1} \sin^2(\theta - \varphi_2) + q_1 m_2 + 2q_2 m_3 e^{2i\varphi_1} \cos^2(\theta - \varphi_2)|. \quad (3.59)$$

We plot $|m_{ee}|$ as a function of the lightest neutrino mass m_{lightest} in figure 11. For the smallest flavor symmetry group A_4 which predicts $(\varphi_1, \varphi_2) = (\pi, 2\pi/3)$, all the three CP violation phases are conserved. As a result, the effective mass $|m_{ee}|$ is close to 0.027eV or 0.042eV in case of IO spectrum. It is notable that there is no cancellation in $|m_{ee}|$ for any values of m_{lightest} in the case of NO, and thus $|m_{ee}|$ has a lower bound $|m_{ee}| \geq 2.52 \times 10^{-3}$ eV.

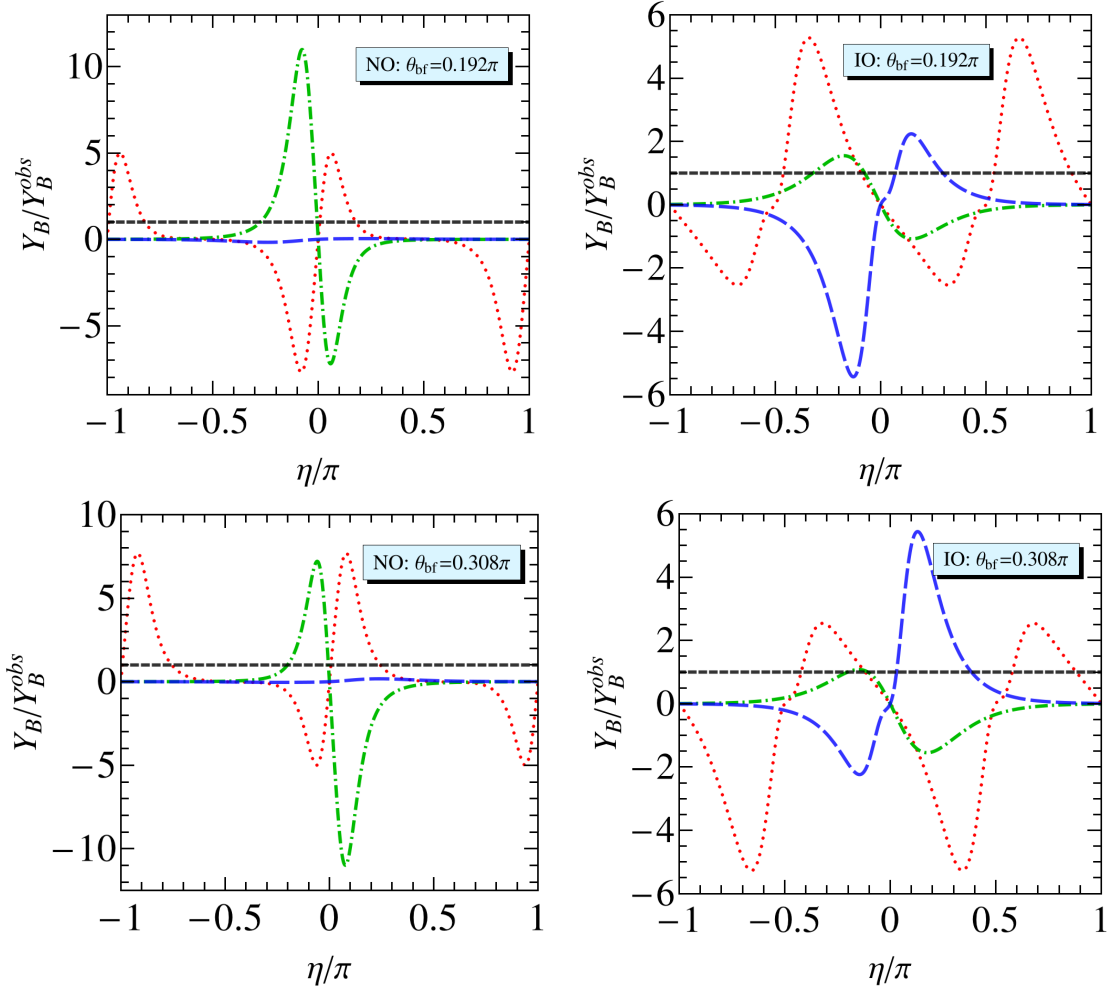


Figure 10: The prediction for Y_B/Y_B^{obs} as a function of η in case II with $(\varphi_1, \varphi_2) = (\pi, 0)$, where θ_{bf} is the best fit value of θ . We choose $M_1 = 5 \times 10^{11}$ GeV and the lightest neutrino mass m_1 (or m_3) = 0.01eV. The red dotted, green dot-dashed, blue dashed lines correspond to $(K_1, K_2, K_3) = (+, \pm, +), (+, \pm, -)$ and $(-, \pm, +)$ respectively. The experimentally observed value Y_B^{obs} is represented by the horizontal black dashed line.

As regards the leptogenesis, we find that both rephase invariant I_{13}^α and the CP asymmetry ϵ_α are vanishing,

$$I_{13}^e = I_{13}^\mu = I_{13}^\tau = 0, \quad \epsilon_e = \epsilon_\mu = \epsilon_\tau = 0. \quad (3.60)$$

Hence the net baryon asymmetry can not be generated in this case, and appropriate subleading corrections are necessary in order to make the leptogenesis viable.

Group Id	(φ_1, φ_2)
$[12, 3], [24, 12]_{\Delta}$	$(\pi, \frac{2\pi}{3})$
$[96, 64]_{\Delta}, [192, 182]$	$(-\frac{3\pi}{4}, \frac{2\pi}{3})$
$[384, 568]_{\Delta}, [768, 1085335]$	$(-\frac{7\pi}{8}, 0)$
$[600, 179]_{\Delta}, [1200, 682]$	$(-\frac{3\pi}{5}, \frac{\pi}{6}), (\frac{4\pi}{5}, \frac{\pi}{6})$
$[648, 259]_{\Delta'}, [648, 260]$	$(\frac{\pi}{3}, \frac{2\pi}{3})$
$[1176, 243]_{\Delta}$	$(\frac{3\pi}{7}, \frac{\pi}{6}), (\frac{5\pi}{7}, \frac{\pi}{6}), (\frac{6\pi}{7}, \frac{2\pi}{3})$
$[1536, 408544632]_{\Delta}$	$(-\frac{7\pi}{16}, \frac{\pi}{6}), (\frac{5\pi}{16}, \frac{\pi}{6})$

Table 6: The predictions for PMNS matrix of the form U^{III} , where the first column shows the group identification in GAP system, and the second column displays the achievable values of the parameters φ_1 and φ_2 . We have shown at most two representatives flavor symmetry groups in the first column. If there is only one group predicting the corresponding values of φ_1 and φ_2 in the second column, this unique group would be listed. The full results of our analysis are provided at the website [45]. The subscripts Δ and Δ' indicate that the corresponding groups belong to the type D group series $D_{n,n}^{(0)} \cong \Delta(6n^2)$ and $D_{9n',3n'}^{(1)} \cong (Z_{9n'} \times Z_{3n'}) \rtimes S_3$, respectively.

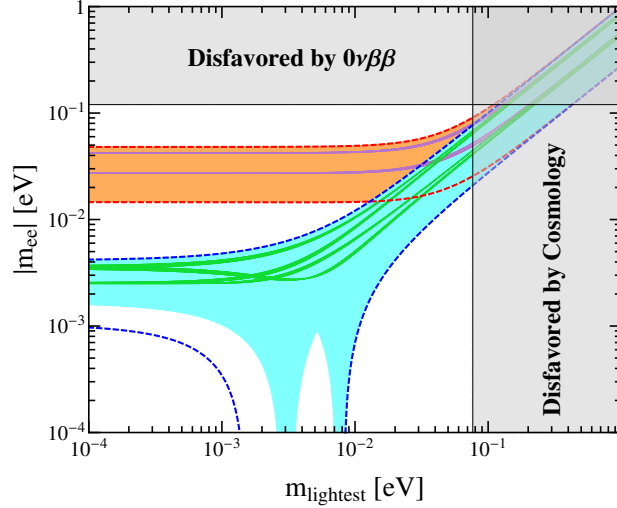


Figure 11: Predictions of the $0\nu\beta\beta$ decay effective mass $|m_{ee}|$ with respect to the lightest neutrino mass m_{lightest} for the mixing pattern U^{III} . The red (blue) dashed lines indicate the most general allowed regions for IO (NO) spectrum obtained by varying the mixing parameters within their 3σ ranges [44]. The orange (cyan) areas denote the achievable values of $|m_{ee}|$ when φ_1 and φ_2 are taken to be free continuous parameters in the case of IO (NO). The purple and green regions are the theoretical predictions of the smallest flavor symmetry group which can generate this mixing pattern. Note that the purple (green) region overlaps the orange (cyan) one. The present most stringent upper limits $|m_{ee}| < 0.120$ eV from EXO-200 [57, 58] and KamLAND-ZEN [59] is shown by horizontal grey band. The vertical grey exclusion band is the current limit on m_{lightest} from the cosmological data of $\sum m_i < 0.230$ eV by the Planck collaboration [60].

Case IV

$$\begin{aligned}
U^{IV(a)} &= \begin{pmatrix} -\sqrt{\frac{\phi_g}{\sqrt{5}}} & \sqrt{\frac{1}{\sqrt{5}\phi_g}} & 0 \\ \sqrt{\frac{1}{2\sqrt{5}\phi_g}} & \sqrt{\frac{\phi_g}{2\sqrt{5}}} & -\frac{1}{\sqrt{2}} \\ \sqrt{\frac{1}{2\sqrt{5}\phi_g}} & \sqrt{\frac{\phi_g}{2\sqrt{5}}} & \frac{1}{\sqrt{2}} \end{pmatrix} S_{13}(\theta) Q_{\nu}^{\dagger}, \\
U^{IV(b)} &= \begin{pmatrix} -i\sqrt{\frac{\phi_g}{\sqrt{5}}} & \sqrt{\frac{1}{\sqrt{5}\phi_g}} & 0 \\ i\sqrt{\frac{1}{2\sqrt{5}\phi_g}} & \sqrt{\frac{\phi_g}{2\sqrt{5}}} & -\frac{1}{\sqrt{2}} \\ i\sqrt{\frac{1}{2\sqrt{5}\phi_g}} & \sqrt{\frac{\phi_g}{2\sqrt{5}}} & \frac{1}{\sqrt{2}} \end{pmatrix} S_{13}(\theta) Q_{\nu}^{\dagger},
\end{aligned} \tag{3.61}$$

where $\phi_g = (\sqrt{5} + 1)/2$ is the golden ratio. Notice that $U^{IV(b)}$ can be obtained from $U^{IV(a)}$ by multiplying the factor i in its first column. Our group scanning reveals that these two mixing patterns can be obtained from the groups $[60, 5] \cong A_5$, $[120, 35]$, $[180, 19]$ and many others shown in the website. Indeed, this case has been found in previous work on A_5 flavor symmetry and generalized CP [17–19], and our results coincide with those. The PMNS mixing matrix $U^{IV(a)}$ leads to the following expressions for the mixing angles

$$\sin^2 \theta_{13} = \frac{\phi_g}{\sqrt{5}} \sin^2 \theta, \quad \sin^2 \theta_{12} = \frac{4 - 2\phi_g}{5 - 2\phi_g + \cos 2\theta}, \quad \sin^2 \theta_{23} = \frac{1}{2} - \frac{\sqrt{3 - \phi_g} \sin 2\theta}{3\phi_g - 2 + \phi_g \cos 2\theta}. \quad (3.62)$$

Obviously $U^{IV(a)}$ is a real matrix, therefore all the three CP invariants vanish,

$$J_{CP} = I_1 = I_2 = 0, \quad (3.63)$$

which implies that each of the CP violation phases $\delta_{CP}, \alpha_{21}, \alpha_{31}$ is either 0 or π . Moreover, we see that the mixing angles fulfill the following sum rules

$$\sin^2 \theta_{12} \cos^2 \theta_{13} = \frac{3 - \phi_g}{5}, \quad \sin^2 \theta_{23} - \frac{1}{2} = \pm(\phi_g - 1) \tan \theta_{13} \sqrt{1 + (\phi_g - 2) \tan^2 \theta_{13}}, \quad (3.64)$$

Using the 3σ range of the reactor mixing angle $0.0188 \leq \sin^2 \theta_{13} \leq 0.0251$ [44], we get

$$0.282 \leq \sin^2 \theta_{12} \leq 0.284, \quad 0.401 \leq \sin^2 \theta_{23} \leq 0.415 \quad \text{or} \quad 0.585 \leq \sin^2 \theta_{23} \leq 0.599. \quad (3.65)$$

These predictions for θ_{12} and θ_{23} will be testable at future neutrino facilities such as JUNO, DUNE, Hyper-Kamiokande and so on. For the mixing matrix $U^{IV(b)}$, the mixing angles read

$$\sin^2 \theta_{13} = \frac{\phi_g}{\sqrt{5}} \sin^2 \theta, \quad \sin^2 \theta_{12} = \frac{4 - 2\phi_g}{5 - 2\phi_g + \cos 2\theta}, \quad \sin^2 \theta_{23} = \frac{1}{2}. \quad (3.66)$$

The solar and reactor mixing angles have the same form as that of $U^{IV(a)}$, and consequently the correlation $\sin^2 \theta_{12} \cos^2 \theta_{13} = (3 - \phi_g)/5$ given in Eq. (3.64) still holds. The minimum value of χ^2 is $\chi_{\min}^2 = 4.045$ (7.742) obtained at the best fitting values $\theta_{\text{bf}} = \pm 0.056\pi$ ($\pm 0.056\pi$) for NO (IO) spectrum. For the CP violating phases, we find δ_{CP} is exactly maximal while both Majorana phases α_{21} and α_{31} are trivial with

$$|J_{CP}| = \frac{1}{4} \sqrt{\frac{\phi_g}{5\sqrt{5}}} |\sin 2\theta|, \quad I_1 = I_2 = 0. \quad (3.67)$$

In this case, the general expression for the effective mass $|m_{ee}|$ is

$$\begin{aligned} |m_{ee}| &= \frac{1}{\sqrt{5}} |\phi_g m_1 \cos^2 \theta + \phi_g^{-1} q_1 m_2 + \phi_g q_2 m_3 \sin^2 \theta|, \quad \text{for } U^{IV(a)}, \\ |m_{ee}| &= \frac{1}{\sqrt{5}} |\phi_g m_1 \cos^2 \theta - \phi_g^{-1} q_1 m_2 + \phi_g q_2 m_3 \sin^2 \theta|, \quad \text{for } U^{IV(b)}, \end{aligned} \quad (3.68)$$

where $q_1, q_2 = \pm 1$. Therefore the same values of $|m_{ee}|$ would be obtained if the parameter q_1 is of opposite sign for $U^{IV(a)}$ and $U^{IV(b)}$. After considering all possible values of q_1 and q_2 , we display the allowed regions of $|m_{ee}|$ in figure 12. We see that $|m_{ee}|$ is close to 0.021eV or 0.048eV for IO while it is smaller than 10^{-4} eV for $0.0016 \text{ eV} \leq m_{\text{lightest}} \leq 0.0024 \text{ eV}$ and $0.0051 \text{ eV} \leq m_{\text{lightest}} \leq 0.0061 \text{ eV}$ in the case NO.

Then we come to study the resulting predictions for leptogenesis. All the rephasing invariants I_{13}^α are determined to be zero for $U^{IV(a)}$ so that the CP asymmetries ϵ_α vanish and the matter-antimatter asymmetry of the universe can not be generated without high order corrections. For the PMNS mixing matrix $U^{IV(b)}$, we find

$$I_{13}^e = 0, \quad I_{13}^\mu = -I_{13}^\tau = -\sqrt{\frac{1}{4\sqrt{5}\phi_g}}. \quad (3.69)$$

We plot the values of Y_B versus η in figure 13. It is easy to see that the observed baryon asymmetry can be obtained via leptogenesis except in the case of NO with $(K_1, K_2, K_3) = (-, \pm, +)$.

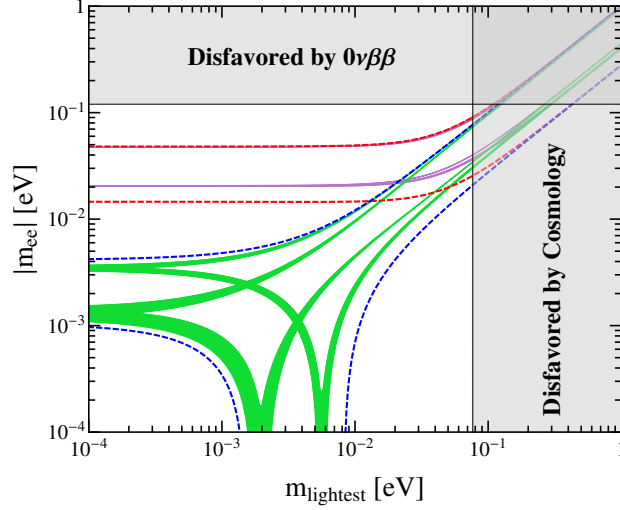


Figure 12: Predictions of the $0\nu\beta\beta$ decay effective mass $|m_{ee}|$ with respect to the lightest neutrino mass m_{lightest} for the mixing patterns $U^{IV(a)}$ and $U^{IV(b)}$. The red (blue) dashed lines indicate the most general allowed regions for IO (NO) spectrum obtained by varying the mixing parameters within their 3σ ranges [44]. The purple and green regions are the theoretical predictions of these two mixing patterns. The present most stringent upper limits $|m_{ee}| < 0.120$ eV from EXO-200 [57, 58] and KamLAND-ZEN [59] is shown by horizontal grey band. The vertical grey exclusion band is the current limit on m_{lightest} from the cosmological data of $\sum m_i < 0.230$ eV by the Planck collaboration [60].

Case V

$$\begin{aligned}
 U^{V(a)} &= \frac{1}{2} \begin{pmatrix} \phi_g & 1 & \phi_g - 1 \\ \phi_g - 1 & -\phi_g & 1 \\ 1 & 1 - \phi_g & -\phi_g \end{pmatrix} S_{23}(\theta) Q_\nu^\dagger \\
 U^{V(b)} &= \frac{1}{2} \begin{pmatrix} \phi_g & 1 & \phi_g - 1 \\ 1 & 1 - \phi_g & -\phi_g \\ \phi_g - 1 & -\phi_g & 1 \end{pmatrix} S_{23}(\theta) Q_\nu^\dagger.
 \end{aligned} \tag{3.70}$$

Notice that these two mixing matrices are related through an exchange of the second and third rows. Similar to case IV, this mixing pattern can be obtained from the flavor symmetry groups [60, 5] $\cong A_5$, [120, 35], [180, 19] etc in combination with generalized CP. Earlier studies of this mixing pattern in the context of A_5 flavor symmetry and CP can be found in Refs. [17–19]. We can extract the following results for the mixing angles

$$\begin{aligned}
 \sin^2 \theta_{13} &= \frac{(\cos \theta - \phi_g \sin \theta)^2}{4\phi_g^2}, \quad \sin^2 \theta_{12} = \frac{(\phi_g \cos \theta + \sin \theta)^2}{4\phi_g^2 - (\cos \theta - \phi_g \sin \theta)^2}, \\
 \sin^2 \theta_{23} &= \frac{\phi_g^2 (\cos \theta + \phi_g \sin \theta)^2}{4\phi_g^2 - (\cos \theta - \phi_g \sin \theta)^2} \quad \text{for } U^{V(a)}, \\
 \sin^2 \theta_{23} &= \frac{(\sin \theta - \phi_g^2 \cos \theta)^2}{4\phi_g^2 - (\cos \theta - \phi_g \sin \theta)^2} \quad \text{for } U^{V(b)}.
 \end{aligned} \tag{3.71}$$

For the mixing pattern $U^{V(a)}$, the global minimum of χ^2 is $\chi_{\text{min}}^2 = 6.190$ (6.434) obtained at the best fitting values $\theta_{\text{bf}} = 0.095\pi$ (0.095π) for NO (IO) spectrum. Accordingly the mixing angles at $\theta = \theta_{\text{bf}}$ are given by $\sin^2 \theta_{12} = 0.331$, $\sin^2 \theta_{13} = 0.022$ and $\sin^2 \theta_{23} = 0.524$ which are in excellent agreement with experimental data. For the PMNS matrix $U^{V(b)}$, χ^2 is minimized at the best fitting point $\theta_{\text{bf}} = 0.095\pi$ (0.094π) with $\chi_{\text{min}}^2 = 4.477$ (11.799), and the values obtained for the mixing angles are $\sin^2 \theta_{12} = 0.331$, $\sin^2 \theta_{13} = 0.022$ and $\sin^2 \theta_{23} = 0.476$. The CP invariants J_{CP} , I_1 and I_2 are found to vanish exactly so that both Dirac and Majorana CP phases take CP conserving values 0 and π . Similarly the bilinear invariants I_{23}^α are also zero. Hence a baryon asymmetry can not be obtained in this case unless the residual symmetries are further broken by higher order contributions. Furthermore, the two PMNS mixing matrices $U^{V(a)}$ and $U^{V(b)}$ yield

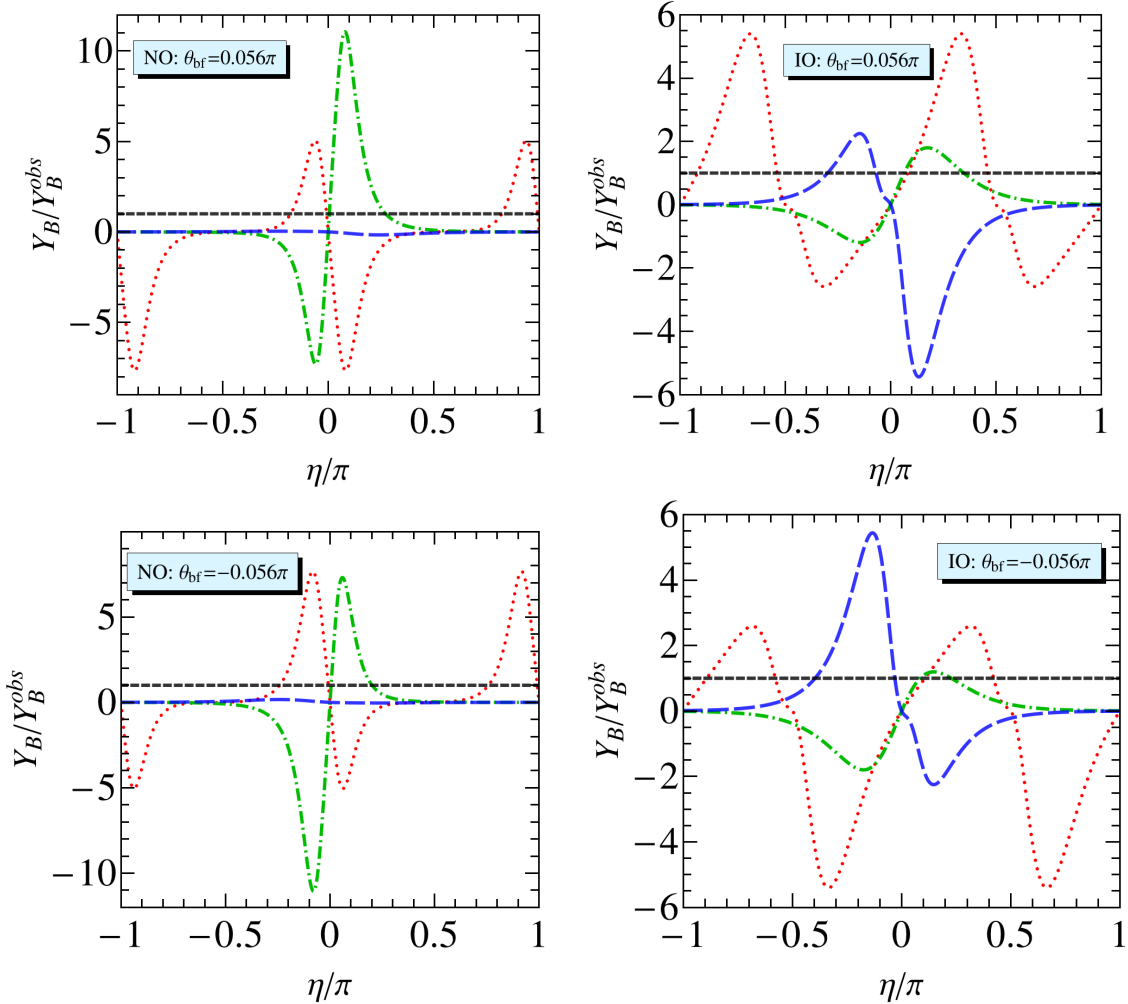


Figure 13: The prediction for Y_B/Y_B^{obs} as a function of η in case IV(b), where θ_{bf} is the best fit value of θ . We choose $M_1 = 5 \times 10^{11}$ GeV and the lightest neutrino mass m_1 (or m_3) = 0.01eV. The red dotted, green dot-dashed, blue dashed lines correspond to $(K_1, K_2, K_3) = (+, \pm, +), (+, \pm, -)$ and $(-, \pm, +)$ respectively. The experimentally observed value Y_B^{obs} is represented by the horizontal black dashed line.

the same expression for the effective Majorana mass $|m_{ee}|$

$$|m_{ee}| = \frac{1}{4} \left| \phi_g^2 m_1 + q_1 m_2 (\cos \theta + \phi_g^{-1} \sin \theta)^2 + q_2 m_3 (\sin \theta - \phi_g^{-1} \cos \theta)^2 \right| \quad (3.72)$$

with $q_1, q_2 = \pm 1$. The predicted values of $|m_{ee}|$ from this mixing pattern are shown in figure 14. We find that $|m_{ee}|$ is around 0.016eV or 0.048eV in the case of IO spectrum, and it can be approximately vanishing for NO due to strong cancellations if the lightest neutrino mass is in the narrow range of $0.0023 \text{ eV} \leq m_{\text{lightest}} \leq 0.0034 \text{ eV}$ and $0.0067 \text{ eV} \leq m_{\text{lightest}} \leq 0.0078 \text{ eV}$.

Case VI

$$U^{VI} = \frac{1}{2\sqrt{3}} \begin{pmatrix} (\sqrt{3}-1)e^{i\varphi} & 2 & -(\sqrt{3}+1)e^{i(\varphi+\frac{3\pi}{4})} \\ -(\sqrt{3}+1)e^{i\varphi} & 2 & (\sqrt{3}-1)e^{i(\varphi+\frac{3\pi}{4})} \\ 2e^{i\varphi} & 2 & 2e^{i(\varphi+\frac{3\pi}{4})} \end{pmatrix} S_{13}(\theta) Q_\nu^\dagger, \quad (3.73)$$

where $\varphi = \arctan(2 - \sqrt{7})$. This mixing pattern has not been discussed in the literature as far as we know. It can be achieved from the flavor symmetry groups [168,42], [336,209], [504,157] and others which are listed at the website [45]. The group [168,42] exactly is the known group $\Sigma(168) \cong PSL(2, 7)$. It is the automorphism group of the Klein quartic as well as the symmetry group of the Fano plane. It is the second-smallest nonabelian simple group after the alternating

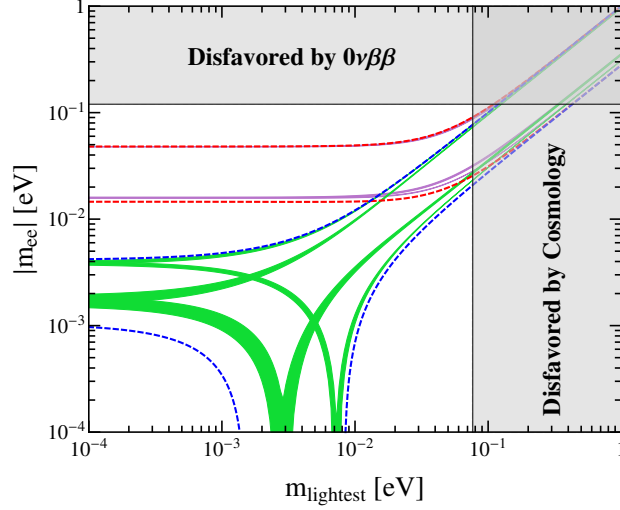


Figure 14: Predictions of the $0\nu\beta\beta$ decay effective mass $|m_{ee}|$ with respect to the lightest neutrino mass m_{lightest} for the mixing patterns $U^{V(a)}$ and $U^{V(b)}$. The red (blue) dashed lines indicate the most general allowed regions for IO (NO) spectrum obtained by varying the mixing parameters within their 3σ ranges [44]. The purple and green regions are the theoretical predictions of these two mixing patterns. The present most stringent upper limits $|m_{ee}| < 0.120$ eV from EXO-200 [57, 58] and KamLAND-ZEN [59] is shown by horizontal grey band. The vertical grey exclusion band is the current limit on m_{lightest} from the cosmological data of $\sum m_i < 0.230$ eV by the Planck collaboration [60].

group A_5 . It has important applications in algebra, geometry, and number theory. $\Sigma(168)$ has also been recognized as quite interesting in discrete flavor symmetry theory [64]. Notice that one column of the PMNS matrix is $(1, 1, 1)^T/\sqrt{3}$ in this case, and it should be identified as the second column in order to be compatible with the experimental data on lepton mixing angles. For the mixing matrices arising from the six possible row permutations of U^{VI} , four of them can accommodate the experimental data

$$\begin{aligned} U^{VI(a)} &= U_{PMNS}^{VI}, & U^{VI(b)} &= P_{132}U_{PMNS}^{VI}, \\ U^{VI(c)} &= P_{213}U_{PMNS}^{VI}, & U^{VI(d)} &= P_{231}U_{PMNS}^{VI}. \end{aligned} \quad (3.74)$$

One see that $U^{VI(b)}$ and $U^{VI(d)}$ can be obtained from $U^{VI(a)}$ and $U^{VI(c)}$ respectively by exchanging the second and third rows. From the mixing matrices $U^{VI(a)}$ and $U^{VI(b)}$, the mixing angles and the three CP rephasing invariants can be read out as

$$\begin{aligned} \sin^2 \theta_{13} &= \frac{1}{12} \left(4 + 2\sqrt{3} \cos 2\theta + \sqrt{2} \sin 2\theta \right), \\ \sin^2 \theta_{12} &= \frac{4}{8 - 2\sqrt{3} \cos 2\theta - \sqrt{2} \sin 2\theta}, \\ \sin^2 \theta_{23} &= \frac{4 - 2\sqrt{3} \cos 2\theta + \sqrt{2} \sin 2\theta}{8 - 2\sqrt{3} \cos 2\theta - \sqrt{2} \sin 2\theta} \quad \text{for } U^{VI(a)}, \\ \sin^2 \theta_{23} &= \frac{4 - 2\sqrt{2} \sin 2\theta}{8 - 2\sqrt{3} \cos 2\theta - \sqrt{2} \sin 2\theta} \quad \text{for } U^{VI(b)}, \\ |J_{CP}| &= \frac{1}{6\sqrt{6}} |\sin 2\theta|, \quad |I_2| = \frac{1}{36} \left| \cos 2\theta - \sqrt{6} \sin 2\theta \right|, \\ |I_1| &= \frac{1}{72} \left| 2\sqrt{7} - \sqrt{3} + (2 - \sqrt{21}) \cos 2\theta - \sqrt{14} \sin 2\theta \right|. \end{aligned} \quad (3.75)$$

	θ_{bf}/π	χ_{min}^2	$\sin^2 \theta_{13}$	$\sin^2 \theta_{12}$	$\sin^2 \theta_{23}$	δ_{CP}/π	α_{21}/π (mod 1)	α'_{31}/π (mod 1)	(K_1, K_2, K_3)
$U^{VI(a)}$	0.572 [0.555]	12.028 [8.007]	0.0222 [0.0218]	0.341 [0.341]	0.554 [0.578]	0.667 [0.763]	0.839 [0.845]	0.106 [0.926]	$(+, \pm, +), (+, \pm, -)$ [[$(+, \pm, +), (+, \pm, -)$]]
$U^{VI(b)}$	0.569 [0.576]	8.133 [20.586]	0.0219 [0.0227]	0.341 [0.341]	0.443 [0.452]	1.680 [1.646]	0.839 [0.837]	0.082 [0.146]	$(+, \pm, +), (+, \pm, -)$ [[$(+, \pm, +), (+, \pm, -)$]]
$U^{VI(c)}$	0.928 [0.945]	12.028 [8.007]	0.0222 [0.0218]	0.341 [0.341]	0.554 [0.578]	1.333 [1.237]	0.392 [0.385]	0.894 [0.074]	$(+, \pm, +), (+, \pm, -)$ [[$(-, \pm, +)$]]
$U^{VI(d)}$	0.931 [0.924]	8.133 [20.586]	0.0219 [0.0227]	0.341 [0.341]	0.443 [0.452]	0.320 [0.354]	0.391 [0.393]	0.918 [0.854]	$(+, \pm, +), (+, \pm, -)$ [[$(-, \pm, +)$]]

Table 7: Results of the χ^2 analysis for case VI. We show the best fit value θ_{bf} of the parameter θ , and χ_{min}^2 is the global minimum of the χ^2 function. The mixing angles and the CP violating phases for $\theta = \theta_{\text{bf}}$ are given as well. Note that the CP parity matrix Q_ν can shift the Majorana phases α_{21} and α'_{31} by π . In the last column we give the values of $K_{1,2,3}$ for which the observed baryon asymmetry can be generated via leptogenesis. The values in the square brackets are the corresponding results for the case of IO mass spectrum.

Then we can derive the following sum rules among the mixing angles

$$\begin{aligned}
\sin^2 \theta_{12} \cos^2 \theta_{13} &= \frac{1}{3}, \\
\sin^2 \theta_{23} \cos^2 \theta_{13} &= \frac{1}{42} \left(9 + 15 \cos 2\theta_{13} \pm 2\sqrt{3} \sqrt{12 \cos 2\theta_{13} - 9 \cos 4\theta_{13} - 4} \right) \quad \text{for } U^{VI(a)}, \\
\sin^2 \theta_{23} \cos^2 \theta_{13} &= \frac{1}{21} \left(6 + 3 \cos 2\theta_{13} \pm \sqrt{3} \sqrt{12 \cos 2\theta_{13} - 9 \cos 4\theta_{13} - 4} \right) \quad \text{for } U^{VI(b)}.
\end{aligned} \tag{3.76}$$

Plugging in the best fitting value of the reactor angle $\sin^2 \theta_{13} = 0.0218$ [44], we have

$$\begin{aligned}
\sin^2 \theta_{12} &= 0.341, \\
\sin^2 \theta_{23} &= 0.559 \quad \text{or} \quad 0.578 \quad \text{for } U^{VI(a)}, \\
\sin^2 \theta_{23} &= 0.441 \quad \text{or} \quad 0.422 \quad \text{for } U^{VI(b)}.
\end{aligned} \tag{3.77}$$

Obviously the atmospheric mixing angle θ_{23} is non-maximal in this case. The results of our χ^2 analysis are summarized in table 7. The mixing matrices $U^{VI(c)}$ and $U^{VI(d)}$ give rise to the following results for mixing angles and CP invariants

$$\begin{aligned}
\sin^2 \theta_{13} &= \frac{1}{12} \left(4 - 2\sqrt{3} \cos 2\theta + \sqrt{2} \sin 2\theta \right), \\
\sin^2 \theta_{12} &= \frac{4}{8 + 2\sqrt{3} \cos 2\theta - \sqrt{2} \sin 2\theta}, \\
\sin^2 \theta_{23} &= \frac{4 + 2\sqrt{3} \cos 2\theta + \sqrt{2} \sin 2\theta}{8 + 2\sqrt{3} \cos 2\theta - \sqrt{2} \sin 2\theta} \quad \text{for } U^{VI(c)}, \\
\sin^2 \theta_{23} &= \frac{4 - 2\sqrt{2} \sin 2\theta}{8 + 2\sqrt{3} \cos 2\theta - \sqrt{2} \sin 2\theta} \quad \text{for } U^{VI(d)}, \\
|J_{CP}| &= \frac{1}{6\sqrt{6}} |\sin 2\theta|, \quad |I_2| = \frac{1}{36} \left| \cos 2\theta + \sqrt{6} \sin 2\theta \right|, \\
|I_1| &= \frac{1}{72} \left| 2\sqrt{7} + \sqrt{3} + \left(2 + \sqrt{21} \right) \cos 2\theta - \sqrt{14} \sin 2\theta \right|.
\end{aligned} \tag{3.78}$$

We find the sum rules in Eq. (3.76) and consequently the estimates given in Eq. (3.77) are satisfied as well. Furthermore, the sum rule of Eq. (3.49) among the mixing angles and Dirac CP phase is fulfilled for all the above four permutations of the PMNS matrix. Consequently the comments below Eq. (3.49) also hold true here. As regards the neutrinoless double beta decay, the predictions

for the effective mass $|m_{ee}|$ are given by

$$|m_{ee}| = \frac{1}{12} \left| \left((\sqrt{3}-1)e^{i\varphi} \cos \theta + (1+\sqrt{3})e^{i(\frac{3\pi}{4}+\varphi)} \sin \theta \right)^2 m_1 + 4q_1 m_2 + q_2 m_3 \left((1+\sqrt{3})e^{i(\frac{3\pi}{4}+\varphi)} \cos \theta - (\sqrt{3}-1)e^{i\varphi} \sin \theta \right)^2 \right| \quad \text{for } U^{VI(a)} \text{ and } U^{VI(b)}, \quad (3.79)$$

$$|m_{ee}| = \frac{1}{12} \left| \left((1+\sqrt{3})e^{i\varphi} \cos \theta + (\sqrt{3}-1)e^{i(\frac{3\pi}{4}+\varphi)} \sin \theta \right)^2 m_1 + 4q_1 m_2 + q_2 m_3 \left((\sqrt{3}-1)e^{i(\frac{3\pi}{4}+\varphi)} \cos \theta - (1+\sqrt{3})e^{i\varphi} \sin \theta \right)^2 \right| \quad \text{for } U^{VI(c)} \text{ and } U^{VI(d)}. \quad (3.80)$$

The parameter θ freely varies in the range of $[0, \pi]$, and the observed values of the lepton mixing angles are required to be reproduced at 3σ level. The admissible regions of $|m_{ee}|$ as a function of m_{lightest} are displayed in figure 15. We can read off from this figure that $|m_{ee}^{\text{IO}}| \simeq 0.019$ eV or 0.046 eV and $|m_{ee}^{\text{NO}}| \geq 0.00052$ eV for the mixing patterns $U^{VI(a)}$ and $U^{VI(b)}$ while $|m_{ee}^{\text{IO}}| \simeq 0.030$ eV or 0.040 eV and $|m_{ee}^{\text{NO}}| \geq 0.0018$ eV for the mixing patterns $U^{VI(c)}$ and $U^{VI(d)}$, where $|m_{ee}^{\text{IO}}|$ and $|m_{ee}^{\text{NO}}|$ are the $0\nu\beta\beta$ decay effective masses corresponding to IO and NO mass orderings respectively.

Then we turn to study the implication for leptogenesis. One can read out the lepton asymmetry parameters I_{13}^α as follows

$$\begin{aligned} I_{13}^e &= I_{13}^\mu = \frac{1}{6\sqrt{2}}, & I_{13}^\tau &= -\frac{1}{3\sqrt{2}} & \text{for } U^{VI(a)} \text{ and } U^{VI(c)}, \\ I_{13}^e &= I_{13}^\tau = \frac{1}{6\sqrt{2}}, & I_{13}^\mu &= -\frac{1}{3\sqrt{2}} & \text{for } U^{VI(b)} \text{ and } U^{VI(d)}, \end{aligned} \quad (3.81)$$

which are constant values. The numerical results for Y_B as a function of η are plotted in figure 16 and figure 17. We can see that the observed baryon asymmetry can be interpreted as an effect of leptogenesis for certain values of the parameters $K_{1,2,3}$, as listed in table 7.

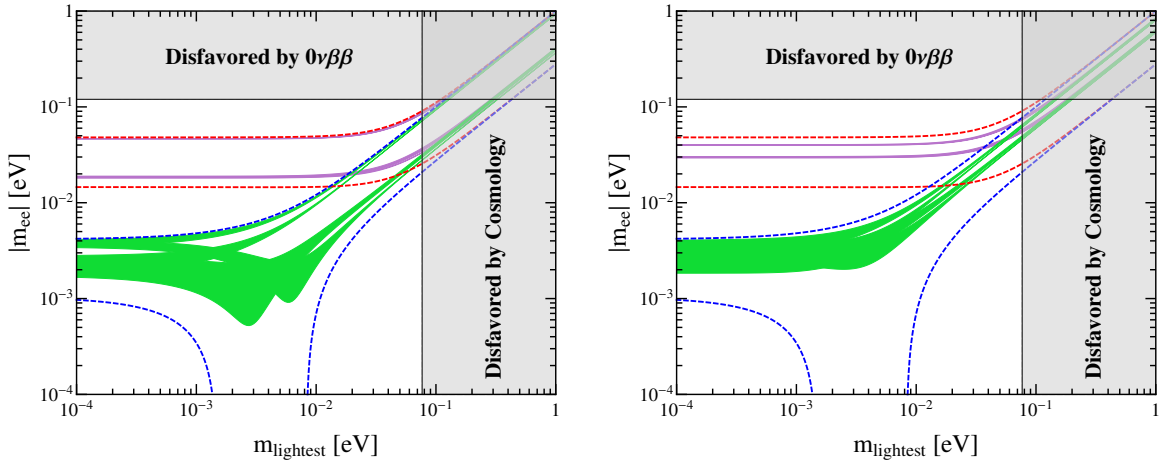


Figure 15: Predictions of the $0\nu\beta\beta$ decay effective mass $|m_{ee}|$ with respect to the lightest neutrino mass m_{lightest} in the case VI. The left panel is the result for the mixing patterns $U^{VI(a)}$ and $U^{VI(b)}$, and the right panel is for $U^{VI(c)}$ and $U^{VI(d)}$. The red (blue) dashed lines indicate the most general allowed regions for IO (NO) spectrum obtained by varying the mixing parameters within their 3σ ranges [44]. The purple and green regions are the theoretical predictions of these two mixing patterns. The present most stringent upper limits $|m_{ee}| < 0.120$ eV from EXO-200 [57, 58] and KamLAND-ZEN [59] is shown by horizontal grey band. The vertical grey exclusion band is the current limit on m_{lightest} from the cosmological data of $\sum m_i < 0.230$ eV by the Planck collaboration [60].

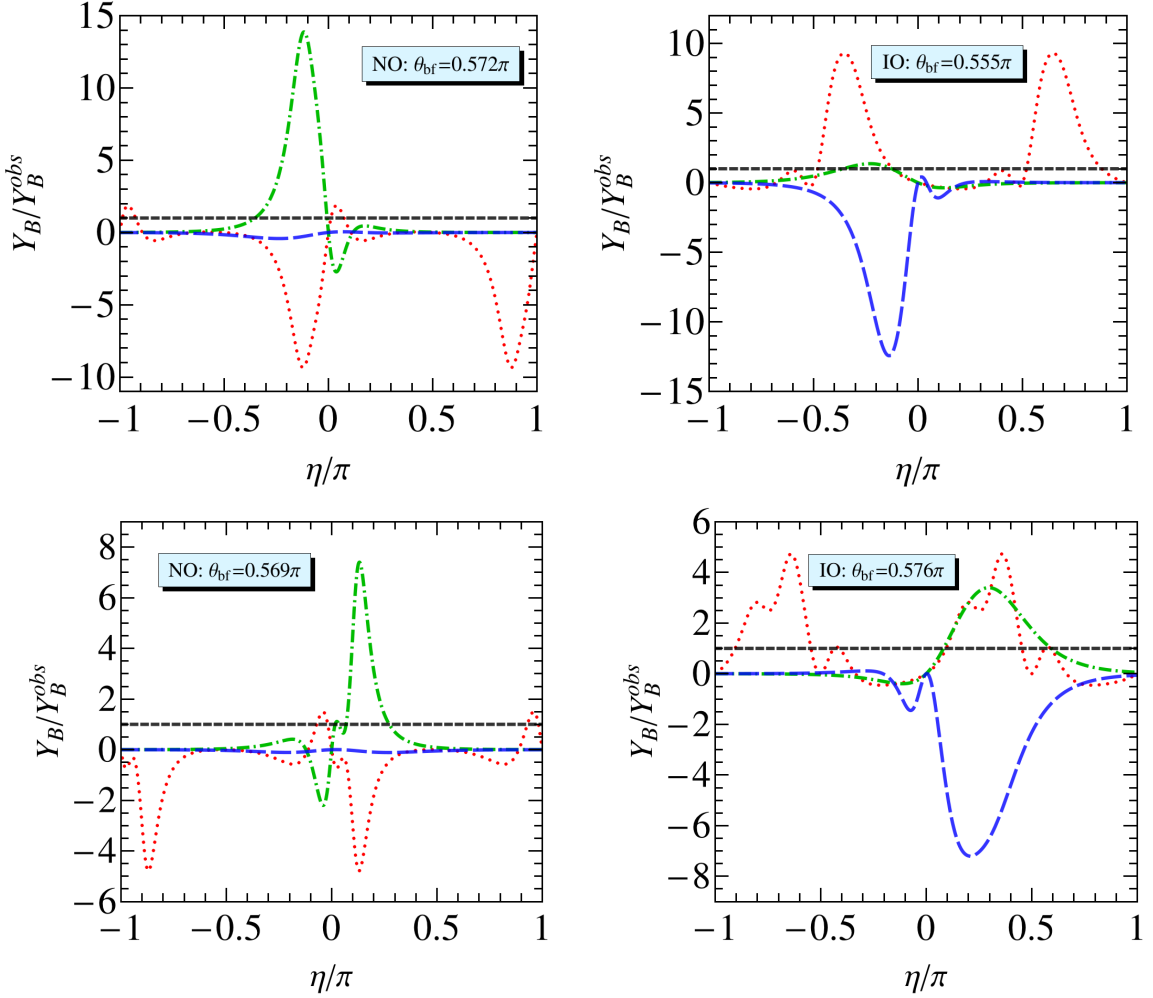


Figure 16: The prediction for Y_B/Y_B^{obs} as a function of η in case VI(a) and case VI(b) at the best fit value θ_{bf} , where the first and second rows correspond to the mixing patterns $U^{VI(a)}$ and $U^{VI(b)}$ respectively. We choose $M_1 = 5 \times 10^{11}$ GeV and the lightest neutrino mass m_1 (or m_3) = 0.01eV. The red dotted, green dot-dashed, blue dashed lines correspond to $(K_1, K_2, K_3) = (+, \pm, +), (+, \pm, -)$ and $(-, \pm, +)$ respectively. The experimentally observed value Y_B^{obs} is represented by the horizontal black dashed line.

Case VII

$$\begin{aligned}
 U^{VII(a)} &= \frac{1}{2\sqrt{6}} \begin{pmatrix} -\frac{\sqrt{3}}{s_3} & 2\sqrt{2} & \frac{s_2-s_1}{s_1 s_2} \\ \frac{\sqrt{3}}{s_2} & 2\sqrt{2} & -\frac{s_1+s_3}{s_1 s_3} \\ \frac{\sqrt{3}}{s_1} & 2\sqrt{2} & \frac{s_2+s_3}{s_2 s_3} \end{pmatrix} S_{23}(\theta) Q_\nu^\dagger, \\
 U^{VII(b)} &= \frac{1}{2\sqrt{6}} \begin{pmatrix} -\frac{\sqrt{3}}{s_3} & 2\sqrt{2} & \frac{s_2-s_1}{s_1 s_2} \\ \frac{\sqrt{3}}{s_1} & 2\sqrt{2} & \frac{s_2+s_3}{s_2 s_3} \\ \frac{\sqrt{3}}{s_2} & 2\sqrt{2} & -\frac{s_1+s_3}{s_1 s_3} \end{pmatrix} S_{23}(\theta) Q_\nu^\dagger,
 \end{aligned} \tag{3.82}$$

where $s_n \equiv \sin(2n\pi/7)$ with $n = 1, 2, 3$. We note that that $U^{VII(a)}$ and $U^{VII(b)}$ are related by the exchange of the second and third rows. Similar to case VI, this mixing pattern can also be obtained from the flavor symmetry groups [168, 42] $\cong \Sigma(168)$, [336, 209], [504, 157] and so forth in combination with generalized CP [45]. In this case, the column fixed by residual symmetry is

$$\frac{1}{2\sqrt{2}} \begin{pmatrix} -1/s_3 \\ 1/s_2 \\ 1/s_1 \end{pmatrix} \approx \begin{pmatrix} -0.815 \\ 0.363 \\ 0.452 \end{pmatrix}, \quad \text{or} \quad \frac{1}{2\sqrt{2}} \begin{pmatrix} -1/s_3 \\ 1/s_1 \\ 1/s_2 \end{pmatrix} \approx \begin{pmatrix} -0.815 \\ 0.452 \\ 0.363 \end{pmatrix}. \tag{3.83}$$

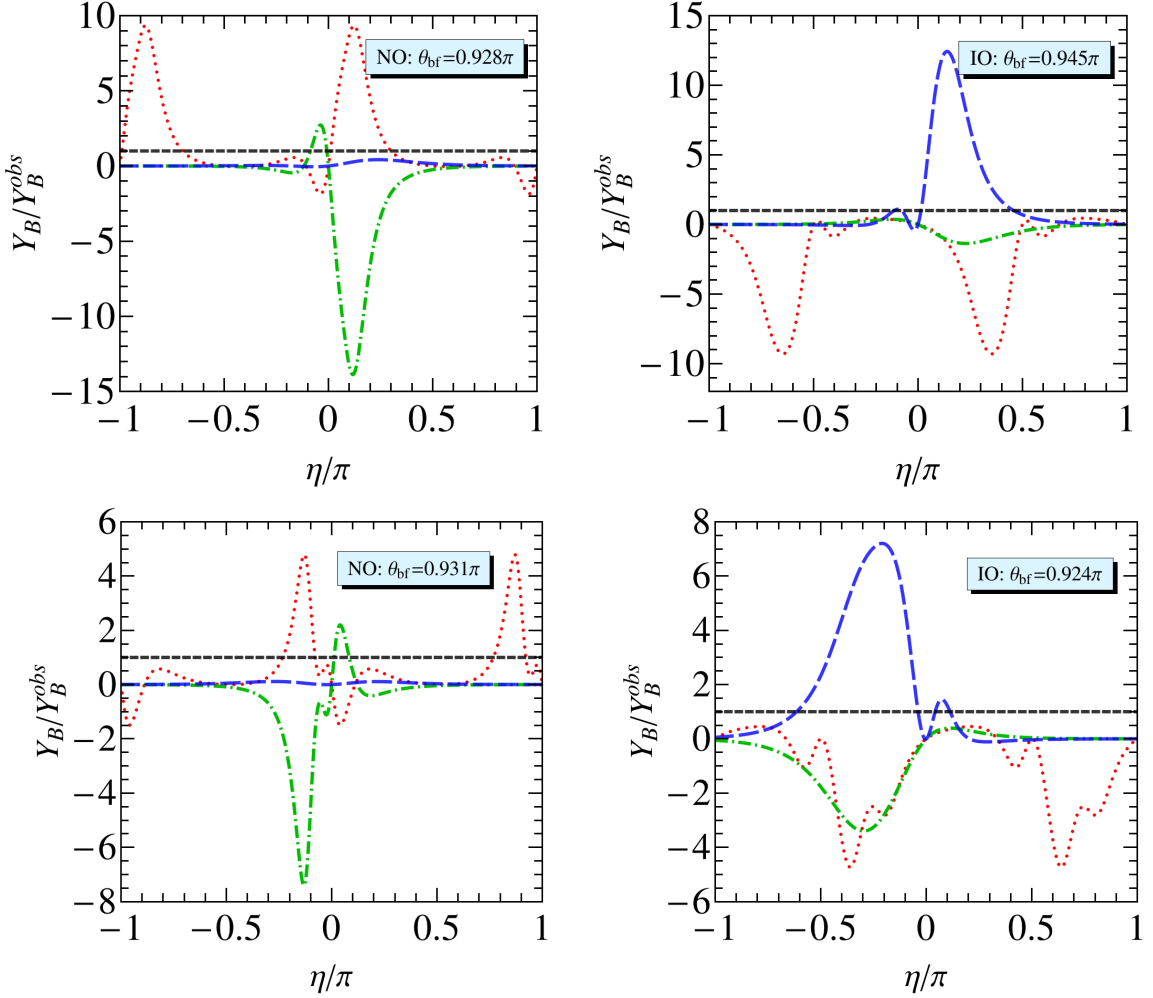


Figure 17: The prediction for Y_B/Y_B^{obs} as a function of η in case VI(c) and case VI(d) at the best fit value θ_{bf} , where the first and second rows correspond to the mixing patterns $U^{VI(c)}$ and $U^{VI(d)}$ respectively. We choose $M_1 = 5 \times 10^{11}$ GeV and the lightest neutrino mass m_1 (or m_3) = 0.01eV. The red dotted, green dot-dashed, blue dashed lines correspond to $(K_1, K_2, K_3) = (+, \pm, +), (+, \pm, -)$ and $(-, \pm, +)$ respectively. The experimentally observed value Y_B^{obs} is represented by the horizontal black dashed line.

It should be identified with the first column of the PMNS matrix to be in accordance with the experimental data. From the mixing matrices in Eq. (3.82), we find the following results for the lepton mixing angles

$$\begin{aligned}
\sin^2 \theta_{13} &= \frac{(2\sqrt{2}s_1s_2 \sin \theta + (s_1 - s_2) \cos \theta)^2}{24s_1^2s_2^2}, \\
\sin^2 \theta_{12} &= \frac{(2\sqrt{2}s_1s_2 \cos \theta + (s_2 - s_1) \sin \theta)^2}{2\sqrt{2}s_1s_2(s_2 - s_1) \sin 2\theta - (s_2 - s_1)^2 \cos^2 \theta + 4s_1^2s_2^2(\cos 2\theta + 5)}, \\
\sin^2 \theta_{23} &= \frac{s_2^2(2\sqrt{2}s_1s_3 \sin \theta + (s_1 + s_3) \cos \theta)^2}{s_3^2(2\sqrt{2}s_1s_2(s_2 - s_1) \sin 2\theta - (s_2 - s_1)^2 \cos^2 \theta + 4s_1^2s_2^2(\cos 2\theta + 5))} \quad \text{for } U^{VII(a)}, \\
\sin^2 \theta_{23} &= \frac{s_1^2(2\sqrt{2}s_2s_3 \sin \theta - (s_2 + s_3) \cos \theta)^2}{s_3^2(2\sqrt{2}s_1s_2(s_2 - s_1) \sin 2\theta - (s_2 - s_1)^2 \cos^2 \theta + 4s_1^2s_2^2(\cos 2\theta + 5))} \quad \text{for } U^{VII(b)},
\end{aligned} \tag{3.84}$$

and

$$J_{CP} = I_1 = I_2 = 0, \tag{3.85}$$

which implies that all the three CP violating phases δ_{CP} , α_{21} and α_{31} are trivial. Expressing the parameter θ in terms of θ_{13} , we can obtain the sum rules among the lepton mixing angles,

$$8 \cos^2 \theta_{12} \cos^2 \theta_{13} = \frac{1}{s_3^2},$$

$$\sin^2 \theta_{23} \cos^2 \theta_{13} = \frac{\left(\sqrt{(8 \cos^2 \theta_{13} s_3^2 - 1)(s_2^2(8s_3^2 - 1) - s_3^2)} \pm s_3 \sin \theta_{13} \right)^2}{s_2^2(8s_3^2 - 1)^2} \quad \text{for } U^{VII(a)}, \quad (3.86)$$

$$\sin^2 \theta_{23} \cos^2 \theta_{13} = \frac{\left(\sqrt{(8 \cos^2 \theta_{13} s_3^2 - 1)(s_1^2(8s_3^2 - 1) - s_3^2)} \pm s_3 \sin \theta_{13} \right)^2}{s_1^2(8s_3^2 - 1)^2} \quad \text{for } U^{VII(b)}.$$

Given the best fitting value of the reactor mixing angle $\sin^2 \theta_{13} = 0.0218$ [44], we obtain

$$\sin^2 \theta_{12} = 0.321, \quad \sin^2 \theta_{23} = 0.399 \quad \text{or} \quad 0.601. \quad (3.87)$$

For this mixing pattern, the effective Majorana neutrino mass $|m_{ee}|$ is given by

$$|m_{ee}| = \frac{1}{24} \left| \frac{3m_1}{s_3^2} + q_1 m_2 \left(2\sqrt{2} \cos \theta + \left(\frac{1}{s_1} - \frac{1}{s_2} \right) \sin \theta \right) + q_2 m_3 \left(-2\sqrt{2} \sin \theta + \left(\frac{1}{s_1} - \frac{1}{s_2} \right) \cos \theta \right) \right|^2, \quad (3.88)$$

As shown in figure 18, $|m_{ee}|$ is around 0.017eV or 0.048eV in the case of IO, while a noticeable cancellation occurs such that $|m_{ee}|$ can be smaller than 10^{-4} eV for NO if the lightest neutrino mass lies in the interval $[0.0022, 0.0032]$ eV or $[0.0064, 0.0074]$ eV. Regarding the predictions for leptogenesis, all the relevant CP invariants I_{23}^α as well as the lepton asymmetries ϵ_α are zero. Thus a model, realizing this pattern at leading order, should receive moderate corrections to interpret the observed baryon asymmetry as an effect of leptogenesis.

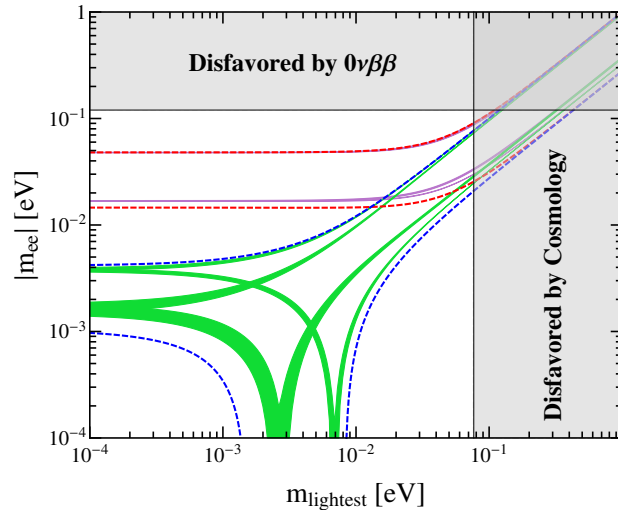


Figure 18: The Predictions of the $0\nu\beta\beta$ decay effective mass $|m_{ee}|$ with respect to the lightest neutrino mass m_{lightest} for the mixing patterns $U^{VII(a)}$ and $U^{VII(b)}$. The red (blue) dashed lines indicate the most general allowed regions for IO (NO) spectrum obtained by varying the mixing parameters within their 3σ ranges [44]. The purple and green regions are the theoretical predictions of these two mixing patterns. The present most stringent upper limits $|m_{ee}| < 0.120$ eV from EXO-200 [57, 58] and KamLAND-ZEN [59] is shown by horizontal grey band. The vertical grey exclusion band is the current limit on m_{lightest} from the cosmological data of $\sum m_i < 0.230$ eV by the Planck collaboration [60].

3.2 Mixing patterns derived from the variant of semidirect approach

In this approach, the residual flavor symmetries in the neutrino and charged lepton sectors are $K_4 \times H_{CP}^\nu$ and $Z_2 \times H_{CP}^l$ respectively. The prediction for the PMNS mixing matrix can be straightforwardly extracted from Eq. (2.51). It is remarkable that the resulting mixing matrix has one column which is determined by the residual symmetries and which does not depend on the free parameter θ . In exactly the same manner as the semidirect approach in section 3.1, we perform a comprehensive scan over all possible finite discrete groups of the order less than 2000 with the help of GAP. We find only one type of mixing pattern which can accommodate the experimental data on lepton mixing angles for particular choices of the free parameter θ

$$U^{VIII(a)} = \frac{1}{2} S_{13}^T(\theta) \begin{pmatrix} \sqrt{2}e^{i\varphi_1} & -\sqrt{2}e^{i\varphi_1} & 0 \\ 1 & 1 & -\sqrt{2}e^{i\varphi_2} \\ 1 & 1 & \sqrt{2}e^{i\varphi_2} \end{pmatrix} Q_\nu^\dagger, \quad U^{VIII(b)} = P_{132} U_{PMNS}^{VIII(a)}, \quad (3.89)$$

where the viable values of φ_1 , φ_2 and the representative flavor symmetry groups are summarized in table 8. Notice that all these mixing patterns can be reproduced from the type D group series $\Delta(6n^2)$ and $D_{9n,3n}^{(1)}$, and the small flavor symmetry groups S_4 and $\Delta(96)$ already allows a reasonable fit to the experimental data for this type of mixing pattern. This is consistent with the findings in Ref. [11]. Obvious $U_{PMNS}^{VIII(b)}$ is obtained from $U_{PMNS}^{VIII(a)}$ by exchanging the second and third rows. In this case, the row that is fixed by residual symmetry is $(1, 1, -\sqrt{2}e^{i\varphi_2})/2$, and it could be the second or the third row of the PMNS mixing matrix. The predictions for the mixing angles read as

$$\begin{aligned} \sin^2 \theta_{13} &= \frac{1}{2} \sin^2 \theta, & \sin^2 \theta_{12} &= \frac{1}{2} + \frac{\sqrt{2} \sin 2\theta \cos \varphi_1}{3 + \cos 2\theta}, \\ \sin^2 \theta_{23} &= \frac{2}{3 + \cos 2\theta} \quad \text{for } U^{VIII(a)}, & \sin^2 \theta_{23} &= \frac{1 + \cos 2\theta}{3 + \cos 2\theta} \quad \text{for } U^{VIII(b)}, \end{aligned} \quad (3.90)$$

and the CP invariants take the form

$$\begin{aligned} |J_{CP}| &= \frac{1}{8\sqrt{2}} |\sin 2\theta \sin \varphi_1|, & |I_1| &= \frac{1}{8\sqrt{2}} |(1 + 3 \cos 2\theta) \sin 2\theta \sin \varphi_1|, \\ |I_2| &= \frac{\sin^2 \theta}{8} \left| \sqrt{2} \sin 2\theta \sin(2\varphi_2 - \varphi_1) - 2 \cos^2 \theta \sin 2(\varphi_2 - \varphi_1) - \sin^2 \theta \sin 2\varphi_2 \right|. \end{aligned} \quad (3.91)$$

We easily see that the reactor and atmospheric mixing angles are related by

$$\sin^2 \theta_{23} = \frac{1}{2 \cos^2 \theta_{13}} \quad \text{for } U^{VIII(a)}, \quad \sin^2 \theta_{23} = \frac{\cos 2\theta_{13}}{2 \cos^2 \theta_{13}} \quad \text{for } U^{VIII(b)}. \quad (3.92)$$

Given the 3σ range $0.0188 \leq \sin^2 \theta_{13} \leq 0.0251$ of θ_{13} [44], the atmospheric mixing angle θ_{23} is determined to lie in the region of

$$0.510 \leq \sin^2 \theta_{23} \leq 0.513 \quad \text{for } U^{VIII(a)}, \quad 0.487 \leq \sin^2 \theta_{23} \leq 0.490 \quad \text{for } U^{VIII(b)}, \quad (3.93)$$

which deviates from maximal mixing slightly. Similarly the sum rule among the reactor and solar mixing angles is given by

$$\sin^2 \theta_{12} = \frac{1}{2} \pm \tan \theta_{13} \sqrt{1 - \tan^2 \theta_{13}} \cos \varphi_1, \quad (3.94)$$

where the “+” and “−” signs are valid $0 < \theta < \pi/2$ and $\pi/2 < \theta < \pi$ respectively. For the experimentally favored 3σ interval of the reactor mixing angle, we get

$$0.342 \leq \sin^2 \theta_{12} \leq 0.363. \quad (3.95)$$

As a example, for $\sin^2 \theta_{13} = 0.0251$ ($\theta \simeq 0.072\pi$ or $\theta \simeq 1.928\pi$) and $\varphi_1 = \pi$ (or 0), we find the value of the solar mixing angle $\sin^2 \theta_{12} \simeq 0.342$ which is within the 3σ range. Therefore $\sin^2 \theta_{12}$ is

Group Id	(φ_1, φ_2)
$[24, 12]_\Delta, [48, 48]$	(π, π)
$[96, 64]_\Delta, [192, 944]$	$(0, \frac{3\pi}{4})$
$[384, 568]_\Delta,$ $[768, 1085727]$	$(\frac{\pi}{8}, -\frac{5\pi}{8}), (\frac{\pi}{8}, \pi), (0, \frac{7\pi}{8}), (\frac{\pi}{8}, -\frac{7\pi}{8}), (-\frac{7\pi}{8}, \frac{3\pi}{4})$
$[600, 179]_\Delta, [1200, 1011]$	$(0, -\frac{4\pi}{5}), (0, -\frac{9\pi}{10}), (-\frac{\pi}{10}, \frac{9\pi}{10}), (-\frac{\pi}{5}, -\frac{4\pi}{5}), (-\frac{\pi}{10}, \frac{7\pi}{10}), (-\frac{\pi}{5}, \pi),$ $(-\frac{\pi}{5}, \frac{9\pi}{10}), (-\frac{\pi}{10}, -\frac{9\pi}{10}), (-\frac{\pi}{5}, \frac{4\pi}{5}), (-\frac{\pi}{10}, \pi), (-\frac{\pi}{10}, -\frac{7\pi}{10}), (-\frac{\pi}{5}, -\frac{9\pi}{10})$
$[648, 259]_{\Delta'}, [648, 260]$	$(-\frac{5\pi}{6}, \frac{2\pi}{3}), (-\frac{5\pi}{6}, \pi), (-\frac{5\pi}{6}, -\frac{2\pi}{3}), (-\pi, -\frac{5\pi}{6})$
$[1176, 243]_\Delta$	$(0, -\frac{5\pi}{7}), (0, -\frac{13\pi}{14}), (\frac{13\pi}{14}, -\frac{13\pi}{14}), (\frac{13\pi}{14}, -\frac{9\pi}{14}), (\frac{13\pi}{14}, -\frac{6\pi}{7}),$ $(-\frac{6\pi}{7}, \frac{13\pi}{14}), (0, -\frac{6\pi}{7}), (-\frac{\pi}{14}, \frac{13\pi}{14}), (\frac{13\pi}{14}, \frac{5\pi}{7}), (\frac{3\pi}{14}, \pi), (\frac{13\pi}{14}, \pi),$ $(\frac{\pi}{7}, \frac{4\pi}{7}), (\frac{3\pi}{14}, \frac{5\pi}{7}), (-\frac{\pi}{14}, \frac{11\pi}{14}), (-\frac{11\pi}{14}, \frac{13\pi}{14}), (\frac{\pi}{7}, \frac{11\pi}{14}), (\frac{3\pi}{14}, -\frac{6\pi}{7}),$ $(\frac{\pi}{7}, \pi), (\frac{3\pi}{14}, \frac{6\pi}{7}), (\frac{\pi}{7}, -\frac{11\pi}{14}), (\frac{3\pi}{14}, -\frac{13\pi}{14}), (\frac{3\pi}{14}, -\frac{5\pi}{7}), (\frac{\pi}{7}, -\frac{6\pi}{7}),$ $(\frac{\pi}{7}, -\frac{9\pi}{14})$
$[1536, 408544632]_\Delta$	$(-\frac{13\pi}{16}, \frac{7\pi}{8}), (\frac{\pi}{16}, \frac{13\pi}{16}), (\frac{\pi}{16}, \pi), (\frac{\pi}{16}, -\frac{13\pi}{16}), (\frac{\pi}{16}, \frac{7\pi}{8}), (-\pi, \frac{15\pi}{16}),$ $(\frac{\pi}{16}, -\frac{15\pi}{16}), (\frac{\pi}{16}, -\frac{3\pi}{4}), (\frac{\pi}{16}, -\frac{9\pi}{16}), (\frac{3\pi}{16}, -\frac{11\pi}{16}), (\frac{\pi}{8}, -\frac{13\pi}{16}), (\frac{3\pi}{16}, -\frac{7\pi}{8}),$ $(\frac{\pi}{8}, \frac{13\pi}{16}), (\frac{3\pi}{16}, \frac{15\pi}{16}), (\frac{3\pi}{16}, -\frac{3\pi}{4}), (\frac{3\pi}{16}, \pi), (0, \frac{11\pi}{16}), (\frac{\pi}{8}, \frac{15\pi}{16}),$ $(\frac{3\pi}{16}, -\frac{15\pi}{16}), (\frac{\pi}{8}, \frac{9\pi}{16}), (\frac{3\pi}{16}, \frac{11\pi}{16}), (-\frac{15\pi}{16}, \frac{5\pi}{8})$

Table 8: The predictions for PMNS matrix of the form $U^{VIII(a)}$ and $U^{VIII(b)}$, where the first column shows the group identification in GAP system, and the second column displays the achievable values of the parameters φ_1 and φ_2 . We have shown at most two representatives flavor symmetry groups in the first column. If there is only one group predicting the corresponding values of φ_1 and φ_2 in the second column, this unique group would be listed. The full results of our analysis are provided at the website [45]. The subscripts Δ and Δ' indicate that the corresponding groups belong to the type D group series $D_{n,n}^{(0)} \cong \Delta(6n^2)$ and $D_{9n',3n'}^{(1)} \cong (Z_{9n'} \times Z_{3n'}) \rtimes S_3$, respectively.

generically predicted to be close to its 3σ upper limit in this case¹. Notice that better agreement of the predicted values of $\sin^2 \theta_{12}$ with the experimental results could be achieved in a concrete model with small corrections.

Moreover, we find that the Dirac CP phase is correlated with the mixing angles as follows

$$\cos \delta_{CP} = \pm \frac{(3 \cos 2\theta_{13} - 1) \cot 2\theta_{12}}{4\sqrt{\cos 2\theta_{13}} \sin \theta_{13}}, \quad (3.96)$$

where the “+” and “-” correspond to $U^{VIII(a)}$ and $U^{VIII(b)}$ respectively. If the reactor and solar mixing angles vary within the 3σ intervals $0.0188 \leq \sin^2 \theta_{13} \leq 0.0251$ and $0.270 \leq \sin^2 \theta_{12} \leq 0.344$ [44], we obtain

$$\cos \delta_{CP} \in \pm[0.983, 1]. \quad (3.97)$$

Hence δ_{CP} is predicted to be around 0 or π in this case. This mixing pattern would be ruled out if large CP violation effect is discovered in planned long baseline experiments.

From the mixing matrix shown in Eq. (3.89), we can extract the expression for the effective Majorana mass $|m_{ee}|$,

$$|m_{ee}| = \frac{1}{4} \left| m_1 \left(\sqrt{2} e^{i\varphi_1} \cos \theta - \sin \theta \right)^2 + q_1 m_2 \left(\sin \theta + \sqrt{2} e^{i\varphi_1} \cos \theta \right)^2 + 2q_2 m_3 e^{2i\varphi_2} \sin^2 \theta \right|, \quad (3.98)$$

with $q_{1,2} = \pm 1$. We plot the possible region of $|m_{ee}|$ as a function of the lightest neutrino mass m_{lightest} in figure 19. In the limit of $|G_f| \rightarrow \infty$, we see that the entire 3σ region for IO and a sizable part for NO can be reproduced. For the particular value of $(\varphi_1, \varphi_2) = (\pi, \pi)$ which can be achieved from S_4 flavor symmetry combined with CP symmetry, we can read off from this figure $|m_{ee}^{\text{IO}}| \simeq$

¹The 3σ ranges of $\sin^2 \theta_{12}$ obtained by distinct global fitting groups have some minor difference: $0.270 \leq \sin^2 \theta_{12} \leq 0.344$ from the NuFIT group [44], $0.278 \leq \sin^2 \theta_{12} \leq 0.375$ from the Valencia group [65] and $0.250 \leq \sin^2 \theta_{12} \leq 0.354$ given by the Italian group [66].

0.015 eV or $|m_{ee}^{\text{IO}}| \simeq 0.048$ eV and $|m_{ee}^{\text{NO}}|$ is highly suppressed for $0.0026 \text{ eV} \leq m_{\text{lightest}} \leq 0.0031$ eV and $0.0079 \text{ eV} \leq m_{\text{lightest}} \leq 0.0084$ eV.

As has been shown in Ref. [27], if a Klein four flavor symmetry is preserved by the neutrino mass matrix, all the leptogenesis CP asymmetries ϵ_α would vanish and this result is independent of the concrete form of the residual Klein flavor symmetry transformation. Since the residual flavor symmetry of the neutrino sector is K_4 in the variant of the semidirect approach, a net baryon asymmetry can not be generated, and appropriate higher order corrections are necessary to have successful leptogenesis.

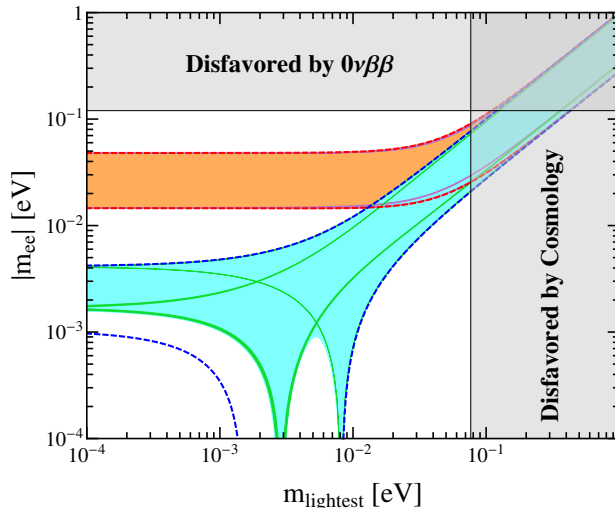


Figure 19: Predictions of the $0\nu\beta\beta$ decay effective mass $|m_{ee}|$ with respect to the lightest neutrino mass m_{lightest} for the mixing patterns $U^{VIII(a)}$ and $U^{VIII(b)}$. The red (blue) dashed lines indicate the most general allowed regions for IO (NO) spectrum obtained by varying the mixing parameters within their 3σ ranges [44]. The orange (cyan) areas denote the achievable values of $|m_{ee}|$ when φ_1 and φ_2 are taken to be free continuous parameters in the case of IO (NO). The purple and green regions are the theoretical predictions of the smallest flavor symmetry group which can generate these two mixing patterns. Note that the purple (green) region overlaps the orange (cyan) one. The present most stringent upper limits $|m_{ee}| < 0.120$ eV from EXO-200 [57, 58] and KamLAND-ZEN [59] is shown by horizontal grey band. The vertical grey exclusion band is the current limit on m_{lightest} from the cosmological data of $\sum m_i < 0.230$ eV by the Planck collaboration [60].

4 Conclusions

Flavor and CP symmetries have been widely used to predict leptonic mixing parameters. In the present work, we take into account the generalized CP symmetry and perform an exhaustive scan of the lepton mixing patterns which can be obtained from the discrete finite groups up to order 2000 with the help of computer program GAP. The generalized CP transformations are required to correspond to class-inverting automorphisms of the flavor symmetry group G_f , so that the consistency conditions between flavor and CP symmetry can be fulfilled. If G_f doesn't possess a class-inverting automorphism, a CP symmetry could possibly be consistently defined in a model which contains only a subset of irreducible representations of G_f .

The flavor and CP symmetries have to be broken at low energy. The PMNS mixing matrix is fully fixed by the residual symmetries of the neutrino and charged lepton mass matrices, and we do not need to consider how the residual symmetries are dynamically realized. In this work, we have considered two scenarios: the semidirect approach and the variant of the semidirect approach. In the semidirect approach, the residual symmetries of the charged lepton and neutrino mass matrices are $G_l \times H_{CP}^l$ and $Z_2 \times H_{CP}^\nu$ respectively, where G_l can be any abelian subgroup of G_f capable of distinguishing the three generations. In the variant of the semidirect approach, the flavor and CP symmetries are assumed to be broken down to $Z_2 \times H_{CP}^l$ and $K_4 \times H_{CP}^\nu$ in the charged lepton and neutrino sectors respectively. The PMNS matrix can be determined from the representation matrix

of the residual symmetry without reconstructing the neutrino and charged lepton mass matrices, and the master formula is given by Eq. (2.27) and Eq. (2.51) respectively. We see that the PMNS matrix depends on only a free parameter θ which can take values in the range of $[0, \pi)$ in both approaches. Nevertheless, one column of the PMNS matrix is fixed to certain constant value by the residual symmetry in the semidirect approach while one row is fixed in its variant.

For each discrete flavor group which has a faithful three-dimensional irreducible representation and a class-inverting outer automorphism, all the possible remnant symmetries and the resulting predictions for lepton flavor mixing are studied. All these results are available at our website [45]. We find that all the mixing patterns which can accommodate the experimental data on the mixing angles can be organized into eight different cases up to possible permutations of rows and columns. It is remarkable that the mixing matrices of case I, case II and case III can be reproduced from the $\Delta(6n^2)$ or $D_{9n,3n}^{(1)}$ groups combined with the CP symmetry. The list of the mixing matrices associated with $\Delta(6n^2)$ and $D_{9n,3n}^{(1)}$ agrees exactly with those given in Refs. [22, 25, 26]. The smallest group which can produce the mixing patterns of case IV and case V is the alternating group A_5 . These two mixing patterns have really been found in the literature of A_5 flavor symmetry with generalised CP [17–19]. The mixing patterns of case VI and case VII are completely new as far as we know. They can be achieved from the flavor symmetry group $\Sigma(168) \cong PSL(2, 7)$ and CP symmetry. The second column of the resulting PMNS mixing matrix is trimaximal in case II, case III and case VI, and therefore the sum rule $3 \sin^2 \theta_{12} \cos^2 \theta_{13} = 1$ is satisfied and the solar mixing angle is bounded from below $\sin^2 \theta_{12} \geq 1/3$. In the variant of the semidirect approach, only one type of mixing matrix denoted as case VIII can yield a good fit to the experimental data, and one row of the PMNS matrix is $(1, 1, -\sqrt{2}e^{i\varphi_2})/2$. The solar mixing angle θ_{12} is predicted to be close to its 3σ upper bound, and the atmospheric mixing angle is around $\sin^2 \theta_{23} \simeq 0.49$ or $\sin^2 \theta_{23} \simeq 0.51$. As a result, the paradigm of the generalized CP symmetry should be testable by precisely measuring θ_{12} and θ_{23} at future reactor neutrino experiments such as JUNO and long baseline experiments DUNE and Hyper-K.

Furthermore, the implications of residual symmetry in $0\nu\beta\beta$ decay and flavored thermal leptogenesis are studied. The predicted values of the effective Majorana mass $|m_{ee}|$ are within the sensitivity of planned experiments for IO neutrino mass spectrum, the known cancellation of the different terms in $|m_{ee}|$ may occur in the case of NO although $|m_{ee}|$ could have a non-trivial lower limit for a certain finite group. As regards the leptogenesis, the R -matrix in the Casas-Ibarra parametrization only depends on one single parameter η because of the constraint imposed by remnant symmetry. The total lepton asymmetry $\epsilon_1 \equiv \epsilon_e + \epsilon_\mu + \epsilon_\tau$ is determined to be zero such that the unflavored leptogenesis does not work. On the other hand, all the lepton charge asymmetries ϵ_α ($\alpha = e, \mu, \tau$) are vanishing in case III, case V, case VII and case VIII, consequently the matter-antimatter asymmetry of the universe can not be explained via leptogenesis unless the postulated residual symmetry is further broken at the subleading level. For the remaining case I, case II, case IV and case VI, the measured value of the baryon asymmetry can be generated for certain values of the parameters η and $K_{1,2,3}$ which are determined by the CP parity of the neutrino states.

Many interesting mixing patterns and the associated residual symmetry provide new opportunity for model building. It would be interesting to construct concrete models in which the breaking of the symmetry group to the residual symmetry is achieved dynamically. Inspired by the above promising results obtained for lepton mixing, it is appealing to investigate whether the quark mixing angles and the precisely measured CP violating phase can be obtained as a result of mismatched remnant symmetries in the down quark and up quark sectors if the generalized CP symmetry is considered.

Acknowledgements

We are grateful to Peng Chen for stimulating discussions on leptogenesis. This work is supported by the National Natural Science Foundation of China under Grant Nos. 11275188, 11179007 and 11522546.

A Equivalent conditions of distinct mixing patterns

In both the semidirect approach and the variant of the semidirect approach discussed in section 2, two distinct residual symmetries could lead to the same PMNS mixing matrix up to permutations of rows and columns and redefinition of the free parameter θ and the CP parity matrix Q_ν . Then the lepton mixing matrices following from these two residual symmetries would be called equivalent. For example, the mixing matrices predicted by two residual symmetries conjugate under a group element are equivalent, as shown in the end of section 2. In the following, we shall derive the most general equivalent conditions for both approaches.

A.1 Equivalence in semidirect approach

Let us consider two generic residual symmetries in the semidirect approach, their predictions for the lepton mixing matrix can be written as

$$\begin{aligned} U_1 &= Q_{l1}^\dagger P_{l1}^T \Sigma_1 S_{23}(\theta_1) P_{\nu 1} Q_{\nu 1}^\dagger, \\ U_2 &= Q_{l2}^\dagger P_{l2}^T \Sigma_2 S_{23}(\theta_2) P_{\nu 2} Q_{\nu 2}^\dagger, \end{aligned} \quad (\text{A.1})$$

where $\Sigma = \Sigma_l^\dagger \Sigma_\nu$, Σ_1 and Σ_2 are the corresponding results of Σ for the two postulated residual symmetries. $Q_{l1,2}$ are arbitrary diagonal phase matrices and $Q_{\nu 1,2}$ are unitary diagonal matrices with nonvanishing entries ± 1 and $\pm i$. $P_{l1,2}$ and $P_{\nu 1,2}$ are permutation matrices, and they can take the six possible forms in Eq. (3.7). Moreover, θ_1 and θ_2 are free continuous parameters within the fundamental interval of $[0, \pi)$. For any given values of θ_1 and the matrices $Q_{l1}, P_{l1}, Q_{\nu 1}, P_{\nu 1}$, if the corresponding values of θ_2 as well as $Q_{l2}, P_{l2}, Q_{\nu 2}, P_{\nu 2}$ can be found such the equality $U_1 = U_2$ is fulfilled, these two residual symmetries would be equivalent, i.e.,

$$Q_{l1}^\dagger P_{l1}^T \Sigma_1 S_{23}(\theta_1) P_{\nu 1} Q_{\nu 1}^\dagger = Q_{l2}^\dagger P_{l2}^T \Sigma_2 S_{23}(\theta_2) P_{\nu 2} Q_{\nu 2}^\dagger, \quad (\text{A.2})$$

from which we can define a matrix Ξ which is independent of θ_1 and θ_2 as follows

$$\Xi \equiv \Sigma_1^\dagger P_{l1} Q_{l1} Q_{l2}^\dagger P_{l2}^T \Sigma_2 = S_{23}(\theta_1) P_{\nu 1} Q_{\nu 1}^\dagger Q_{\nu 2} P_{\nu 2}^T S_{23}^T(\theta_2). \quad (\text{A.3})$$

For convenience, introducing the notations $P_l = P_{l1} P_{l2}^T$, $Q_l = P_{l2} Q_{l1} Q_{l2}^\dagger P_{l2}^T$, $P_\nu = P_{\nu 1} P_{\nu 2}^T$ and $Q_\nu = P_{\nu 2} Q_{\nu 1} Q_{\nu 2}^\dagger P_{\nu 2}^T$, then we have

$$\Xi = \Sigma_1^\dagger P_l Q_l \Sigma_2 = S_{23}(\theta_1) P_\nu Q_\nu S_{23}^T(\theta_2), \quad (\text{A.4})$$

which implies

$$\Xi \Xi^T = S_{23}(\theta_1) Q_\nu'^2 S_{23}^T(\theta_1), \quad (\text{A.5})$$

where $Q_\nu' = P_\nu Q_\nu P_\nu^T$. Since Ξ doesn't depend on the parameters θ_1 and θ_2 , the right hand side of the above equation has to be independent of θ_1 . This requires Q_ν' should be of the form

$$Q_\nu'^2 = \pm \text{diag}(1, \pm 1_{2 \times 2}). \quad (\text{A.6})$$

Therefore the (22) and (33) elements of Q_ν' are either ± 1 or $\pm i$ simultaneously while the (11) element denoted as q_ν is independently ± 1 and $\pm i$. Without loss of generality, we assume that the fixed column by residual symmetries is the first column of the PMNS matrix, thus the permutation matrices $P_{\nu 1}$ and $P_{\nu 2}$ as well as P_ν can be either P_{123} or P_{132} . Using the properties $S_{23}^T(\theta) = S_{23}(-\theta)$, $P_{132} S_{23}(\theta) = S_{23}(-\theta) P_{132}$ and $\text{diag}(1, 1, -1) S_{23}(\theta) = S_{23}(-\theta) \text{diag}(1, 1, -1)$, we can obtain

$$\Xi = \Sigma_1^\dagger P_l Q_l \Sigma_2 = S_{23}(\theta_1) Q_\nu' P_\nu S_{23}^T(\theta_2) = S_{23}(\theta_0) Q_\nu' P_\nu, \quad (\text{A.7})$$

where $\theta_0 = \theta_1 \pm \theta_2$, “+” and “-” depend on the values of Q_ν' and P_ν . Assuming the common first column of Σ_1 and Σ_2 is v_1 , the (11) entry of then the (11) entry of the Ξ matrix is

$$v_1^\dagger P_l Q_l v_1 = q_\nu. \quad (\text{A.8})$$

We parameterize v_1 and Q_l as $v_1 = (a, b, c)^T$ and $Q_l = \text{diag}(e^{i\alpha_1}, e^{i\alpha_2}, e^{i\alpha_3})$, where a, b, c can be set to be positive real numbers by redefining the charged lepton fields with the property $a^2 + b^2 + c^2 = 1$. In the following we shall discuss the constraints of Eqs. (A.7, A.8) for the six possible forms of P_l one by one.

Firstly, in the case of $P_l = P_{123} = \mathbb{1}_{3 \times 3}$, Eq. (A.8) becomes

$$e^{i\alpha_1} a^2 + e^{i\alpha_2} b^2 + e^{i\alpha_3} c^2 = q_\nu. \quad (\text{A.9})$$

Taking the absolute value of the both sides of this equation, we obtain

$$|e^{i\alpha_1} a^2 + e^{i\alpha_2} b^2 + e^{i\alpha_3} c^2| \leq a^2 + b^2 + c^2 = 1 = |q_\nu|. \quad (\text{A.10})$$

This equality is fulfilled if and only if

$$e^{i\alpha_1} = e^{i\alpha_2} = e^{i\alpha_3} = q_\nu. \quad (\text{A.11})$$

Thus $Q_l = q_\nu \mathbb{1}_{3 \times 3}$, and Eq. (A.7) reduces to

$$\Omega \equiv \Sigma_1^\dagger P_l \Sigma_2 = q_\nu^* S_{23}(\theta_0) Q'_\nu P_\nu, \quad (\text{A.12})$$

which can be written into a equivalent and more compact form

$$\Omega \Omega^T = q_\nu^{*2} Q_\nu'^2 = \text{diag}(1, \pm \mathbb{1}_{2 \times 2}), \quad (\text{A.13})$$

Conversely, if the condition of Eq. (A.12) or Eq. (A.13) is satisfied, one can easily see that the two PMNS mixing matrices U_1 and U_2 in Eq. (A.1) would be equivalent.

For the case of $P_l = P_{132}$, then Eq. (A.8) becomes

$$e^{i\alpha_1} a^2 + e^{i\alpha_2} bc + e^{i\alpha_3} bc = q_\nu. \quad (\text{A.14})$$

Taking the absolute value on both sides of this equation, we get

$$|e^{i\alpha_1} a^2 + e^{i\alpha_2} bc + e^{i\alpha_3} bc| \leq a^2 + 2bc \leq a^2 + b^2 + c^2 = 1, \quad (\text{A.15})$$

which requires

$$e^{i\alpha_1} = e^{i\alpha_2} = e^{i\alpha_3}, \quad b = c. \quad (\text{A.16})$$

Consequently the equivalent condition in Eq. (A.12) and Eq. (A.13) is also fulfilled with $P_l = P_{132}$. In other words, if the second and third elements b and c of the fixed column are the same, we should further consider the equivalent condition of Eq. (A.13) with $P_l = P_{132}$. In the same manner, we can analyze the remaining cases of $P_l = P_{213}, P_{321}, P_{231}$ and P_{312} . The resulting constraints on the phases $\alpha_{1,2,3}$ and the constraints on the elements a, b and c are summarized in table 9. One can see that $e^{i\alpha_1} = e^{i\alpha_2} = e^{i\alpha_3} = q_\nu$ always needs to be satisfied. As a consequence, we summarize that the most general equivalent condition of two mixing pattern is given by Eq. (A.13) in the semidirect approach, and P_l is the permutation matrix under which the fixed column v_1 is invariant $P_l v_1 = v_1$.

A.2 Equivalence in variant of the semidirect approach

Given two distinct set of residual symmetries in this approach, as shown in section 2.2, the lepton mixing matrices read as

$$\begin{aligned} U_1 &= Q_{l1} P_{l1}^T S_{23}^T(\theta_1) \Sigma_1 P_{\nu 1} Q_{\nu 1}^\dagger, \\ U_2 &= Q_{l2} P_{l2}^T S_{23}^T(\theta_2) \Sigma_2 P_{\nu 2} Q_{\nu 2}^\dagger, \end{aligned} \quad (\text{A.17})$$

where $\Sigma = \Sigma_l^\dagger \Sigma_\nu$. In the following, we shall derive the criteria to determine whether the above two PMNS matrices U_1 and U_2 are essentially the same up to rows and columns permutations and the redefinition of the parameter θ . In other words, if the solution(s) for θ_2 and the $P_{l1,2}, Q_{l1,2}, P_{\nu 1,2}, Q_{\nu 1,2}$

P_l	Constraint on $\alpha_{1,2,3}$	Constraint on a, b and c
P_{123}	$e^{i\alpha_1} = e^{i\alpha_2} = e^{i\alpha_3} = q_\nu$	—
P_{132}		$b = c$
P_{213}		$a = b$
P_{321}		$a = c$
P_{231}		$a = b = c$
P_{312}		$a = b = c$

Table 9: Constraints on the fixed column $v_1 = (a, b, c)^T$ and the phase matrix $Q_l = \text{diag}(e^{i\alpha_1}, e^{i\alpha_2}, e^{i\alpha_3})$ imposed by the equivalent condition in the semidirect approach.

matrices can be found for any given value of θ_1 , so that the equality $U_1 = U_2$ is fulfilled, and then U_1 and U_2 would be equivalent, i.e.

$$Q_{l1} P_{l1}^T S_{23}^T(\theta_1) \Sigma_1 P_{\nu 1} Q_{\nu 1}^\dagger = Q_{l2} P_{l2}^T S_{23}^T(\theta_2) \Sigma_2 P_{\nu 2} Q_{\nu 2}^\dagger, \quad (\text{A.18})$$

which leads to

$$\Xi \equiv \Sigma_1 P_\nu Q_\nu \Sigma_2^\dagger = S_{23}(\theta_1) P_l Q_l S_{23}^T(\theta_2), \quad (\text{A.19})$$

with $P_\nu = P_{\nu 1} P_{\nu 2}^T$, $Q_\nu = P_{\nu 2} Q_{\nu 1}^\dagger Q_{\nu 2} P_{\nu 2}^T$, $P_l = P_{l1} P_{l2}^T$ and $Q_l = P_{l2} Q_{l1}^\dagger Q_{l2} P_{l2}^T$. Thus the product of Ξ and its transpose is

$$\Xi \Xi^T = S_{23}(\theta_1) Q_l'^2 S_{23}^T(\theta_1), \quad (\text{A.20})$$

where $Q_l' = P_l Q_l P_l^T$ is a diagonal phase matrix. Since Ξ is a constant matrix and it doesn't depend on θ_1 , we have

$$Q_l' = \text{diag}(\pm e^{i\gamma/2}, \pm e^{i\alpha/2}, \pm e^{i\alpha/2}), \quad (\text{A.21})$$

where α and γ are real, and “ \pm ” can be chosen independently. In the variant of the semidirect approach, one row of the PMNS matrix is fixed by the postulated residual symmetry. Without loss of generality, we assume that the fixed row is the first row of the PMNS matrix. As a result, the permutation matrices P_{l1} , P_{l2} and P_l can be either P_{123} or P_{132} , thus we obtain the equivalent condition

$$\Xi = \Sigma_1 P_\nu Q_\nu \Sigma_2^\dagger = S_{23}(\theta_1) P_l Q_l S_{23}^T(\theta_2) = S_{23}(\theta_1) Q_l' P_l S_{23}^T(\theta_2) = Q_l' P_l S_{23}^T(\theta_0), \quad (\text{A.22})$$

with $\theta_0 = \theta_2 \pm \theta_1$. If the two mixing patterns U_1 and U_2 are equivalent, the first row of Σ_1 and Σ_2 must be equal, and it is denoted as $u_1 = (c_1, c_2, c_3) = (|c_1|e^{i\delta_1}, |c_2|e^{i\delta_2}, |c_3|e^{i\delta_3})$ with $|c_1|^2 + |c_2|^2 + |c_3|^2 = 1$. Notice that we can set the phases $\delta_1 = 0$ and $\delta_{2,3} \in [0, \frac{\pi}{2})$ by redefining the matrices Q_l and Q_ν . The (11) element of Ξ can be read from Eq. (A.22) as

$$u_1 P_\nu Q_\nu u_1^\dagger = \pm e^{i\gamma/2} \equiv q_l. \quad (\text{A.23})$$

We parameterize $Q_\nu = \text{diag}(q_{\nu 1}, q_{\nu 2}, q_{\nu 3})$ and $q_{\nu 1,2,3} = \pm 1, \pm i$. In the following, we shall analyze the equivalent condition of Eq. (A.22) and the constraint of Eq. (A.23) for the six possible values of P_ν .

If $P_\nu = P_{123} = \mathbb{1}_{3 \times 3}$, Eq. (A.23) reduces to

$$q_{\nu 1} |c_1|^2 + q_{\nu 2} |c_2|^2 + q_{\nu 3} |c_3|^2 = q_l, \quad (\text{A.24})$$

Subsequently taking absolute value of the both sides of this equation, we obtain

$$\left| q_{\nu 1} |c_1|^2 + q_{\nu 2} |c_2|^2 + q_{\nu 3} |c_3|^2 \right| = 1, \quad (\text{A.25})$$

which requires

$$q_{\nu 1} = q_{\nu 2} = q_{\nu 3} = q_l. \quad (\text{A.26})$$

Therefore the equivalent condition of Eq. (A.22) becomes

$$\Omega \equiv \Sigma_1 P_\nu \Sigma_2^\dagger = q_l^* Q_l' P_l S_{23}^T(\theta_0), \quad (\text{A.27})$$

or equivalently

$$\Omega \Omega^T = q_l'^2 Q_l'^2 = \text{diag}(1, e^{i\alpha'}, e^{i\alpha'}), \quad (\text{A.28})$$

where $\alpha' = \alpha - \gamma$.

For the case of $P_\nu = P_{132}$, Eq. (A.23) takes the form

$$q_{\nu 1} |c_1|^2 + q_{\nu 2} c_3 c_2^* + q_{\nu 3} c_2 c_3^* = q_l, \quad (\text{A.29})$$

from which we obtain

$$\left| q_{\nu 1} |c_1|^2 + q_{\nu 2} c_2^* c_3 + q_{\nu 3} c_2 c_3^* \right| \leq |c_1|^2 + 2|c_2||c_3| \leq |c_1|^2 + |c_2|^2 + |c_3|^2 = 1 = |q_l|. \quad (\text{A.30})$$

Thus Eq. (A.29) is satisfied if and only if

$$q_{\nu 1} = e^{i(\delta_3 - \delta_2)} q_{\nu 2} = e^{-i(\delta_3 - \delta_2)} q_{\nu 3}, \quad |c_2| = |c_3|, \quad (\text{A.31})$$

which leads to $e^{i(\delta_3 - \delta_2)} = \pm 1, \pm i$. Considering $\delta_3 - \delta_2 \in (-\frac{\pi}{2}, \frac{\pi}{2})$, we have

$$\delta_2 = \delta_3, \quad q_{\nu 1} = q_{\nu 2} = q_{\nu 3} = q_l. \quad (\text{A.32})$$

Therefore the equivalent condition is still $\Omega \Omega^T = \text{diag}(1, e^{i\alpha'}, e^{i\alpha'})$ given by Eq. (A.28) with $\Omega = \Sigma_1 P_\nu \Sigma_2^\dagger$ and $P_\nu = P_{132}$.

For all the six possible values of P_ν , the corresponding constraints on the fixed row $u_1 = (|c_1|, |c_2|e^{i\delta_2}, |c_3|e^{i\delta_3})$ and the phase matrix $Q_\nu = \text{diag}(q_{\nu 1}, q_{\nu 2}, q_{\nu 3})$ are summarized in table 10. We see that the equivalent condition can be written as $\Omega \Omega^T = \text{diag}(1, e^{i\alpha'}, e^{i\alpha'})$ with $\Omega = \Sigma_1 P_\nu Q_\nu' \Sigma_2^\dagger$. The matrix Q_ν' is an identity matrix $Q_\nu' = \mathbb{1}_{3 \times 3}$ in the case of $P_\nu = P_{123}, P_{132}, P_{213}$ and P_{321} . Nevertheless, depending on the values of δ_2 and δ_3 , we have $Q_\nu' = \mathbb{1}_{3 \times 3}, e^{-i\pi/6} \text{diag}(1, i, 1), e^{-i\pi/6} \text{diag}(1, 1, i)$ or $e^{-i\pi/3} \text{diag}(1, i, i)$ for $P_\nu = P_{231}, P_{312}$. Using this simple criteria, one can easily determine whether two residual symmetries give rise to the same lepton mixing patten.

P_ν	Constraint on $q_{\nu 1,2,3}$	Constraint on $ c_{1,2,3} $	Constraint on $\delta_{2,3}$
P_{123}	$q_{\nu 1} = q_{\nu 2} = q_{\nu 3} = q_l$	—	—
P_{132}	$q_{\nu 1} = q_{\nu 2} = q_{\nu 3} = q_l$	$ c_2 = c_3 $	$\delta_2 = \delta_3$
P_{213}	$q_{\nu 1} = q_{\nu 2} = q_{\nu 3} = q_l$	$ c_1 = c_2 $	$\delta_2 = 0$
P_{321}	$q_{\nu 1} = q_{\nu 2} = q_{\nu 3} = q_l$	$ c_1 = c_3 $	$\delta_3 = 0$
P_{231}	$q_{\nu 1} = q_{\nu 2} = q_{\nu 3} = q_l$	$ c_1 = c_2 = c_3 = \frac{1}{\sqrt{3}}$	$\delta_2 = \delta_3 = 0$
	$q_{\nu 1} = -iq_{\nu 2} = q_{\nu 3} = e^{-i\pi/6} q_l$		$\delta_2 = \pi/3, \delta_3 = \pi/6$
	$q_{\nu 1} = -iq_{\nu 2} = -iq_{\nu 3} = e^{-i\pi/3} q_l$		$\delta_2 = \pi/6, \delta_3 = \pi/3$
P_{312}	$q_{\nu 1} = q_{\nu 2} = q_{\nu 3} = q_l$	$ c_1 = c_2 = c_3 = \frac{1}{\sqrt{3}}$	$\delta_2 = \delta_3 = 0$
	$q_{\nu 1} = -iq_{\nu 2} = -iq_{\nu 3} = e^{-i\pi/3} q_l$		$\delta_2 = \pi/3, \delta_3 = \pi/6$
	$q_{\nu 1} = q_{\nu 2} = -iq_{\nu 3} = e^{-i\pi/6} q_l$		$\delta_2 = \pi/6, \delta_3 = \pi/3$

Table 10: Constraints on the fixed row $u_1 = (|c_1|, |c_2|e^{i\delta_2}, |c_3|e^{i\delta_3})$ and the phase matrix $Q_\nu = \text{diag}(q_{\nu 1}, q_{\nu 2}, q_{\nu 3})$ imposed by the equivalent condition in the variant of the semidirect approach.

References

- [1] G. Altarelli and F. Feruglio, *Rev. Mod. Phys.* **82**, 2701 (2010) doi:10.1103/RevModPhys.82.2701 [arXiv:1002.0211 [hep-ph]].
- [2] H. Ishimori, T. Kobayashi, H. Ohki, Y. Shimizu, H. Okada and M. Tanimoto, *Prog. Theor. Phys. Suppl.* **183**, 1 (2010) doi:10.1143/PTPS.183.1 [arXiv:1003.3552 [hep-th]].
- [3] S. F. King and C. Luhn, *Rept. Prog. Phys.* **76**, 056201 (2013) doi:10.1088/0034-4885/76/5/056201 [arXiv:1301.1340 [hep-ph]]; S. F. King, A. Merle, S. Morisi, Y. Shimizu and M. Tanimoto, *New J. Phys.* **16**, 045018 (2014) doi:10.1088/1367-2630/16/4/045018 [arXiv:1402.4271 [hep-ph]]; S. F. King, *J. Phys. G* **42**, 123001 (2015) doi:10.1088/0954-3899/42/12/123001 [arXiv:1510.02091 [hep-ph]].
- [4] F. Feruglio, C. Hagedorn and R. Ziegler, *JHEP* **1307**, 027 (2013) doi:10.1007/JHEP07(2013)027 [arXiv:1211.5560 [hep-ph]].
- [5] M. Holthausen, M. Lindner and M. A. Schmidt, *JHEP* **1304**, 122 (2013) doi:10.1007/JHEP04(2013)122 [arXiv:1211.6953 [hep-ph]].
- [6] K. Abe *et al.* [T2K Collaboration], *Phys. Rev. D* **91**, no. 7, 072010 (2015) doi:10.1103/PhysRevD.91.072010 [arXiv:1502.01550 [hep-ex]].
- [7] P. Chen, C. C. Li and G. J. Ding, *Phys. Rev. D* **91**, 033003 (2015) doi:10.1103/PhysRevD.91.033003 [arXiv:1412.8352 [hep-ph]].
- [8] P. Chen, C. Y. Yao and G. J. Ding, *Phys. Rev. D* **92**, no. 7, 073002 (2015) doi:10.1103/PhysRevD.92.073002 [arXiv:1507.03419 [hep-ph]].
- [9] G. J. Ding, S. F. King and A. J. Stuart, *JHEP* **1312**, 006 (2013) doi:10.1007/JHEP12(2013)006 [arXiv:1307.4212 [hep-ph]].
- [10] G. J. Ding, S. F. King, C. Luhn and A. J. Stuart, *JHEP* **1305**, 084 (2013) doi:10.1007/JHEP05(2013)084 [arXiv:1303.6180 [hep-ph]].
- [11] C. C. Li and G. J. Ding, *JHEP* **1508**, 017 (2015) doi:10.1007/JHEP08(2015)017 [arXiv:1408.0785 [hep-ph]].
- [12] F. Feruglio, C. Hagedorn and R. Ziegler, *Eur. Phys. J. C* **74**, 2753 (2014) doi:10.1140/epjc/s10052-014-2753-2 [arXiv:1303.7178 [hep-ph]].
- [13] C. Luhn, *Nucl. Phys. B* **875**, 80 (2013) doi:10.1016/j.nuclphysb.2013.07.003 [arXiv:1306.2358 [hep-ph]].
- [14] C. C. Li and G. J. Ding, *Nucl. Phys. B* **881**, 206 (2014) doi:10.1016/j.nuclphysb.2014.02.002 [arXiv:1312.4401 [hep-ph]].
- [15] G. C. Branco, I. de Medeiros Varzielas and S. F. King, *Nucl. Phys. B* **899**, 14 (2015) doi:10.1016/j.nuclphysb.2015.07.024 [arXiv:1505.06165 [hep-ph]]; G. C. Branco, I. de Medeiros Varzielas and S. F. King, *Phys. Rev. D* **92**, no. 3, 036007 (2015) doi:10.1103/PhysRevD.92.036007 [arXiv:1502.03105 [hep-ph]].
- [16] G. J. Ding and Y. L. Zhou, *Chin. Phys. C* **39**, no. 2, 021001 (2015) doi:10.1088/1674-1137/39/2/021001 [arXiv:1312.5222 [hep-ph]]; G. J. Ding and Y. L. Zhou, *JHEP* **1406**, 023 (2014) doi:10.1007/JHEP06(2014)023 [arXiv:1404.0592 [hep-ph]].
- [17] C. C. Li and G. J. Ding, *JHEP* **1505**, 100 (2015) doi:10.1007/JHEP05(2015)100 [arXiv:1503.03711 [hep-ph]].

- [18] A. Di Iura, C. Hagedorn and D. Meloni, JHEP **1508**, 037 (2015) doi:10.1007/JHEP08(2015)037 [arXiv:1503.04140 [hep-ph]].
- [19] P. Ballett, S. Pascoli and J. Turner, Phys. Rev. D **92**, no. 9, 093008 (2015) doi:10.1103/PhysRevD.92.093008 [arXiv:1503.07543 [hep-ph]].
- [20] G. J. Ding and S. F. King, Phys. Rev. D **89**, no. 9, 093020 (2014) doi:10.1103/PhysRevD.89.093020 [arXiv:1403.5846 [hep-ph]].
- [21] S. j. Rong, arXiv:1604.08482 [hep-ph].
- [22] C. Hagedorn, A. Meroni and E. Molinaro, Nucl. Phys. B **891**, 499 (2015) doi:10.1016/j.nuclphysb.2014.12.013 [arXiv:1408.7118 [hep-ph]].
- [23] G. J. Ding and S. F. King, Phys. Rev. D **93**, 025013 (2016) doi:10.1103/PhysRevD.93.025013 [arXiv:1510.03188 [hep-ph]].
- [24] S. F. King and T. Neder, Phys. Lett. B **736**, 308 (2014) doi:10.1016/j.physletb.2014.07.043 [arXiv:1403.1758 [hep-ph]].
- [25] G. J. Ding, S. F. King and T. Neder, JHEP **1412**, 007 (2014) doi:10.1007/JHEP12(2014)007 [arXiv:1409.8005 [hep-ph]].
- [26] C. C. Li, C. Y. Yao and G. J. Ding, JHEP **1605**, 007 (2016) doi:10.1007/JHEP05(2016)007 [arXiv:1601.06393 [hep-ph]].
- [27] P. Chen, G. J. Ding and S. F. King, JHEP **1603**, 206 (2016) doi:10.1007/JHEP03(2016)206 [arXiv:1602.03873 [hep-ph]].
- [28] C. Hagedorn and E. Molinaro, arXiv:1602.04206 [hep-ph].
- [29] P. Chen, G. J. Ding, F. Gonzalez-Canales and J. W. F. Valle, arXiv:1604.03510 [hep-ph]; P. Chen, G. J. Ding, F. Gonzalez-Canales and J. W. F. Valle, Phys. Lett. B **753**, 644 (2016) doi:10.1016/j.physletb.2015.12.069 [arXiv:1512.01551 [hep-ph]].
- [30] The GAP Group, *GAP - Groups, Algorithms, and Programming, Version 4.5.6* (2012), <http://www.gap-system.org>.
- [31] C. S. Lam, Phys. Rev. D **87**, no. 1, 013001 (2013) doi:10.1103/PhysRevD.87.013001 [arXiv:1208.5527 [hep-ph]].
- [32] M. Holthausen, K. S. Lim and M. Lindner, Phys. Lett. B **721**, 61 (2013) doi:10.1016/j.physletb.2013.02.047 [arXiv:1212.2411 [hep-ph]].
- [33] M. Holthausen and K. S. Lim, Phys. Rev. D **88**, 033018 (2013) doi:10.1103/PhysRevD.88.033018 [arXiv:1306.4356 [hep-ph]].
- [34] L. Lavoura and P. O. Ludl, Phys. Lett. B **731**, 331 (2014) doi:10.1016/j.physletb.2014.03.001 [arXiv:1401.5036 [hep-ph]].
- [35] A. S. Joshipura and K. M. Patel, JHEP **1404**, 009 (2014) doi:10.1007/JHEP04(2014)009 [arXiv:1401.6397 [hep-ph]].
- [36] A. S. Joshipura and K. M. Patel, Phys. Rev. D **90**, no. 3, 036005 (2014) doi:10.1103/PhysRevD.90.036005 [arXiv:1405.6106 [hep-ph]].
- [37] J. Talbert, JHEP **1412**, 058 (2014) doi:10.1007/JHEP12(2014)058 [arXiv:1409.7310 [hep-ph]].
- [38] C. Y. Yao and G. J. Ding, Phys. Rev. D **92**, no. 9, 096010 (2015) doi:10.1103/PhysRevD.92.096010 [arXiv:1505.03798 [hep-ph]].

- [39] I. d. M. Varzielas, R. W. Rasmussen and J. Talbert, arXiv:1605.03581 [hep-ph].
- [40] S. F. King and P. O. Ludl, arXiv:1605.01683 [hep-ph].
- [41] G. Ecker, W. Grimus and W. Konetschny, Nucl. Phys. B **191**, 465 (1981). doi:10.1016/0550-3213(81)90309-6; G. Ecker, W. Grimus and H. Neufeld, Nucl. Phys. B **247**, 70 (1984). doi:10.1016/0550-3213(84)90373-0; J. Bernabeu, G. C. Branco and M. Gronau, Phys. Lett. B **169**, 243 (1986). doi:10.1016/0370-2693(86)90659-3; G. Ecker, W. Grimus and H. Neufeld, J. Phys. A **20**, L807 (1987). doi:10.1088/0305-4470/20/12/010; H. Neufeld, W. Grimus and G. Ecker, Int. J. Mod. Phys. A **3**, 603 (1988). doi:10.1142/S0217751X88000254.
- [42] M. C. Chen, M. Fallbacher, K. T. Mahanthappa, M. Ratz and A. Trautner, Nucl. Phys. B **883**, 267 (2014) doi:10.1016/j.nuclphysb.2014.03.023 [arXiv:1402.0507 [hep-ph]].
- [43] R. M. Fonseca and W. Grimus, JHEP **1409**, 033 (2014) doi:10.1007/JHEP09(2014)033 [arXiv:1405.3678 [hep-ph]].
- [44] M. C. Gonzalez-Garcia, M. Maltoni and T. Schwetz, JHEP **1411**, 052 (2014) doi:10.1007/JHEP11(2014)052 [arXiv:1409.5439 [hep-ph]].
- [45] http://staff.ustc.edu.cn/~dinggj/cp_scan.html.
- [46] C. Jarlskog, Phys. Rev. Lett. **55**, 1039 (1985). doi:10.1103/PhysRevLett.55.1039
- [47] G. C. Branco, R. G. Felipe and F. R. Joaquim, Rev. Mod. Phys. **84**, 515 (2012) doi:10.1103/RevModPhys.84.515 [arXiv:1111.5332 [hep-ph]].
- [48] G. C. Branco, L. Lavoura and M. N. Rebelo, Phys. Lett. B **180**, 264 (1986). doi:10.1016/0370-2693(86)90307-2
- [49] E. E. Jenkins and A. V. Manohar, Nucl. Phys. B **792**, 187 (2008) doi:10.1016/j.nuclphysb.2007.09.031 [arXiv:0706.4313 [hep-ph]].
- [50] K. A. Olive *et al.* [Particle Data Group Collaboration], Chin. Phys. C **38**, 090001 (2014). doi:10.1088/1674-1137/38/9/090001
- [51] L. Covi, E. Roulet and F. Vissani, Phys. Lett. B **384**, 169 (1996) doi:10.1016/0370-2693(96)00817-9 [hep-ph/9605319].
- [52] T. Endoh, T. Morozumi and Z. h. Xiong, Prog. Theor. Phys. **111**, 123 (2004) doi:10.1143/PTP.111.123 [hep-ph/0308276].
- [53] A. Abada, S. Davidson, A. Ibarra, F.-X. Josse-Michaux, M. Losada and A. Riotto, JHEP **0609**, 010 (2006) doi:10.1088/1126-6708/2006/09/010 [hep-ph/0605281].
- [54] A. Abada, S. Davidson, F. X. Josse-Michaux, M. Losada and A. Riotto, JCAP **0604**, 004 (2006) doi:10.1088/1475-7516/2006/04/004 [hep-ph/0601083].
- [55] C. S. Fong, E. Nardi and A. Riotto, Adv. High Energy Phys. **2012**, 158303 (2012) doi:10.1155/2012/158303 [arXiv:1301.3062 [hep-ph]].
- [56] J. A. Casas and A. Ibarra, Nucl. Phys. B **618**, 171 (2001) doi:10.1016/S0550-3213(01)00475-8 [hep-ph/0103065].
- [57] M. Auger *et al.* [EXO-200 Collaboration], Phys. Rev. Lett. **109**, 032505 (2012) doi:10.1103/PhysRevLett.109.032505 [arXiv:1205.5608 [hep-ex]].
- [58] J. B. Albert *et al.* [EXO-200 Collaboration], Nature **510**, 229 (2014) doi:10.1038/nature13432 [arXiv:1402.6956 [nucl-ex]].

- [59] A. Gando *et al.* [KamLAND-Zen Collaboration], Phys. Rev. Lett. **110**, no. 6, 062502 (2013) doi:10.1103/PhysRevLett.110.062502 [arXiv:1211.3863 [hep-ex]].
- [60] P. A. R. Ade *et al.* [Planck Collaboration], Astron. Astrophys. **571**, A16 (2014) doi:10.1051/0004-6361/201321591 [arXiv:1303.5076 [astro-ph.CO]].
- [61] F. An *et al.* [JUNO Collaboration], J. Phys. G **43**, no. 3, 030401 (2016) doi:10.1088/0954-3899/43/3/030401 [arXiv:1507.05613 [physics.ins-det]].
- [62] R. Acciarri *et al.* [DUNE Collaboration], arXiv:1601.05471 [physics.ins-det]; R. Acciarri *et al.* [DUNE Collaboration], arXiv:1512.06148 [physics.ins-det]; J. Strait *et al.* [DUNE Collaboration], arXiv:1601.05823 [physics.ins-det]; R. Acciarri *et al.* [DUNE Collaboration], arXiv:1601.02984 [physics.ins-det].
- [63] E. Kearns *et al.* [Hyper-Kamiokande Working Group Collaboration], arXiv:1309.0184 [hep-ex].
- [64] C. Luhn, S. Nasri and P. Ramond, J. Math. Phys. **48**, 123519 (2007) doi:10.1063/1.2823978 [arXiv:0709.1447 [hep-th]]; R. Zwicky and T. Fischbacher, Phys. Rev. D **80**, 076009 (2009) doi:10.1103/PhysRevD.80.076009 [arXiv:0908.4182 [hep-ph]]; S. F. King and C. Luhn, Nucl. Phys. B **832**, 414 (2010) doi:10.1016/j.nuclphysb.2010.02.019 [arXiv:0912.1344 [hep-ph]]; R. de Adelhart Toorop, F. Feruglio and C. Hagedorn, Nucl. Phys. B **858**, 437 (2012) doi:10.1016/j.nuclphysb.2012.01.017 [arXiv:1112.1340 [hep-ph]].
- [65] D. V. Forero, M. Tortola and J. W. F. Valle, Phys. Rev. D **90**, no. 9, 093006 (2014) doi:10.1103/PhysRevD.90.093006 [arXiv:1405.7540 [hep-ph]].
- [66] F. Capozzi, E. Lisi, A. Marrone, D. Montanino and A. Palazzo, Nucl. Phys. B **908**, 218 (2016) doi:10.1016/j.nuclphysb.2016.02.016 [arXiv:1601.07777 [hep-ph]].